



**HAL**  
open science

# Colloidal stability of native and cross-linked casein micelles and their potential use as nanocarrier for cyanidin-3-0 glucoside

Federico Casanova

► **To cite this version:**

Federico Casanova. Colloidal stability of native and cross-linked casein micelles and their potential use as nanocarrier for cyanidin-3-0 glucoside. Food and Nutrition. Universidade Federal de Viçosa, 2017. English. NNT: . tel-02789435

**HAL Id: tel-02789435**

**<https://hal.inrae.fr/tel-02789435v1>**

Submitted on 5 Jun 2020

**HAL** is a multi-disciplinary open access archive for the deposit and dissemination of scientific research documents, whether they are published or not. The documents may come from teaching and research institutions in France or abroad, or from public or private research centers.

L'archive ouverte pluridisciplinaire **HAL**, est destinée au dépôt et à la diffusion de documents scientifiques de niveau recherche, publiés ou non, émanant des établissements d'enseignement et de recherche français ou étrangers, des laboratoires publics ou privés.



Distributed under a Creative Commons Attribution - ShareAlike 4.0 International License

FEDERICO CASANOVA

**COLLOIDAL STABILITY OF NATIVE AND CROSS-LINKED CASEIN MICELLES  
AND THEIR POTENTIAL USE AS NANOCARRIER FOR CYANIDIN-3-O-  
GLUCOSIDE**

Dissertationthesis presented to  
Universidade Federal de Viçosa as part of  
the requirements for the PostGraduate  
Program in Food Science and Technology  
to obtain the title of Doctor Scientiae.

VIÇOSA  
MINAS GERAIS – BRASIL  
2017

**Ficha catalográfica preparada pela Biblioteca Central da Universidade  
Federal de Viçosa - Câmpus Viçosa**

T

C335c  
2017 Casanova, Federico, 1984-  
Colloidal stability of native and cross-linked casein micelles  
and their potential use as nanocarrier for cyanidin-3-O-glucoside  
/ Federico Casanova. – Viçosa, MG, 2017.  
xiv, 113f. : il. (algumas color.) ; 29 cm.

Orientador: Antônio Fernandes de Carvalho.  
Tese (doutorado) - Universidade Federal de Viçosa.  
Referências bibliográficas: f.103-113.

1. Tecnologia de alimentos. 2. Antocianidinas. 3. Leite.  
4. Proteína. 5. Físico-química. I. Universidade Federal de  
Viçosa. Departamento de Tecnologia de Alimentos. Programa de  
Pós-graduação em Ciência e Tecnologia de Alimentos. II. Título.

CDD 22 ed. 664.02

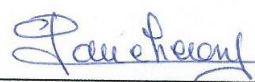
FEDERICO CASANOVA

**COLLOIDAL STABILITY OF NATIVE AND CROSS-LINKED CASEIN MICELLES  
AND THEIR POTENTIAL USE AS NANOCARRIER FOR CYANIDIN-3-O-  
GLUCOSIDE**

Dissertation thesis presented to  
Universidade Federal de Viçosa as part of  
the requirements for the PostGraduate  
Program in Food Science and Technology  
to obtain the title of Doctor Scientiae.


APPROVED: March 14, 2017.

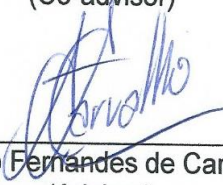
  
\_\_\_\_\_  
Guilherme Miranda Tavares

  
\_\_\_\_\_  
Frédéric Gaucheron

  
\_\_\_\_\_  
Evandro Martins

  
\_\_\_\_\_  
Alvaro V. N. de Carvalho Teixeira

  
\_\_\_\_\_  
Naaman Francisco Nogueira Silva  
(Co-advisor)

  
\_\_\_\_\_  
Antônio Fernandes de Carvalho  
(Advisor)

## **Acknowledgments**

To my family.

To Adèle.

To Universidade Federal de Viçosa and to Inovaleite Laboratory for the opportunity, material and structuresupport.

To CAPES, for the financial support to this research.

To my advisor, Professor Antônio Fernandes de Carvalho, for the advice, trustworth, motivation, for the transmitted knowledgments and mainly for all the words of incentive.

To my friend and co-advisor, Professor Naaman Nogueira Silva for the teachings, motivation, attendance and assistance in France and in Brazil.

To Michele for all his help before, during and after the Ph.D.

To INRA-STLO for the scientific collaboration and for the hospitality during one year.

To all the Brazilian peoples, thanks for their help.

To all the other peoples (and the list is very long) that I have known in recent years in France and Brazil.

I dedicate to my mother, my father, my aunt and my grandmother

## TABLE OF CONTENTS

<b>LIST OF FIGURES</b> .....	<b>vi</b>
<b>LIST OF TABLES</b> .....	<b>ix</b>
<b>ABSTRACT</b> .....	<b>xi</b>
<b>RESUMO</b> .....	<b>xiii</b>
<b>1. GENERAL INTRODUCTION</b> .....	<b>1</b>
<b>2. LITERATURE REVIEW</b> .....	<b>6</b>
<b>2.1 Interaction between casein and interest molecules: a review</b> .....	<b>7</b>
2.1.1 Introduction .....	8
2.1.2 Physico-chemical methods to characterize nanoparticles .....	8
2.1.3 Physico-chemical characteristics of casein .....	12
2.1.4 Physico-chemical interactions between casein and interesting molecules.	14
2.1.5 Conclusions and future applications.....	32
<b>3. OBJECTIVES AND STRATEGIES</b> .....	<b>34</b>
<b>4. RESULTS AND DISCUSSION</b> .....	<b>38</b>
<b>2.1 Stability of casein micelles cross-linked with genipin: a physicochemical study as a function of pH</b> .....	<b>40</b>
2.1.1 Introduction .....	41
2.1.2 Material and methods.....	42
2.1.3 Results and discussion.....	45
2.1.4 Conclusion .....	50
<b>2.2 Physico-chemical stability of casein micelles cross-linked with transglutaminase as a function of acidic pH</b> .....	<b>52</b>
2.2.1 Introduction .....	53
2.2.2 Material and methods.....	54
2.2.3 Results and discussion.....	57
2.2.4 Conclusion .....	66
<b>2.3 Interaction of cyanidin-3-O-glucoside with sodium caseinate</b> .....	<b>68</b>
2.3.1 Introduction .....	69
2.3.2 Materials and methods.....	71
2.3.3 Results and discussion.....	72

2.3.4 Conclusion .....	82
<b>2.4 Interaction between transglutaminase cross-linked casein micelles and cyanidin-3-O-glucoside .....</b>	<b>84</b>
2.4.1 Introduction .....	85
2.4.2 Materials and methods .....	87
2.4.3 Results .....	89
2.4.4 Discussion .....	96
2.4.5 Conclusion .....	98
<b>5. GENERAL CONCLUSION AND PERSPECTIVES.....</b>	<b>99</b>
<b>6. REFERENCES.....</b>	<b>103</b>



## LISTOF FIGURES

Figure 1: Chemical structure of cyanidin-3-O-glucoside .....	3
Figure 2: Outline of the main analytical techniques used to analyze nanoparticles (NP), from “Advancements in characterization techniques of nanoparticles and sophisticated instruments”, with modifications [17]. .....	9
Figure 3: Example of TEM images (a)–(c) of gold samples obtained in casein solution at different concentration at pH 2.0 (from [18]). .....	10
Figure 4: Example of hydrodynamic diameter measurements with corresponding microscopy images (from [19]). .....	11
Figure 5 : Outline of the strategy adopted in the part A of the manuscript. We star with native CMs and after cross-linking by GP or Tgase, we realize the stability test.....	36
Figure 6 : Interaction between Tgase cross-linking CMs and C3G at pH 2 and pH 7.....	37
Figure 7 : Z-average diameter (nm) as a function of pH of native CMs (●) and CMs-GP (○). Data corresponded to average values (n=3) and the vertical error bars indicate the standard error. For native CMs and CMs-GP, the determinations between pH 5.0 and 3.0 were not possible due to the presence of precipitate. At pH below 3.0, native CMs were not monodisperse. ....	46
Figure 8 : ζ-potential (mV) as a function of pH of native CMs (●) and CMs-GP (○). The determinations between -5 and +5 mV (horizontal dotted lines) were not possible due to the presence of visible aggregates. The standard deviation was < 5%. ....	47
Figure 9 : Effect of pH on the ethanol stability for native CMs (●) and CMs-GP (○). Determinations were performed in triplicate for 3 different preparations of suspensions. The standard deviation was < 5%. For native CMs and CMs-GP, the determinations between pH 5.0 and 3.0 were not possible due to the presence of precipitate. At pH below 3.0, native CMs were not monodisperse.....	49
Figure 10: Z-average $D_h$ (nm) as a function of pH of native CMs (○) and CM-Tgase (●). Data corresponded to an average of 3 determinations. The vertical error bars indicate the standard error. For native CMs and CMs-Tgase, the determinations between pH 5.0 and 3.0 were not possible due to the presence of precipitate. At pH below 3.0, native CMs were not monodisperse. ....	58
Figure 11: ζ-potential as a function of pH of native CMs (○) and CMs+Tgase (●).The determinations between -5 and +5 mV (horizontal dotted lines) were not possible due	

to the presence of visible aggregates. The standard deviation was < 5%. Data corresponded to an average of 4 determinations. The vertical error bars, comprised in points, indicate the standard error. ....	59
Figure 12: Z-average $D_h$ (nm) as a function of pH of CMs-Tgase in presence of 8 M urea. Data corresponded to an average of 6 determinations. The standard deviation was < 5%. The vertical error bars, comprised in points, indicate the standard error. For native CMs the determinations were not possible due to their dissociation.....	60
Figure 13: Z-average $D_h$ (nm) as a function of pH of CMs+Tgase in the presence of 100 mM sodium citrate. Data correspond to an average of 6 determinations. The standard deviation was < 5%. The vertical error bars, comprised in points, indicate the standard error. For native CMs determination of $D_h$ were not possible due to their dissociation.....	62
Figure 14 : Chemical structure of cyanidin-3-O-glucoside .....	71
Figure 15: Fluorescence emission spectra of Cas (4 $\mu$ M) at pH 7 (A) and pH 2 (B) and at 295 °K in the absence and presence of increasing concentrations of C3G (from 0.4 to 40 $\mu$ M). Black line corresponds to the fluorescence spectra of C3G at 40 $\mu$ M in the absence of caseins. ....	74
Figure 16: Stern-Volmer plots of the quenching of Cas fluorescence by C3G at pH 7 (A) and Cas pH 2 (B) and at 295 °K. ....	74
Figure 17: Scatchard plot of Cas (4 $\mu$ M) at pH 7 (A) and pH 2 (B) titrated with an increasing concentration of C3G (from 0.4 to 40 $\mu$ M) at 295 °K. ....	76
Figure 18: Variation of $\ln K_a$ as a function of $1/T$ for the two C3G classes of binding site on Cas at pH 7 (A) and at pH 2(B). ( $\circ$ ) correspond to the first class of binding site and ( $\square$ ) correspond to the second class of binding site. ....	79
Figure 19: Fluorescence spectra (a. u.) of Cas (4 $\mu$ M) in the absence (blue line) or saturated with C3G (C3G/Cas molar ratio of 10) without NaCl added (green line) or with 100, 150, 200 mM NaCl (red, black and orange line) at pH 7 (A) and pH 2 (B). Grey line represent C3G alone. Insert in (A) and (B) show the Stern-Volmer plot of the titration in the absence and the presence of 0 (O), 100 ( $\square$ ) and 200 ( $\diamond$ ) mM of NaCl. ....	81
Figure 20: Scatchard plot of Cas (4 $\mu$ M) at pH 7 and 100 mM NaCl titrated with an increasing concentration of C3G (from 0.4 to 40 $\mu$ M) at 295 °K. ....	81
Figure 21: Volume (%) as a function of particle diameter of Cas (0.4 $\mu$ M) in the absence (black line) and presence of 40 $\mu$ M of C3G (red line) at pH 2 monitored by dynamic light scattering (DLS).....	82

Figure 22 : Intensity (%) as a function of particle diameter of native CMs (red line), CMs-Tgase (blue line) at pH 7 and CMs-Tgase at pH 2 (green line) with 40 $\mu$ l of C3G monitored by dynamic light scattering (DLS). .....	90
Figure 23 : Fluorescence emission spectra of native CMs-Tgase at pH 7 (A) and pH 2 (B) at 295 °C in the absence and presence of increasing concentrations of C3G (from 0.4 to 40 $\mu$ M). Stern-Volmer plots of native CMs (O) and CMs-Tgase ( $\square$ ) at pH 7 (C) and CMs-Tgase at pH 2 (D).....	92
Figure 24 : Scatchard plot of the interaction of C3G with native CMs (O) and CMs-Tgase ( $\square$ ) at pH 7 (A) and CMs-Tgase at pH 2 (B) at 295 °K. ....	93
Figure 25 : $\ln K_a$ as a function of $1/T$ for the two classes of binding site. Figure 3 A represents the first ( $\circ$ and $\circ$ ) and the second ( $\square$ and $\square$ ) class of C3G binding sites for native CMs and CMs-Tgase, respectively, at pH 7. Figure 3 B showed the first ( $\circ$ ) and the second ( $\square$ ) class of C3G binding sites at pH 2.....	95
Figure 26 : Gradual release of C3G molecules under gastric conditions (pH 2). .....	102

## LISTOF TABLES

Table 1: Average characteristics of CMs [25]. .....	14
Table 2: Casein-based nanoparticles as nanocarriers in food applications (rCMs = reassembled casein micelles; CMs = native casein micelles; NaCas= sodium caseinate). .....	22
Table 3: Casein as nanocarriers for anticancer drugs. ....	27
Table 4: Casein-based nanoparticles as nanocarriers in pharmaceuticals applications.....	29
Table 5: Casein interacting with natural or synthetic nanoparticles. ....	31
Table 6 : HCT (s) at different pH values at 140 °C of native CMs and CMs-GP. Measurements were performed in triplicate for 3 different suspensions. For native CMs and CMs-GP, the determinations between pH 5.0 and 3.0 were not possible due to the presence of precipitate. At pH below 3.0, native CMs are not monodisperse. ....	48
Table 7: Pearson correlation coefficients among variables for native CMs and CMs-GP structures. $\varnothing$ = diameter (nm); Eth = ethanol stability; $\zeta$ = $\zeta$ potential; HCT= Heat coagulation time. Correlation established from pH 7.0 to pH 2.0; *correlations established from pH 7.0 to pH 5.5. ....	50
Table 8 : Heat Coagulation Time (HCT) (s) at different pH values at 140 °C of native CMs and CMs-Tgase. Measurements were performed in triplicate for 3 different suspensions. For native CMs and CMs-Tgase, the determinations between pH 5.0 and 3.0 were not possible due to the presence of precipitate. At pH below 3.0, native CMs were not monodisperse and $D_h$ was not determined. ....	63
Table 9 : Ethanol stability (v/v) at different pH values of native CMs and CMs-Tgase. Measurements were performed in triplicate for 3 different suspensions. For native CMs and CMs-Tgase, the determinations between pH 5.0 and 3.0 were not possible due to the presence of precipitate. At pH below 3.0, native CMs were not monodisperse. ....	64
Table 10 : Pearson correlation coefficients among variables for native CMs and CMs-Tgase structures. $D_h$ = hydrodynamic diameter (nm); Eth = ethanol stability; $\zeta$ = zeta potential; HCT= Heat coagulation time. <sup>1</sup> correlations established from pH 7.0 to 5.5 for native CMs; <sup>2</sup> correlation established from pH 7.0 to 2.0 for CMs-Tgase; .....	65

Table 11 : Binding affinity of C3G to Cas at different temperatures.....	76
Table 12. Thermodynamic parameters of Cas / C3G interaction at pH 7 and pH 2 at different temperatures. ....	79
Table 13: Binding parameters of the interaction of C3G with native CMs at pH 7 and CMs-Tgase at pH 7 and pH 2 at different temperatures. ....	94
Table 14: Thermodynamic parameters of native CMs at pH 7 and CMs-Tgase at pH 7 and pH 2 at different temperatures. ....	96

## ABSTRACT

CASANOVA, Federico, D.Sc., Universidade Federal de Viçosa, March, 2017. **Colloidal stability of native and cross-linked casein micelles and their potential use as nanocarrier for cyanidin-3-O-glucoside.** Adviser: Antônio Fernandes de Carvalho. Co-advisers: Naaman Francisco Nogueira Silva, Italo Tuler Perrone and Paulo Cesar Stringheta.

Casein micelles (CMs) are natural supramolecular assemblies present in milk. Their average hydrodynamic diameter is about 200nm and they present a hydrophobic core and a hydrophilic shell. CMs can be used as natural nanocarriers to deliver various molecules of interest. Although CMs are quite stable against heat, their structure is highly sensitive to ionic changes, especially at acid pH. An interesting method to stabilize casein structure consists on its cross-linking, by joining casein molecules through covalent bonds. In this context, the objective of the present work is first to investigate the stability of cross-linked CMs under different pH, dissociating agents, temperature, and ethanol conditions. Then, verify their potential use as nanocarrier for entrapped cyanidine-3-O-glucoside (C3G), an anthocyanin present in several Brazilian's fruits, that shows diverse bioactive properties in acid conditions. Two cross-linking agents were evaluated: genipin (GP) and transglutaminase (Tgase). We present a comparative study of the stability between native CMs and CMs cross-linked with GP or Tgase as a function of pH. Stabilities at different temperatures and ethanol concentrations were investigated in a pH range between 7.0 – 2.0 and results showed that the cross-linking reaction stabilized CMs under the conditions tested. However, GP is not recognized as GRAS (safe for food applications) and further researches on toxicity would be required to implement their use as a food-grade cross-linker. For this reason, in the second part of our work, we focalize only on Tgase cross-linked CMs with perspectives of using it for food applications. Firstly we investigated on the possible interaction between casein molecules and C3G under acidic (pH 2.0) and neutral (pH 7.0) conditions. Then, the use of Tgase cross-linked CMs as nanocarrier for C3G at pH 2.0 and at pH 7.0 was explored. Binding constant as well as driving forces at different pH values were determined by thermodynamic analysis at different temperatures. At pH 2.0,

hydrophobic association drive the interactions between caseins and C3G, whereas at pH 7.0, electrostatic interactions are the dominant binding forces. CMs Cross-linking by Tgase don't affect the interactions between C3G and caseins meaning it can be used as efficient nanocarriers for anthocyanins such as C3G under acid conditions.

## RESUMO

CASANOVA, Federico, D.Sc., Universidade Federal de Viçosa, março de 2017. **Estabilidade coloidal da micela de caseína nativa e reticulada e seu potencial uso como nanocarreador de cianidina-3-O-glicosídeo.** Orientador: Antônio Fernandes de Carvalho. Coorientador: Naaman Francisco Nogueira Silva, Italo Tuler Perrone e Paulo Cesar Stringheta.

Micelas de caseína (MCs) são estruturas supramoleculares naturais presentes no leite. Seu diâmetro hidrodinâmico médio é de 200 nm e apresenta um núcleo hidrofóbico e uma membrana hidrofílica. MCs podem ser usadas como nanocarreadores naturais para liberar várias moléculas de interesse. Apesar das MCs serem bastante estáveis ao calor, sua estrutura é altamente sensível a mudanças iônicas especialmente em pH ácido. Um interessante método para estabilizar a estrutura da caseína consiste na sua reticulação pela união de moléculas de caseínas por meio de ligações covalentes. Neste contexto, o objetivo desse presente trabalho é investigar a estabilidade de MCs reticuladas sob diferentes pHs, agentes dissociadores, temperatura e condições alcólicas. Assim, verificar o seu potencial como nanocarreador para aprisionar cianidina-3-O-glicosídeo (C3G), um antocianina presente em várias frutas brasileiras que apresenta diversificada propriedade bioativa em condições ácidas. Dois agentes reticuladores foram avaliados: genipina (GP) e transglutaminase (Tgase). Nós apresentamos um estudo comparativo da estabilidade entre MCs nativas e MCs reticuladas com GP ou Tgase em função do pH. A estabilidade em diferentes temperaturas e concentrações de etanol foram investigadas em uma faixa de pH entre 2,0 - 7,0 e os resultados apresentaram que a reação de reticulação estabilizou as MCs sob as condições testadas. No entanto, GP não é reconhecida como GRAS (segura para aplicação em alimentos) a pesquisas adicionais sobre sua toxicidade devem ser requeridas para implementar o seu uso como reticulador em alimentos. Por essa razão, na segunda parte do nosso trabalho, nós restringimos somente nas MCs reticuladas com Tgase com a perspectiva do seu uso em aplicações alimentícias. Primeiramente nós investigamos sobre a possibilidade de interação



entre as moléculas de caseína e C3G em condições ácida (pH 2,0) e neutra (pH 7,0). Desta forma, o uso de MCs reticuladas por Tgase como nanocarreadores de C3G a pH 2,0 e a pH 7,0 foram exploradas. A constante de ligação tão bem quanto as forças dirigentes a diferentes valores de pH foram determinadas por meio de análises termodinâmicas a diferentes temperaturas. A pH 2,0, a associação hidrofóbica dirigiu as interações entre a caseína e C3G, enquanto a pH 7,0, as interações eletrostáticas são as forças dirigentes dominantes. MCs reticulada com Tgase não afeta as interações entre C3G e as caseínas significando que elas podem ser usadas como eficientes nanocarreadores para antocianinas como a C3G em condições ácidas.

## **1. GENERAL INTRODUCTION**

According to the Food and Agriculture Organization of the United Nations, in the last three decades, world milk production has increased by more than 50 percent, from 500 million tons in 1983 to 769 million tons in 2013. India is the world's largest milk producer, with 18 percent of global production, followed by the United States of America, China, Pakistan and Brazil whereas the countries with the highest milk surpluses are New Zealand, United States of America, Germany, France, Australia and Ireland.

Milk can make a significant contribution to the required nutrient intakes for protein, lipid, calcium, magnesium, selenium, riboflavin, vitamin B12 and pantothenic acid. Milk and milk products are nutrient-dense foods and their consumption can add diversity to plant-based diets.

Milk processing can produce a wide range of milk products such as liquid and fermented milks, cheeses, butter and ghee, condensed and evaporated milks, milk powder, cream, whey products and casein. Casein is the principal protein in bovine milk (approximately 80% of the total milk protein) and is used as an ingredient in several products, including cheese, bakery products, paints and glues. It is extracted from skimmed milk by precipitation with rennet or by harmless lactic acid-producing bacteria. The singularity of caseins is their ability of self-assembly in the presence of calcium and phosphate into micelles, called casein micelles (CMs). CMs are porous, highly hydrated supramolecular structures, with a mean diameter of about 200 nm. The caseins are assembled in such a way they have a hydrophobic core and a hydrophilic shell[1]. CMs are natural nano-capsules to deliver nutrients, such as calcium and phosphate to the neonate [2]. CMs are unique in nature, and its supramolecular organization is in equilibrium with the surrounding medium. Only in the last 10 years, they are employed as a versatile, cheap and raw materials for the development of natural nanocarrier with applications in food and pharmaceutical area. However, physico-chemical conditions and processes, such as temperature, high pressure, alkalisation or acidification, and addition of chelators can affect their colloidal stability[3]. Therefore, stabilisation of CMs against the above stresses would improve their use as nanocarrier for molecules of interest and widen their spectra of utilisation. According to the literature a possible way to increase their stability is their cross-linking by natural agents, such as genipin or transglutaminase[4][5].

In recent years, several groups of molecules such as antioxidants, probiotics, fatty acids and vitamins present in the fruits, have received increasing attention for their health-promoting activities. Actually, one of the main challenge in academic and industrial research is (1) to protect the properties of the active molecule until the time of consumption and (2) to deliver it to the physiological target within the organism.

Brazil is one of the three major fruit producers in the world. Native and/or exotic Brazilian fruits have great nutritional and economic potentials. Among the Brazilian fruits, Amazon açai [6] and jaboticaba [7], naturally present in several Brazilian areas, show high antioxidant activity due to the presence of anthocyanins. A typical representative anthocyanin in these fruits is cyanidin-3-O-glucoside (C3G), represent in Schema 1.

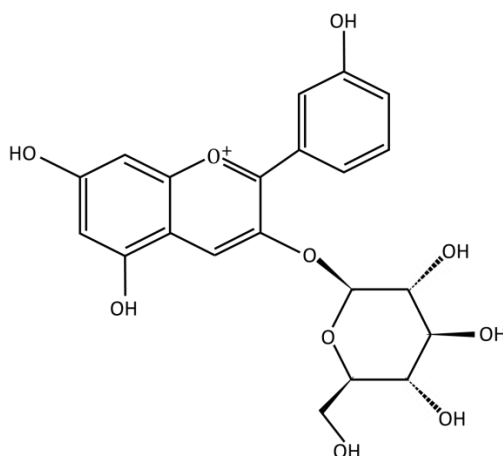


**Figure 1: Chemical structure of cyanidin-3-O-glucoside**

In recent decades, interest in this molecule has been growing in the scientific community due to recent evidence of their beneficial effects on health. Numerous publications have reported the wellness properties of anthocyanins: vasoprotective [8], anti-inflammatory [9], anticancer [10], antimicrobial [11] and antidiabetic effects [12]. Anthocyanins are quite sensitive to environmental conditions, which may decrease their bioavailability. pH is the main factor that affects the stability of C3G. They are stable between pH 2 – 3 [13] and unstable between pH 6 – 8 [14], causing a reduction of its bioavailability. Other factors that influence the stability of

anthocyanins, are ionic strength, UV light, oxygen, temperature and the presence of other solutes [15]. Therefore, the formulation of processed food products delivering the active form of the anthocyanins is a real challenge.

The objective of the present work is to study the potential cross-linked CMs as potential nanocarrier for C3G in acid and neutral pH conditions. In this context, we analyzed, in the first part of this work, the behaviour of cross-linked CMs in acid conditions. Then, in the second part, we investigated on the mechanism of interactions between cross-linked CMs and C3G.

This document is divided in 3 sections:

- **Review of literature** section presents an overview on the analytical techniques employed to characterize the interactions between caseins in different states (monomer, aggregates and supramolecular states) and molecules of interest in food and pharmaceutical applications. A discussion on the major advances on the interactions between caseins and molecules of interest is presented. Part of this chapter is under preparation for a submission in *Journal of Control Release* as “Interaction between casein and interest molecules: a review”.

- **Results and Discussion section** is divided into two parts (PART A and PART B), each divided into two chapters (chapters 4.1 – 4.2 for PART A and 4.3 – 4.4 for PART B).

#### PART A

The paragraph (4.1) presents the stability of the casein micelles cross-linked with genipin as a function of pH. These results are published in *International Dairy Journal* as “Stability of casein micelles cross-linked with genipin: a physicochemical study as a function of pH”.

The paragraph (4.2) presents the stability of the casein micelles cross-linked with transglutaminase as a function of pH. This paper is under revision for a publication in *LWT – Food Science and Technology* as “Casein micelles cross-linked with transglutaminase: stability under stress conditions as a function of acid pH”.

#### PART B

The paragraph (4.3) presents a study on the interactions between casein molecules and cyanidin-3-O-glucoside analyzed by fluorescence spectroscopy and dynamic light scattering. This paper is under revision for a publication in *Food Chemistry* as “Interaction of cyanidin-3-O-glucoside with sodium caseinate”.

The paragraph (4.4) describe the results on cross-linked casein micelles with transglutaminase for using it as nanocarrier for cyanidin-3-O-glucoside. The interactions are characterized at different temperatures by fluorescence spectroscopy and dynamic light scattering. This paper is under revision for a publication “Interaction between transglutaminase cross-linked casein micelles and cyanidin-3-O-glucoside”.

- General conclusions and perspectives in food or pharmaceutical applications are presented at the end of the manuscript.

## **2. LITERATURE REVIEW**

## 2.1 Interaction between casein and interest molecules: a review

The content of this chapter is under preparation for submission to:

*Journal of Control Release.*

Federico Casanova, Naaman F. N. Silva, Antonio F. Carvalho, Frédéric Gaucheron

This review was realized in collaboration with Frédéric Gaucheron during my visiting as  
Ph.D. student at INRA-STLO (Rennes, France)



### 2.1.1 Introduction

Several definitions are proposed to describe nanotechnology. For example, from the National Cancer Institute website, nanotechnology is a “technology development at the atomic, molecular or macromolecular range of approximately 1-100 nanometers to create and use structures, devices and systems that have novel properties”. For U.S. Food and Drug Administration (FDA) is a “technology that use engineered material or end product exhibits properties or phenomena, including physical or chemical properties or biological effects, that are attributable to its dimension(s), even if these dimensions fall outside the nanoscale range, up to one micrometer”.

Scientists work with nanoscience since more than a century, for example with bacteria, structure of DNA or blood cells. In food, “nano” has been part during all the time, since many foods, such as proteins structures, naturally exist at the nanoscale. In milk for example, casein micelles (with size ranged from 200 to 500 nm), whey proteins (with ranging in size from 1 to 10 nm) and fat globules (with ranging in size from 1 to 5  $\mu\text{m}$ ) can be considered as nanoparticles. However, only in the last years, nanotechnology in food science has known a growing interest. This was driven by the development of instrumentation and the availability of tools that (1) allow to scientists to see nanostructure that they were unable to see in the past and (2) find new ways of controlling and structuring foods with greater functionality and added value.

This chapter present, in the first part, the principal techniques employed to characterize the structure of nanoparticles and their interactions with interesting molecules. In the second part, a detailed overview on the last advanced concerning the interactions between casein as natural nanocarrier and interesting molecules is discussed. Finally, cross-linking is proposed as a possible way to increase their spectra of application in different physico-chemical conditions.

### 2.1.2 Physico-chemical methods to characterize nanoparticles

Understanding the fundamental interactions between biomolecules and nanoparticles is essential in nanoscience. Physico-chemical characteristics of nanomaterials such as size, surface composition, surface energy, and surface charge are important to understand their behavior in food or pharmaceuticals matrices for future *in vivo* and *in vitro* applications. Figure 2 presents an overview of the principal analytical

techniques used to characterize the structure of nanoparticles [16]. In the following paragraph, the principal advantages and disadvantages of some techniques are briefly commented.

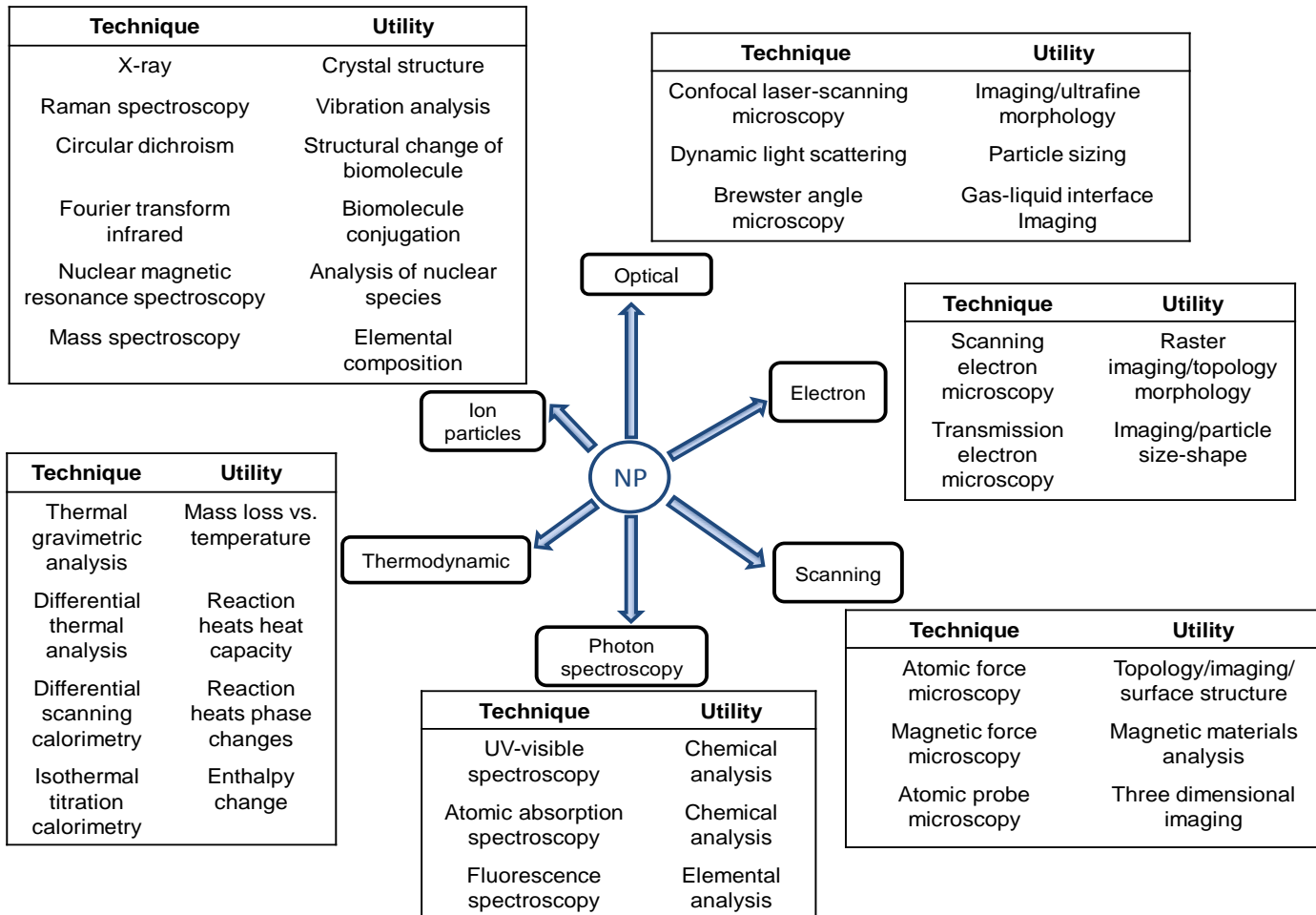


Figure 2: Outline of the main analytical techniques used to analyze nanoparticles (NP), from “Advancements in characterization techniques of nanoparticles and sophisticated instruments”, with modifications [17].

**Microscopies** - To determine the size distribution and the shape of nanomaterial, scanning and transmission electronic microscopies (SEM or TEM) are widely employed (Figure 3). These techniques provide direct images of nanomaterials with a precision of 1 nm. Observation of nanoparticle surface by atomic force microscopy (AFM) allows to analyze surface at sub-nanometer scale without causing appreciable damage of the sample.

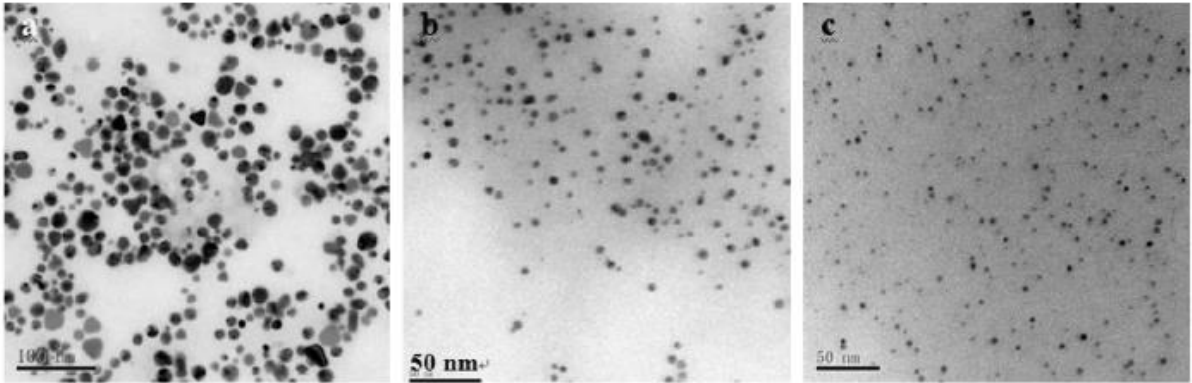
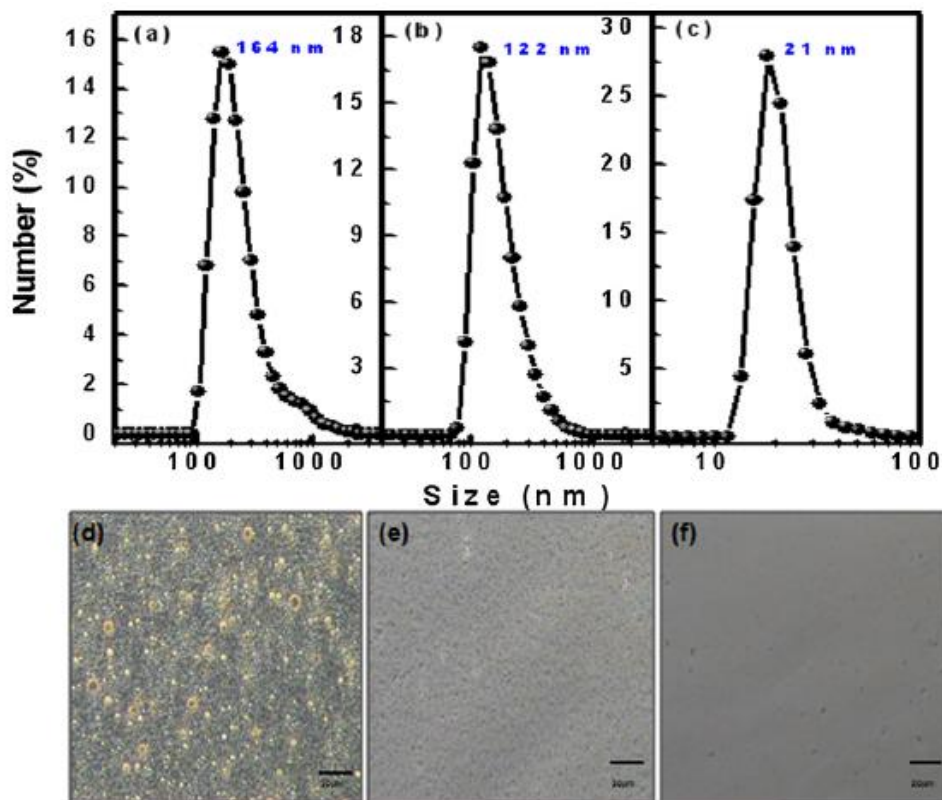


Figure 3: Example of TEM images (a)–(c) of gold samples obtained in casein solution at different concentration at pH 2.0 (from [18]).

**Spectroscopic methods** - Dynamic light scattering (DLS) is one of the most popular and non-invasive light scattering analysis to obtain informations about hydrodynamic size, structure and possible aggregation of nanomaterials (Figure 4). However this technique presents some disadvantages, such a restricted range of particle analysis (between 1 nm and 3  $\mu\text{m}$ ) and some difficulties to determine the size fractions in the presence of aggregates of different sizes.



**Figure 4: Example of hydrodynamic diameter measurements with corresponding microscopy images (from [19]).**

Raman scattering is used to characterize nanostructures with a submicron spatial resolution for light-transparent material without the requirement of sample preparation. This technique is employed for studying biological samples in aqueous solution. The behavior of biomolecules interacting with nanoparticles and the structure of drug-delivery nanocarriers can be investigated using circular dichroism (CD) [20]. This technique focuses on the characterization of the structure of the asymmetric molecule as a function of different absorptions of circularly polarized lights. To analyze biomolecule conjugation, for example conformational states of bound protein to nanoparticles surfaces, Fourier transform infrared (FTIR) is also employed. To obtain structural information at long-range order, for example the crystalline property, nuclear magnetic resonance (NMR) is commonly used to characterize the structures of amorphous materials, polymers and biomolecules.

Mass spectroscopy (MS) is an analytical technique employed to determine the elemental composition of bioconjugates nanomaterial and chemical structure of a

compound with a small quantity of sample ( $10^{-9}$  to  $10^{-21}$  mol). With a different X-ray spectroscopic techniques, we can resolve the tertiary structures of crystalline materials at the atomic scale and we can evaluate size, distribution, shape, orientation, and structure of a protein and protein-nanomaterial systems in solution [21]. Based on photon spectroscopy, UV–visible absorbance spectroscopy is utilized to investigate the concentration and aggregation of the sample. In parallel, fluorescence spectroscopy is used for evaluate the interaction between host (*i.e.* protein) and ligand (*i.e.* bioactive molecule), to obtain information on type of quenching, binding constant and number of binding sites. Different thermal techniques can be employed to obtain informations on the amount of nanomaterial conjugates.

**Thermodynamic methods-** Differential scanning calorimetry (DSC) is used to characterize melting, crystallization, glass transition and decomposition of nanomaterial. Isothermal titration calorimetry (ITC) can determine the affinity and enthalpy between nanomaterial and biomolecule. With a theoretical approach, molecular dynamics simulations is a complementary method to deep understanding these interactions. Simulation can been applied for exploring protein–surface binding mechanisms, determine binding constant, as well as the thermodynamics and kinetics of absorption.

**Separative methods** - Other routinely techniques are normally applied. Analytical ultracentrifugation, for example, can be used to incremented the investigation on conformation, structure, stoichiometry and self-aggregation state of nanomaterials. High performance liquid chromatography (HPLC) can be used to purify the nanomaterial conjugate. Gel electrophoresis and capillary electrophoresis can provide the relative and absolute hydrodynamic size and zeta potential of nanomaterial.

All these methods are complementary and contribute to a best understanding of the nanoparticle in interaction with other molecules.

### 2.1.3 Physico-chemical characteristics of casein

Actually, one of the major challenge in food or pharmaceutical formulations is the delivery of interesting molecules. This requires two mainly features (1) maintain the active molecular form (2) deliver this form to the physiological target in the organism. In this way, some proteins are excellent and cheap vehicles for bioactive material [22]. Food proteins based nanoparticles were used in formulated foods because they have high nutritional value and are generally recognized as safe [23]. The protein-based nanoparticles are known to be easy to prepare and their size distribution can be monitored. Milk contains several proteins with important functional properties, such as the abilities to bind hydrophobic or ionic molecules, to interact with other biopolymers, to stabilize emulsions, to form gels, and, to some extent, retard oxidation [24]. Because of these properties, milk proteins are an ideal material for entrapment and delivery of interesting molecules.

Caseins represent 76 – 86 % of total milk proteins and are the best studied food proteins [25]. Besides their primarily role as source of amino acids, they present the biological function of calcium vectors from mother to neonates, and avoid the pathological calcification of the mammary gland [26]. Caseins exhibit open and flexible conformations and are referred as rheomorphic proteins [25][27]. Their high proportions in proline residues prevent the formation globular structures [25]. There are four casein molecules called  $\alpha_{s1}$ ,  $\alpha_{s2}$ ,  $\beta$  and  $\kappa$ -caseins. These caseins contains different amino acid sequences and exhibit additional heterogeneity due to two post-translational modifications, namely phosphorylation and glycosylation especially for  $\kappa$ -casein [28]. Caseins present minimum solubility near the isoelectric points (pI) [29]. Temperature and pH affect the solubility of casein near their pI [30]. Due to their amphiphilic nature, caseins in aqueous solution have a tendency to self-assembly into casein micelles (CMs). CMs represent the most abundant proteins in cow milk. The proportion of casein molecules into CMs are respectively:  $\alpha_{s1}$  (30.1 wt%),  $\alpha_{s2}$  (10.2 wt%),  $\beta$  (35.7 wt%) and  $\kappa$ -caseins (12.8 wt%) [31]. Caseins represent ~94% of dry matter of CMs while the remaining 6 % corresponded to colloidal calcium phosphate (CCP) associated to small amounts of magnesium and citrate [25]. CMs have a porous structure that retains 4.5 g water / g protein [32]. They have a spherical form with an average diameter of about 200 nm [1] and molecular masses

between  $10^6$  and  $3 \times 10^9$  Da. They scatter the light and are mainly responsible for the white color of milk. The main characteristics of CMs are listed in table 1.

**Table 1: Average characteristics of CMs [25].**

<b>Characteristic</b>	<b>Value</b>
Diameter	130 – 160 nm
Surface	$8 \times 10^{-10} \text{ cm}^2$
Volume	$2.1 \times 10^{-15} \text{ cm}^3$
Density (hydrated)	$1.0632 \text{ g/cm}^3$
Mass	$2.2 \times 10^{-15} \text{ g}$
Water content	63%
Hydration	3.7 g H <sub>2</sub> O / g protein
Voluminosity	$4.4 \text{ cm}^3/\text{g}$
Molecular weight (hydrated)	$1.3 \times 10^9 \text{ Da}$
Molecular weight (dehydrated)	$5 \times 10^4 \text{ Da}$
Number of peptides chains (molecular weight : 30000 Da)	$10^4$
Number of particles per mL milk	$10^{14} - 10^{16}$
Whole surface of particle	$5 \times 10^4 \text{ cm}^2/\text{mL milk}$
Mean free distance	240 nm

#### **2.1.4 Physico-chemical interactions between casein and interesting molecules**

The studies described in this section were principally performed with (1) purified casein molecules, (2) sodium caseinate (NaCas), (3) reassembled casein micelles (rCMs), (4) native casein micelles (CMs) also named native phosphocaseinate or (5) casein nanoparticles obtained according to [33][34][35]. Schematically, these different casein systems are completely different in terms of composition (especially their casein and mineral contents), size and surface properties. These differences are due to the methods of preparation/purification. This methodology is necessary to eliminate the majorities of components of the soluble phase of milk (minerals, whey proteins, peptides, lactose...) with the aim to understand the mechanism of interaction between host-ligand. With purified system, binding constants, number of binding sites as well as dynamic or static quenching can be determined.

##### **2.1.4.1 Vitamins**

Vitamins are essential molecules for life. Human organism is not able to synthesize them and food is one of the main source of these molecules. However, some of these vitamins are sensitive to different conditions such as light, oxygen, and temperature. Due to these sensitivities inducing losses of their activities, it is interesting and necessary to protect them. Different methodologies are proposed and one is the encapsulation/interaction between casein and some vitamins especially hydrophobic.

Semo *et al.* [2] proposed CMs as nanovehicle for hydrophobic molecules. CMs were constituted according to a procedure developed by Knoop, and Wiechen [36]. The authors incorporated lipophilic vitamin D<sub>2</sub> into the hydrophobic core of rCMs and showed that rCMs stabilized the vitamin D<sub>2</sub> (27% of the vitamin recovered from the micelle suspension was found in rCMs) and provided protection against UV-light degradation.

With a different experimental approach using high pressure, Menéndez-Aguirre *et al* [37][38] incorporated vitamin D<sub>2</sub> in CMs. In this work, native CMs were treated with vitamin D<sub>2</sub> at different hydrostatical pressures (0.1, 200, 400, and 600 MPa) and temperatures (10-50 °C) in order to increase interaction between the different compound and consequently load the vitamin. This process allowed to have casein micelles with an average hydrodynamic diameter of  $272 \pm 10$  nm, with hydrophobic compounds in their structures. The authors concluded that the loading of vitamin D<sub>2</sub> per casein increased from  $2.2 \pm 0.2$  µg/mg (native CMs) to  $10.4 \pm 0.2$  µg/mg (rCMs). Next, the bioavailability of encapsulated vitamin D<sub>3</sub> was confirmed with a clinical trial with 87 human volunteers. Results showed that (a) rCMs is mixed as Tween-80 (a synthetic emulsifier used for vitamin solubilization) (b) rCMs could be used to promote stability and bioavailability vitamin D<sub>3</sub>[39]. More recently, enriched fat-free yogurt with vitamin D<sub>3</sub> loaded into either rCMs or Polysorbate-80 were compared [40]. *In vivo* bioavailability of vitamin D<sub>3</sub> was evaluated by clinical trial. No significant difference was observed. These results complemented the study proposed by Haham *et al.* [39] showing higher protection against thermal treatment, UV irradiation, and deterioration during shelf-life. This suggests the advantageous use of rCMs against the synthetic emulsifier as a delivery system for the enrichment of food with vitamin D<sub>3</sub> and other hydrophobic nutraceuticals.



Penalva et al. [41] prepared casein nanoparticles for the oral delivery of folic acid (vitamin B9). These nanoparticles were prepared by a coacervation process, stabilized with either lysine or arginine and, finally, spray-dried. Nanoparticles have a mean diameter close to 150 nm and a folic acid content of 25 µg per mg nanoparticle. *In vitro* and *in vivo* release studies showed that the oral bioavailability of folic acid, when it was administered associated to casein nanoparticles was around 52% *i.e* 50% higher than free in aqueous solution.

By different analytical methods (FTIR, UV–visible, fluorescence spectroscopic methods and molecular modelling), Bourassa et al. [42] studied the interaction between vitamin A and α- and β-caseins. The authors showed that both hydrophilic and hydrophobic interactions were mainly responsible for the formation of new complex with binding constants of the complex comprised between  $10^5$  and  $10^4$  M<sup>-1</sup> and a number of bound vitamin molecules per protein (n) equal to 1.5 (±0.1). At industrial scale, Chevalier-Lucia et al. [43] showed that ultra-high pressure homogenization (≥ 200 MPa) allowed the interaction between CMs and α-tocopherol acetate (Vitamin E), an antioxidant able to bind free radicals in cell membranes and other lipids preventing therefore oils from rancidity during storage [44]. The possibility to use this technique in an industrial continuous flow was highlighted but further studies seemed necessary to evaluate the stability of CMs-vitamin E during storage. β-caroten is a carotenoid usually applied in the food industry as a precursor of vitamin A or as a colorant. This molecule is easily degraded by light, heat and oxygen. Recently, Sáiz-Abajo et al. [45] and Jarunglumlert et al. [46] to avoid this problem applied high hydrostatic pressure processing and spray-dried to encapsulate β-caroten in rCMs *via* hydrophobic interactions. rCMs protected β-caroten from degradation during heat stabilisation or storage, high pressure processing and the most commonly processes used in the food industry (sterilization, pasteurization) including baking. This opens new possibilities for introducing thermolabile ingredients in bakery products.

#### **2.1.4.2 Polyphenols**

Polyphenolic compounds are used in a wide range of pharmacological due to their antioxidant, anti-inflammatory, antimicrobial, antiamyloid, and antitumor properties.

The major problem of polyphenol is (a) their extremely low solubility in aqueous solution, which can be caused poor bioavailability and limits its clinical efficacy (*i.e.* curcumin); (b) their low stability against pH, light, temperature (*i.e.* anthocyanins). One possible way to increase their solubility or maintain their stability until consumption is their interaction and encapsulation in proteins.

A number of relevant studies have been focused on the entrapment of curcumin, an hydrophobic anticancer drug, into casein as nanoparticles [47][48][49][50][51][52][53][54][55]. Curcumin (diferuloylmethane) is a natural polyphenol isolated from the rhizome of turmeric (*Curcuma longa*). It has a low intrinsic toxicity and a wide range of pharmacological activities including antioxidant, anti-inflammatory, antimicrobial, antiamyloid, antitumor and anticancer properties [56][57]. Curcumin interacts with low polar regions of CMs. The main problem of curcumin as anticancer drug is their extremely low aqueous solubility which causes low bioavailability and clinical efficacy. Encapsulation in CasNa, using spray drying process, increase their solubility [52]. Otherwise, encapsulation in  $\beta$ -CMs increased its aqueous solubility around 2500 folds [51].

In 2013, Mehranfar et al. [55] investigated the interaction between diacetylcurcumin (DAC), a synthetic derivative of curcumin, with bovine  $\beta$ -casein using fluorescence quenching experiments, Forster energy transfer measurements and molecular docking calculations. DAC showed higher antibacterial activity and formed a complex with  $\beta$ -casein with relatively high affinity (binding constant value equals to  $4.40 \times 10^4 \text{ M}^{-1}$ ). *In vitro* studies indicated a high cytotoxicity of  $\beta$ -casein-DAC against MCF-7 breast cancer cells compared to individual DAC doses. Although further studies are necessary to explore the molecular mechanism of the reaction,  $\beta$ -casein-DAC is proposed as an easily accepted, economically, viable and safe drug. To improve microbiological safety and quality of foods, Li et al [58] produced zein-Na caseinate nanoparticle - based films, for food packaging applications, to load thymol, an antimicrobial agent, against *Escherichia coli* and *Salmonella*. The complex was prepared under continuous stirring and antimicrobial assay was conducted by contact of the film on agar surface diffusion assay. The authors suggested the use of this film as inner packaging for foods such as the flavoring of instant noodles in view of their antimicrobial activities.

In another study, Pan et al. [59] encapsulated thymol, in Na caseinate nanoparticles using high shear homogenization at pH 6.8. This complex, showed stability during 30-days storage at room temperature. The encapsulated thymol significantly improved anti-Listerial activity in milk with different fat levels when compared to thymol crystal. To have a better understanding of the behavior and characteristics of caseins, Zhou et al. [60], investigated the interactions between caseins and phenolic acids (*i.e* protocatechuic acid or *p*-coumaric acid), such as the ones present in chocolate. Electrophoresis results revealed that casein *p*-coumaric acid interactions were induced by incubation at 55 °C. According to the authors, *in vitro* hydrolysis using trypsin of casein control, casein–protocatechuic acid, casein-*p*-coumaric acid, caseins isolated from milk chocolate and white chocolate showed degree of hydrolysis of 19.3, 18.6, 17.7, 10.4 and 17.8% respectively. The presence of protocatechuic acid and *p*-coumaric acid in the model system and the presence of phenolic compounds in milk chocolate, in addition to the structural changes occurring during processing, affected the peptide profiles of casein hydrolysates. To prevent oxidation and to ensure thermal and photo stability of malvidin-3-O-glucoside, the major anthocyanin in grape skin anthocyanin extract, He et al. [61] investigated by different analytical methods the positive addition of  $\alpha$ - and  $\beta$ -caseins. The results showed that  $\alpha$ - and  $\beta$ -caseins bound with malvidin-3-O-glucoside *via* hydrophilic (van der Waals forces or hydrogen bonding) and hydrophobic interactions, respectively, with strong binding affinity ( $\sim 10^3 \text{ M}^{-1}$ ).

With a physico-chemical approach, Ye et al. [62] studied the affinity of black and green tea polyphenols with CMs and whey proteins. According to the authors, Fourier Transforms InfraRed Spectroscopy (FT-IR) analysis showed that tea polyphenols altered the secondary structures. Hydrophobic interactions drive the binding between proteins and tea polyphenols. Others studies present a characterization of interactions at a molecular level between gallic acid (EGCG) with  $\alpha$ - and  $\beta$ -caseins [63][64][65][66][67]. FT-IR, UV–visible, circular dichroism, fluorescence spectroscopic methods as well as molecular modelling were employed to determine the binding constant and the effects of polyphenol complexation on casein stability. The level of bioefficacy of this complex, against colon cancer cell HT-29, was also investigated. Results showed that EGCG was able to bind casein *via* both hydrophilic and

hydrophobic interactions. Binding constant between CMs and EGCG was calculated between  $10^{-4}$  and  $10^{-3} \text{ M}^{-1}$ . The binding would not affect the bioaccessibility of EGCG and *in vitro* digestion model showed a decrease in proliferation of cancer cells without reduce their bioavailability, confirming that CMs are an appropriate delivery system of polyphenols [68][69][70]. Flavonoids, from *Phaleria macrocarpa* from Papua Island, were encapsulated in CMs with a homogenizer followed by sonication. The sample was separated by ultra-filtration system and created nanoparticles. Encapsulations capacity of the CM was about one milligram flavonoids per gram of CMs. According to the authors, CMs can be employed as potential nanovehicle for the *Phaleria macrocarpa* extract [71]. Mehranfar et al. [72] studied, by molecular docking calculations, molecular dynamics simulation and different spectral methods, the interactions between flavonol quercetin, a free radical scavenger and a metal chelator, and  $\beta$ -casein nanoparticles. According to the authors, the negative values of entropy and enthalpy changes represented the predominate role of hydrogen binding and van der Waals interactions in the binding process. Docking calculations showed the probable binding site of quercetin was located in the hydrophobic core of  $\beta$ -casein. Furthermore, molecular dynamic simulation results suggested that this flavonoid could interact with  $\beta$ -casein, without affecting the secondary structure of  $\beta$ -casein. Interactions between naringenin, a nutraceutical flavonoid present in tomato and citrus fruits and  $\beta$ -casein was investigated using fluorescence quenching spectroscopy [73]. Binding constant was calculated at  $10^5 \text{ M}^{-1}$ . Thermodynamic analysis showed that the interaction was spontaneous with van der Waals forces, hydrogen bonds and hydrophobic interactions that played the main roles in the binding process. Ferraro et al. [74] by using optical and thermodynamic methods studied the interactions between rosmarinic acid and bovine milk casein. Chromatography techniques, dynamic light scattering (DLS), zeta-potential, FT-IR and DSC were used for the screening the interactions at 0, 3 and 24 h of storage time and at 4 °C. Interactions were assessed at the pH of the complexes in water, 6.8, and at acidic pH 3 and 4.5. Interactions was mainly hydrophobic and hydrogen and favoured at pH comprise between 3 and 4.5.

#### 2.1.4.3 Omega-3 polyunsaturated fatty acids

Hydrophobic compounds, like fat-soluble vitamins and essential fatty acids are highly sensitive to oxidation, and thus require stabilization in an aqueous medium and protection against deteriorating factors. The formation of nanocarrier for the delivery of hydrophobic nutraceuticals has been shown to facilitate their dissolution and protection. To enrich foods and beverages for promoting health of wide populations, Zimet et al. [75] demonstrated that rCMs can be used as a potential effective ways to protect and deliver omega-3 polyunsaturated fatty acids, such as docosahexaenoic acid (DHA), an important nutraceutical lipid, providing protection against cardiovascular and the metabolic syndrome. Using fluorescence spectroscopy, the authors showed that rCMs can bind DHA with a relative high affinity ( $\sim 10^6 \text{ M}^{-1}$ ). DLS particle characterization experiments showed the formation of nanoparticles upon addition of DHA (pre-dissolved in ethanol) to a casein solution. When rCMs-DHA suspensions were prepared at 4 °C, a size of 50-60 nm was determined. No significant effect of the thermal treatment (74 °C, 20 s) on particle size was observed. rCMs showed a remarkable protective effect against DHA oxidation, demonstrating good colloidal stability and bioactive conservation.

#### 2.1.4.4 Minerals

It is admitted that calcium interacts with casein molecules *via* the phosphoseryl residues present in the sequences of the different casein molecules. In milk, the situation is more complex because calcium is bound to casein by forming nanoclusters constituted of calcium and inorganic phosphate. In spite of the presence of minerals in dairy products, addition of supplementary minerals to dairy matrices is way to improve functional, technological and nutritional properties. CasNa or CMs enriched with iron and / or other minerals (zinc, copper, magnesium, manganese,...) in required quantities to the consumer were proposed by different authors [76][77][78][79]. However, further steps are necessary to evaluate the benefits and the bioavailability of these fortified food matrices. With another interest, the adsorption properties of some oxide minerals such as sepiolite and kaolinite and

expanded and unexpanded perlites minerals on casein were investigated [80]. These minerals are excellent filter aids and fillers in various process and materials. By using Langmuir and Freundlich isotherm models, the adsorption of casein increases with temperature from 15 to 45 °C and with ionic strength of the solutions over the range of 0.0 to 0.1 mol L<sup>-1</sup>. The adsorption decreased with increasing pH from 7.0 to 11.0 and the concentration of phosphate ions from 0.02 to 0.10 mol L<sup>-1</sup>.

Pomastowski et al. [81] studied the kinetics of zinc ions binding to the casein protein. Casein were characterized with the use of capillary electrophoresis, zeta potential analysis, field flow fractionation technique and FT-IR respectively. The kinetics of the metal-binding process was investigated in batch adsorption experiments. Results showed that the kinetic process of zinc binding to casein was not homogeneous with an initial rapid stage with about 70% of zinc ions immobilized by casein and with a much slower second step. Maximum amount of bound zinc in the experimental conditions was 30.04 mg Zn/g casein.

#### 2.1.4.5 Lipids

Only in the last three years, few studies were published on the interactions between lipids and casein. The structural characterization of the interaction between milk caseins and lipids is of a major importance in elucidating the nature of the lipid association with milk proteins and the possibility of lipid transportation by caseins. Bourassa et al. [82] studied the nature of association between cholesterol, 1,2-dioleoyl-3-trimethylammonium-propane, dioctadecyldimethyl-ammoniumbromide and dioleoylphosphatidylethanolamine with  $\alpha$ - and  $\beta$ -caseins by FT-IR, fluorescence spectroscopic methods, circular dichroism and molecular modeling. Structural analysis showed that lipids bind casein *via* mainly hydrophobic interactions with association constants comprised between 10<sup>4</sup> and 10<sup>3</sup> M<sup>-1</sup>. The average number of binding sites occupied by lipid molecules on protein (n) were from 0.7 to 1.1. Docking showed different binding sites for  $\alpha$ - and  $\beta$ -caseins with lipid complexation with the free binding energies from -10 to -13 kcal/mol.

Cheema et al. [83] studied the association of low molecular weight hydrophobic compounds (including phosphatidylcholine, lyso-phosphatidylcholine, phosphatidylethanolamine, and sphingomyelin) with CMs. The main contribution of

this study lies in the identification of hydrophobic compounds associated with CMs in their native form by using liquid chromatography-tandem mass spectrometry. According to the authors, hydrophobic compounds were preferentially associated with native CMs in raw bovine milk, rather than to whey protein and PFS (protein free serum) fractions. In contrast, hydrophilic compounds were found to be uniformly distributed among the CMs, whey protein, and PFS pooled fractions. These observations support the hypothesis that CMs have natural affinity toward hydrophobic compounds in their native state.

More recently, Semenova et al. [84] investigated, by different techniques (differential scanning calorimetry, electron spin resonance spectroscopy and small angle X-ray scattering), the impact of polyunsaturated soy phospholipids on covalent conjugates combining sodium caseinate with maltodextrins. Results supported the hypothesis that sodium caseinate play an important role as hydrophobic bioactive compound carriers in addition to their other biological functions.

**Table 2: Casein-based nanoparticles as nanocarriers in food applications (rCMs = reassembled casein micelles; CMs = native casein micelles; NaCas= sodium caseinate).**

Group	Molecule	Nanocarrier	Constant association	Techniques	Ref.	
vitamins	vitamin D <sub>2</sub>	CMs		HPLC	[2]	
				UV-Vis		
				spectroscopic		
				HPLC		
	vitamin D <sub>3</sub>	rCMs			HPLC	[38]
					HPLC	[37]
	vitamin B9 (folic acid)	NaCas			DLS	[39]
					HPLC	
vitamin A	α- and β-caseins		1.2x10 <sup>5</sup> M <sup>-1</sup> 1.1x10 <sup>5</sup> M <sup>-1</sup>	HPLC	[41]	
				DLS		
vitamin E	CMs			FTIR – CD - Fluorescence spectroscopy	[42]	
				DLS		
β-Carotene	rCMs	rCMs		DLS	[43]	
				TEM	[45]	
				X-ray scattering	[46]	

polyphenols	curcumin	CMs	1.5x10 <sup>4</sup> M <sup>-1</sup>	Fluorescence spectroscopy	[18]
				Fluorescence spectroscopy	[48]
			5.6x10 <sup>4</sup> M <sup>-1</sup>	Fluorescence spectroscopy DLS	[49]
		from 0.6x10 <sup>4</sup> M <sup>-1</sup> to 6.6x10 <sup>4</sup> M <sup>-1</sup>	Fluorescence spectroscopy DLS X-ray scattering	[50]	
		β-casein	1.8x10 <sup>4</sup> M <sup>-1</sup>	Fluorescence spectroscopy UV-Vis spectroscopic	[51]
			NaCas		AFM DSC X-ray diffraction
	α- and β-casein	from 1.9x10 <sup>4</sup> M <sup>-1</sup> to 3.1x10 <sup>4</sup> M <sup>-1</sup>		Fluorescence spectroscopy FTIR FTIR CD	[53]
		NaCas		Fluorescence spectroscopy DLS NMR TEM UV-Vis spectroscopic	[54]
	diacetylcurcumin	β-casein	4.4x10 <sup>4</sup> M <sup>-1</sup>	Fluorescence spectroscopy Molecular simulation	[55]
	thymol	NaCas - Zein		DLS AFM	[58]
		NaCas		DLS AFM	[59]
	coumaric acids malvidin-3-O-	casein		Fluorescence spectroscopy HPLC	[60]
α- and β-		0.5x10 <sup>3</sup> M <sup>-1</sup>	Fluorescence	[61]	



glucoside	casein	$0.4 \times 10^3 \text{ M}^{-1}$	spectroscopy FTIR CD	
Green and black tea	CMs and whey protein		Fluorescence spectroscopy UV-Vis spectroscopic FTIR	[62]
Tea polyphenols	$\alpha$ - and $\beta$ -casein	From $1.8 \times 10^3 \text{ M}^{-1}$ to $1.6 \times 10^4 \text{ M}^{-1}$	Fluorescence spectroscopy FTIR Molecular simulation	[63]
		From $1.0 \times 10^3 \text{ M}^{-1}$ to $3.0 \times 10^4 \text{ M}^{-1}$	Fluorescence spectroscopy HPLC	[64]
	Casein $\beta$ -casein Casein	From $3.6 \times 10^3 \text{ M}^{-1}$ to $9.3 \times 10^3 \text{ M}^{-1}$	Electrophoresis AFM DLS TEM Fluorescence spectroscopy	[65] [66] [67]
	$\alpha$ - and $\beta$ -casein			[68](a)
		From $6.5 \times 10^3 \text{ M}^{-1}$ to $2.7 \times 10^4 \text{ M}^{-1}$	HPLC	[69](b) [70](c)
phaleria macrocarpa flavonoids quercitin	CMs		DLS	[42]
naringenin	$\beta$ -casein		Molecular simulation UV-Vis spectroscopic	[72]
	$\beta$ -casein	$3.2 \times 10^5 \text{ M}^{-1}$	Fluorescence spectroscopy DLS FTIR DSC DLS	[73] [74]
rosmarinic acid	$\alpha$ - $\beta$ -K-casein			
<b>fatty acids</b>	omega-3	rCMs	$8.4 \times 10^6 \text{ M}^{-1}$	Fluorescence spectroscopy [75]

					DLS
<b>minerals</b>	Fe	NaCas			[76]
		CMs			[77]
		NaCas		DLS	[78]
	Fe; Zn;Ca;Cu; Mg sepiolite, kaolinite, expanded and unexpanded perlites Zn	CMs casein		NMR DLS FTIR	[79] [80]
	Zn	casein		DLS FTIR	[81]
<b>lipids</b>	CHOL, DOTAP, DDAB, DOPE	$\alpha$ - and $\beta$ - caseins	From $5.0 \times 10^3 \text{ M}^{-1}$ to $2.1 \times 10^4 \text{ M}^{-1}$	Fluorescence Spectroscopy FTIR Molecular simulation	[82]
	phosphatidylcholine, lyso- phosphatidylcholine, phosphatidylethanolamine, and sphingomyelin, soy phospholipids	CMs		SDS-PAGE Mass spectroscopy	[83]
		NaCas		DSC Static and dynamic light scattering X-ray scattering	[84]

#### 2.1.4.6 Anticancer drugs

The research of protein and nanoparticles interactions as drug carriers, has substantially expanded in the past decade due to nanotechnology contributions in nanomedicine [85]. Casein based nanocarrier can be deliver high concentrations of cytotoxic drugs reducing the agent's side effects on the rest of the body.

Elzoghby et al. [86] published an exhaustive review on protein nanoparticles as potential vehicles for anticancer drugs, with an overview on casein based nanoparticles (Table 4). According to the authors, hydrophobic anticancer drugs can be loaded in casein nanoparticles in two main steps: solubilization of interesting

molecule in organic solvent (e.g. ethanol) with addition of aqueous micellar suspension, followed, in a second step, by solvent evaporation or dialysis to remove the residual solvent. The other advantage is that casein and especially  $\beta$ -casein is highly digestible [86].

$\beta$ -casein was used as nanocarrier for solubilization of several hydrophobic anticancer drugs such as celecoxib [87][88], mitoxantrone [89], docetaxel, paclitaxel [90] and flutamide [91][92][93][94]. All these drugs have a low solubility in water. Incorporation into the hydrophobic core of casein nanoparticles allowing them to be thermodynamically stable in aqueous solutions and used for oral-delivery applications. Further, the gastric digestibility of  $\beta$ -casein was suggested as a possible targeting mechanism for stomach cancer. Their structure is easily digested providing an excellent target-activated release mechanism for unloading the drug in the stomach [86].

Razmi et al. [95] proposed a novel platinum complex (used in chemotherapy treatment) within nanoparticles composed of  $\beta$ -casein and chitosan. The authors obtained nanoparticles with size ranged between 200 and 300 nm. Results indicated also that cytotoxicity against cell line (HCT-116) and cellular uptake of platinum were limited by its entrapment in  $\beta$ -casein nanovehicles. The authors suggested that this novel drug-delivery system was stable in aqueous solutions and potentially useful for targeted oral-delivery applications.

Sequential release of both hydrophobic and hydrophilic anticancer drugs was proposed by Narayanan et al. [96]. A simple emulsion-precipitation was prepared to obtain monodisperse nanoparticles of poly-L-lactide-co-glycolic acid (PLGA)-casein polymer with paclitaxel in the core and epigallocatechin gallate (EGCG) in the shell. The use of casein for encapsulating EGCG can be justified by the affinity of EGCG toward proline, whereas the hydrophobic paclitaxel could be associated with PLGA (poly-L-lactide-co-glycolic acid). The objective of the authors was that an early release of EGCG to increase the sensitivity of paclitaxel to cancer, thereby providing improved therapeutics at lower concentrations, with less toxicity. *In vivo* pharmacokinetic studies in rats revealed a sustained and sequential release of both the drug in plasma: paclitaxel releasing 28% and EGCG releasing 60% of the total entrapped drugs in 10 days.

Acharya et al. [97] proposed sodium caseinate as nanocarrier of resveratrol which is insoluble in both water and oils. Binding constants for the complex was calculated at  $10^5 \text{ M}^{-1}$  with a prevalence of hydrogen bonding and hydrophobic interaction.

Zhen et al. [98], to improve tumor penetration, proposed cispatin-loaded casein nanoparticles cross-linked by transglutaminase. The authors employed a natural cross-linker, transglutaminase to replace glutaraldehyde, which commonly used but toxic. Transglutaminase significantly decreased the size of casein particles and improve the particle stability in various pH media. Then, the penetration of the casein nanoparticles in two-dimensional monolayer cells and three-dimensional multicellular tumor spheroids was investigated. Cispatin-loaded casein nanoparticles have the capabilities to penetrate cell membrane barriers, target tumor and inhibit tumor growth. According to the authors, the tumor growth inhibition of cispatin-loaded nanoparticles was 1.5-fold higher than that of free cispatin.

**Table 3: Casein as nanocarriers for anticancer drugs.**

Group	Molecule	Nanocarrier	Constant association	Techniques	Ref.
Anti-cancer drug	celecoxib	$\beta$ -casein		DLS TEM	[87]
				X-ray diffraction X-ray scattering	[88]
				NMR TEM	
	paclitaxel docetaxel mitoxantrone	$\beta$ -casein		DLS	[89]
				Fluorescence spectroscopy DLS	[90]
				Fluorescence spectroscopy	
		flutamide	$\beta$ -casein		
				UV-Vis spectroscopic HPLC	
				DLS	[93]
				HPLC	[94]
				DLS	
				DSC	

				FTIR	
platinum complex	$\beta$ -casein and chitosan			DLS SEM	[95]
paclitaxel and EGCG	(PLGA)–casein			HPLC	[96]
resveratrol	NaCas	$5.1 \times 10^5 \text{ M}^{-1}$		Fluorescence spectroscopy	[97]
cispatin	Casein			DLS FTIR	[98]

#### 2.1.4.7 Others pharmaceuticals molecules

Casein based nanocarrier are great drug delivery systems for a targeted and sustained drug release.

Raj and Uppuluri [99] proposed CMs as nanovehicle for metformin hydrochloride (MET). MET is an oral antidiabetic agent against Type II diabetes. Its free form shows poor oral bioavailability. *In vitro* experiment, by using Dissolution apparatus USP, showed that half of the drug was released during first 3h and 85% of the drug is released after 15h of its administration. That 50 % and 85 % of the drug was released after 3 and 15 h after its administration, respectively.

Corzo-Martínez et al. [100] developed a milk-based powder formulation for pediatric delivery of ritonavir (RIT). RIT is a potent HIV protease inhibitor with high hydrophobicity and low solubility in water. The authors showed that RIT interacted efficiently with milk proteins, especially with casein micelles after high pressure treatment at 0.1 MPa, RIT interacted with caseins at the micellar surface while at 300 and 500 MPa, RIT was integrated to the protein matrix. *In vitro* experiments under simulated gastrointestinal conditions showed that release of RIT associated with casein micelles was pH-dependent. CMs protected RIT from degradation in the acid environment of the stomach, bypassing the gastric environment and deliver RIT until the small intestine.

Turovsky et al. [101] examined the effect of the hydrophobic non-steroidal anti-inflammatory drug named ibuprofen on the structure of  $\beta$ -casein micelles as a

function of temperature and loading. Using cryo-transmission electron microscopy (cryo-TEM), the authors showed the coexistence of small assemblies (35–60 nm in size) and large aggregates (110–160 nm) containing ibuprofen. At temperature of 50°C and at critical micelle concentration of  $\beta$ -casein, drug was located at the surface instead than being encapsulated in the micellar core. In another study, Zhang et al [102] improved the stability of insulin against enzymatic degradation in solution. This protection against proteolytic enzymes was obtained thanks to interactions of insulin with  $\beta$ -casein.

Kütt et al. [103], in a recent study, investigated on the interactions between native CMs and piscidin-1, an antimicrobial peptide from fish. By using size exclusion chromatography, the interaction between piscidin-1 and native CMs was characterized. The authors proposed native CMs as nanovehicle for antimicrobial peptides in milk.

**Table 4: Casein-based nanoparticles as nanocarriers in pharmaceuticals applications.**

<b>Group</b>	<b>Molecule</b>	<b>Nanocarrier</b>	<b>Constant association</b>	<b>Techniques</b>	<b>Ref.</b>
<b>antidiabetic</b>	metformin	CMs		DLS UV-Vis spectroscopy	[99]
<b>HIV-protease inhibitor</b>	ritonavir	CMs		HPLC Fluorescence spectroscopy FTIR SEM	[100]
<b>anti-inflammatory agent</b>	ibuprofen	$\beta$ -casein		DLS DSC TEM	[101]
<b>hormones</b>	insulin	$\beta$ -casein		HPLC UV-Vis spectroscopy	[102]
<b>anti-microbial agent</b>	piscidin-1	CMs		Mass spectroscopic	[103]

#### 2.1.4.8 Casein interacting with nanoparticles

Design and development of new selective nanocatalytic systems, like casein-nanoparticles complex, plays important role in biomedical applications. Interaction between CMs with gold nanoparticles (GNPs) was studied by Liu et al. [104][18] by using several spectroscopy methods. GNPs were able to be bound to CMs surface, presumably *via* interaction with the carboxylate or amine groups of CMs, leading to the formation of stable GNPs–CMs conjugates. This fabrication is relatively mild, convenient, low-cost and reproducible. GNPs with size below 10.0 nm were synthesized easily by adjusting the casein concentration and pH. This new complex, which presented good stability against salt concentration and pH, could be used for future applications in genomics, proteomics, biomedical and bioanalytical areas.

With the same challenge, Ashrafa et al. [105] used casein to produce biotolerable and highly stable silver nanoparticles for potential bio-applications. The complex protein-silver nanoparticles was formed in several steps to produce uniform spherical agglomerates. These silver nanoparticles undergo reversible agglomeration to form protein–silver nanoparticle composite agglomerates as pH approaches to the isoelectric point of casein protein. The nanoparticles can withstand high salt concentration ( $\sim 0.5$  M), and can also be freeze-dried, stored as dry powder and then dispersed in aqueous media when required.

The interaction of iron oxide nanoparticles (with a core size of 15 nm) and milk protein, the stability of this complexes and their response to an external magnetic field, were studied by Sangeetha and Philip [19], Huang et al. [106][107], Cowger et al. [108] and Singh et al. [109]. These particles could be proposed as a new class of biomarker for MRI contrast enhancement and related biomedical applications.

Interactions between corn zein nanoparticles and CasNa were also investigated. Cheng and Zhong proposed a new solution to increase the dispersibility of spray-dried corn zein nanoparticles [110], by dispersing aqueous ethanol solutions of zein into CasNa dispersion. At the same time, Yin et al. [111], to improve the barrier ability of CasNa films, use corn zein nanospheres (size between 0.5 and 1.0  $\mu\text{m}$ ) *via* direct coatings.

Table 5: Casein interacting with natural or synthetic nanoparticles.

Group	Molecule	Nanocarrier	Constant association	Techniques	Ref.
nanoparticles	gold	CMs		UV-Vis spectroscopic TEM Fluorescence spectroscopic FTIR	[104]
		CMs		UV-Vis spectroscopic TEM X-ray diffraction	[18]
	silver	casein		TEM UV-Vis spectroscopic FTIR	[105]
	iron	CMs		DLS UV-Vis spectroscopic FTIR X-ray diffraction	[19]
		casein		DLS TEM FTIR	[106]
		casein		DLS TEM NMR	[107]
		casein		TEM	[108]
		casein		FTIR TEM SEM Raman spectroscopic	[109]
	zein	NaCas		TEM FTIR	[110]
		NaCas		AFM	[111]



### 2.1.5 Conclusions and future applications

CMs are quite stable against physico-chemical treatments. However, drastic conditions like acid pH, temperature, ethanol and dissociating agents can induce their colloidal instability [3]. An interesting methods of stabilisation are modify casein structure by cross-linking, by joining two or more casein molecules by covalent bonds. Glutaraldehyde is a well-known cross-linking agent especially used in the sample preparation before microscopical observations. Silva et al. [112] showed that this compound was able to link lysyl residues to form aggregates with high molecular weight. However, due to their toxicity no intensive research was realized. Another cross-linking agent is genipin. This compound is a natural molecule extracted from *Gardenia jasminoides* [113]. *In vitro* studies, using 3T3 fibroblasts (BALB/3T3 C1A31-1-1), indicated that genipin is  $10^4$  less cytotoxic than glutaraldehyde [114] and its role as cross-linking agents was investigated in some biological applications [115]. Silva et al. [4] and Nogueira Silva et al. [116] characterized the CMs cross-linked by genipin. After 50 h of reaction, micellar suspension was blue. Modified CMs were (1) formed *via* cross-linking with lysyl and arginyl residues, (2) smaller in size, and (3) more negatively charged with a smoother surface than native CMs. Casanova et al. [117] completed this research with a comparative study of stability between native CMs and CMs cross-linked with genipin (CMs-GP) as a function of pH in different physico-chemicals conditions (alcohol test, thermal stability) was conducted. CMs-GP have high stability compared to native CMs. Casein can be enzymatically cross-linked by transglutaminase (Tgase), a natural agent of microbial origin recognized as safe. Tgase cross-links covalently proteins between the  $\gamma$ - carboxyamide group of glutamine residues and the  $\epsilon$ -amino group of lysyl residues [118]. Analysis by X-ray scattering (SAXS) and small angle neutron scattering (SANS) showed that their internal structure was not affected [119]. Different authors investigated on their stability. Thus, Huppertz et al. [120] demonstrated that CMs cross-linked with Tgase were entirely stable to disruption by urea and/or citrate. Huppertz and de Kruif [121] showed that reticulated CMs were more stable than native CMs against ethanol-induced coagulation. Recently, Huppertz [122] demonstrated that incubation of milk with Tgase increased their heat stability by preventing dissociation of  $\kappa$ -casein. In a

recent paper, Nogueira et al. (*paper under preparation*) presented a comparative study between CMs and CMs-Tgase as a function of pH in different physico-chemical conditions. Higher stabilities for CMs-Tgase compared to native CMs were observed in the presence of 8 M of urea or 100 mM of sodium citrate. Visible coagulations for CMs-Tgase were determined at 500 s at 140 °C and 99.5% (v/v) of ethanol at pH 2 against 99 s and 61 % for native CMs at pH 7.

As mentioned in the previous section, Anema and de Kruif, investigated on the interactions between lactoferrin and CMs cross-linked with transglutaminase [123-124]. The authors demonstrated that cross-linking prevented their disintegration upon binding with lactoferrin. All these results allowed the potential application of cross-linking on CMs to improve their spectra of utilization in different physico-chemical conditions.

### **3. OBJECTIVES AND STRATEGIES**

The objectives of this Thesis want to bring answers to the following questions :

Does cross-linking by GP or Tgase increase the stability of CMs ?

What the factors determining this increase of stability ?

Does cross-linked CMs interact with C3G ? What is the mechanism of interaction ?

Cross-linked CMs can be used as potential nanocarrier for C3G ?

As mentioned previously, the first part of the present work is to verify the physico-chemical stability of cross-linked CMs compared to native CMs against acid pH, temperature, ethanol and dissociating agents. Then, in the second part, we investigate on the possible interactions between cross-linked CMs and C3G in acid and neutral pH conditions.

To answer these questions, we divide this work in two parts: PART A and PART B.

The strategy adopted in a PART A (Figure 5) is to investigated on the physico-chemical stability of native CMs cross-linked with GP or Tgase against acid pH (from 7.0 to 2.0), dissociating agent (citrate and urea), temperature (140 °C as a fonction of the time) and ethanol (% vol/vol). Acid condition were chosen to adapt this nanocarrier for C3G (which present bioactive properties only in pH range from 2 to 3), citrate and urea to obtain the demineralization of native and cross-linked CMs, high temperature for the future industrial applications whereas ethanol for a proof of concept. Hydrodynamic diameter and  $\zeta$ -potential in acid conditions, or in the presence of dissociating agents of native and cross-linked CMs, were determined by Dynamic light scattering (DLS). Visual coagulation was chosen to investigate the stability against ethanol and temperature.

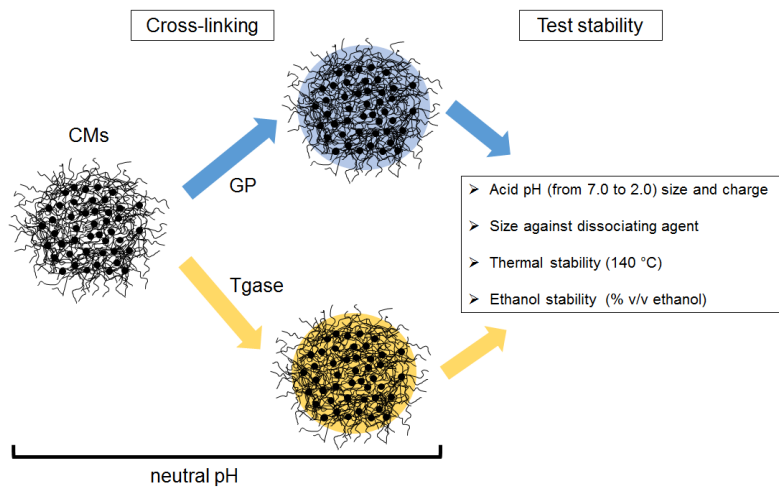


**Figure 5 : Outline of the strategy adopted in the part A of the manuscript. We start with native CMs and after cross-linking by GP or Tgase, we realize the stability test.**

In a PART B, with the perspectives of using cross-linked CMs for food applications, we choose Tgase as cross-linker. Cyanidine-3-O-glucoside (C3G) is an anthocyanin present in several Brazilian's fruits, especially Amazon açai and jaboticaba, which shows high antioxidant activity in acid conditions. The strategy adopted in this section is to investigate first on the possible interaction between casein molecules and C3G under acidic (pH 2.0) and neutral (pH 7.0) conditions. Then, Tgase cross-linked CMs as nanocarrier for C3G at pH 2.0 and at pH 7.0 was explored. Fluorescence spectroscopy, the most popular and perhaps the most sensitive technique that allows to realize routine measurements in the micromolar ( $\mu\text{M}$ ), even nanomolar (nM) concentrations, is chosen to investigate on the possible interactions. Dynamic light scattering were chosen as a complementary technique to investigate on the possible variations in the size of native and cross-linked CMs after interaction with C3G (Figure 6).

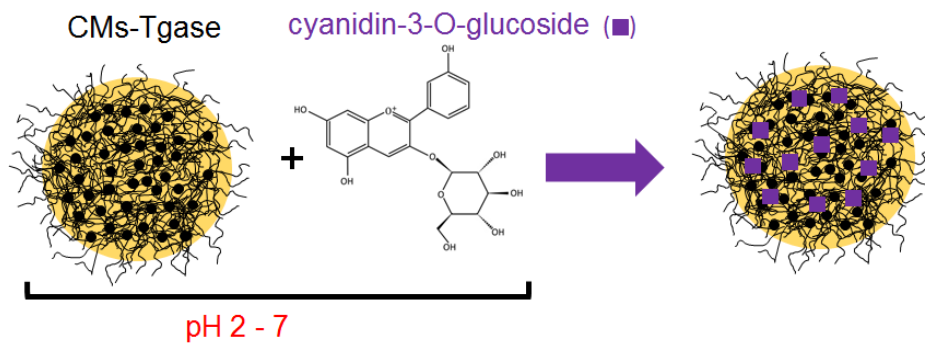


Figure 6 : Interaction between Tgase cross-linking CMs and C3G at pH 2 and pH 7.

## **4. RESULTS AND DISCUSSION**

## PART A

In the following section, we present a comparative study between native CMs and cross-linked CMs with genipin (chapter 3.1) and transglutaminase (chapter 3.2).

The objective was (a) to evaluate the stability of cross-linked CMs under different physicochemical conditions (acid pH, dissociating agents, high temperature and different ethanol concentrations) and (b) understand if cross-linked CMs can be used as versatile nanocarrier that can tolerate a wide range of physico-chemical conditions, which have not yet been exploited due to sensitivity of protein particles.

### Questions

- Does cross-linking by genipin or transglutaminase increase the stability of CMs against acidic pH, dissociating agents, temperature and ethanol ?
- In positive case, what are the factors determining this increase of stability ?

### Main results

- Cross-linking increasing stability of CMs against acidic pH, temperature (140 °C as a function of the time), ethanol (% ethanol), dissociating agents to all conditions studied. We assumed that intramolecular cross-linking and stabilization of polyelectrolyte brush of  $\kappa$ -casein are probably the factors that stabilize cross-linked CMs against disruption.



## 2.1 Stability of casein micelles cross-linked with genipin: a physicochemical study as a function of pH

The content of this chapter has been published in:

*International Dairy Journal*, 68, 70-74 (2017)

Federico Casanova, Naaman F. Nogueira Silva, Frédéric Gaucheron, Márcio H. Nogueira, Alvaro V. N. C. Teixeira, Italo Tuler Perrone, Maura Pinhero Alves, Priscila Cardoso Fidelis and Antonio F. de Carvalho

The experimental part as well as the discussion of this paper was realized at the Inovaleite laboratory and the department of physics at the Universidade Federal de Viçosa (Brazil) in collaboration with Frédéric Gaucheron (INRA-STLO, Rennes, France).

### 2.1.1 Introduction

Casein micelles (CMs) are the major fraction of milk proteins (approximately 80 %). They are formed by interaction of highly phosphorylated  $\alpha_{S1}$  - (40%) -  $\alpha_{S2}$  - (10%)  $\kappa$  (35%) and  $\beta$  - casein (15%) with calcium phosphate [1]. Their hydrodynamic diameter is about 200 nm [125] and the  $\zeta$ -potential is about -20 mV [126]. The stability of CMs depends on the physicochemical conditions of the medium. Therefore, increasing the stability of CMs would allow their use in a greater range of application. Casein micelles have a dynamic structure that can be modified in different ways, including chemical and enzymatic cross-linking. Physico-chemical investigations on cross-linked CMs showed that they are more resistant against destabilizing conditions than native CMs. Enzymatic cross-linking by transglutaminase (TGase), an agent of microbial origin [127], did not affect the size and the internal structure of cross-linked CMs when analyzed by dynamic light-scattering (DLS) [128], X-ray scattering (SAXS) and small-angle neutron-scattering (SANS) [119]. Another alternative to modifying the structure of CMs is chemical cross-linking by glutaraldehyde [112]. Unfortunately, due to its toxicity, only few studies have been conducted in that area. Recently, Nogueira Silva [129][116], investigated the cross-linking of CMs by genipin (GP), a natural molecule extracted from *Gardenia jasminoides* [113]. A study of GP cytotoxicity, tested *in vitro* using 3T3 fibroblasts (BALB/3T3 C1A31-1-1), indicated that this compound was less cytotoxic than glutaraldehyde [114]. These authors showed that cells cultured in medium containing 100 ppm of GP were as confluent as observed in the control without GP, while 0.5 ppm glutaraldehyde induced the death of all cells. In another test, these same authors indicated that the concentrations of glutaraldehyde (0.01 ppm) and GP (100 ppm) reduced by 50 % the optical density of cell culture. This suggests that GP was 10<sup>4</sup>-fold less cytotoxic than glutaraldehyde. Covalent links are formed between GP and lysil or arginyl residues of CMs, leading to the formation of hydrophobic aggregates with high molecular weight (personal communication of Nogueira). Analysis by DLS and rheology showed that the reaction between GP and casein molecules was mainly intramicellar, with the presence of only one population of cross-linked particles. CMs cross-linked with GP did not dissociate at air–water interfaces and formed a solid interface rather than a

viscoelastic gel (Nogueira Silva et al., 2014). Nogueira Silva et al (2014) showed that the structure of cross-linked CMs was resistant to the presence of dissociating agents such as citrate and urea. These results suggest the possibility of using CMs-GP as adaptable nanovehicles. Recent studies have investigated the potential use of CMs as nanocarriers for hydrophobic nutraceuticals [130][47]. Some bioactive molecules cannot be used in their pure form due to their sensitivity to deterioration during process or their sensitivity to light, acid pH or high temperature. The objective of this study was to evaluate the stability of CMs cross-linked with GP under different physicochemical conditions: acid pH, high temperature (140 °C) and different ethanol concentrations. For each pH value, the charge ( $\zeta$  -potential) and size of the particles were determined by DLS. Heat coagulation time (HCT) at 140 °C and ethanol stability (% ethanol, v/v) were also determined as a function of pH. This study is a proof of concept and we test only the stability of the cross-linked micelle system. Finally, the possibility of using this nanocarrier for possible future scientific studies is proposed.

## **2.1.2 Material and methods**

### **2.1.2.1 Sample preparation**

Purified native CMs was obtained by two successive microfiltration steps of raw skimmed milk and spray-dried. The first microfiltration step used a membrane with 1.4  $\mu\text{m}$  pore size to remove bacteria, an average permeation flux of 145  $\text{l}\cdot\text{h}^{-1}$ , with a total membrane area of 0.24  $\text{m}^2$  and a transmembrane pressure of 0.5 bar at a temperature of 38°C. The second was performed using a membrane with pore size 0.1  $\mu\text{m}$  to remove constituents of the soluble phase, a permeation flux of 35  $\text{l}\cdot\text{h}^{-1}$ , a total membrane area of 0.24  $\text{m}^2$ , and a transmembrane pressure of 0.5 bar. A concentration factor equal to 3 was applied to obtain microfiltered whey at an average temperature for the process of 45°C. This second microfiltration step was completed by diafiltration against Milli-Q water, and the retentate was spray-dried as described by [131] and [132]. The powder was comprised of 96 % (w/w) of proteins, and was predominantly casein (97 % (w/w)). Residual whey proteins (3%) (w/w), lactose and diffusible calcium were also present in the powder. A suspension containing 27.5  $\text{g}\cdot\text{L}^{-1}$  of CMs was obtained by solubilization of powder in a buffer

solution containing 25 mmolL<sup>-1</sup> 4-(2-hydroxyethyl)-1-piperazine ethanesulfonic acid (HEPES) and 2 mmolL<sup>-1</sup> CaCl<sub>2</sub> at pH 7.10. In order to prevent microbial growth, 0.30 gL<sup>-1</sup> sodium azide (Acros Organics, New Jersey, USA) was added. GP was purchased from Challenge Bioproducts Co. Ltd. (Yun-Lin Hsien, Taiwan, Republic of China) with a purity of 98%. GP was dissolved in a mixture of 74/26 % (w/w) HEPES buffer and absolute ethanol to give a stock solution of 200 mmolL<sup>-1</sup>. The CM suspension and GP solution were mixed in order to achieve final concentration of 10 mmolL<sup>-1</sup> GP. This concentration of GP is at the same order as lysine in our suspensions containing 25 gL<sup>-1</sup> casein. The dilutions caused by the addition of GP were corrected by adding HEPES buffer and absolute ethanol to the CM suspensions. The cross-linking reaction was performed at 50 °C for 24 h and then at 4°C for 26 h before analysis. A control sample consisting only of suspended CMs was treated under the same conditions. Visible spectroscopy was used to follow the reaction between CMs and GP as a function of time over 50 h (data not shown). Reaction of GP with CMs induced a blue coloration with a maximum of absorption at 607 nm, which was as described by [129].

#### **2.1.2.2 Sample acidification**

The samples were aliquoted and acidified with HCl (1 M) at different pH values from 7 to 2, at intervals of 0.5, at 4 °C to prevent precipitation. Then, temperature was raised to 25 °C and the samples were kept under stirring for 2 h before analysis.

#### **2.1.2.3 Dynamic light scattering (DLS)**

Hydrodynamic diameter ( $D_h$ ) was determined by DLS on a Zetasizer Nano-S (Malvern Instrument, Worcestershire, UK). Measurements were performed at a scattering angle of 173° and a wavelength of 633 nm. Suspensions were diluted 1/25 in the corresponding ultrafiltrate and left at room temperature for 20 min at 20 °C before analysis. Ultrafiltrate was obtained by centrifugation (25 min at 1800 g) in Vivaspin® centrifugal filters (10000 Da molecular weight cut-off, Vivascience, Palaiseau, France) of suspensions at different pH values. The viscosity of suspension was 1.033 mPa.s<sup>-1</sup>. Experiment duration was 2 min and each experiment was repeated five times.  $D_h$  was expressed as the Z average value.

#### 2.1.2.4 $\zeta$ -Potential measurements

Zeta-potential ( $\zeta$ ) was determined by Zetasizer Nano-ZS (Malvern Instruments, Worcestershire, UK) using capillary cells. Suspensions were diluted 1/25 in the corresponding ultrafiltrate and left at room temperature for 20 min at 20 °C before analysis. Ultrafiltrate was obtained by centrifugation (25 min at 1800 g) in Vivaspin® centrifugal filters (10000 Da molecular weight cut-off, Vivascience, Palaiseau, France) of suspensions at different pH values. The measurements were performed with an applied voltage of 50 V. Zeta potential ( $\zeta$ ) was calculated from the electrophoretic mobility ( $\mu$ ) using the Henry equation, as follows:

$$\zeta = \frac{3\eta\mu}{2\varepsilon f(\kappa R_H)} \quad (1)$$

where  $\eta$  is the solvent viscosity ( $\text{Pa s}^{-1}$ ),  $\mu$  is the electrophoretic mobility ( $\text{V Pa}^{-1} \text{s}^{-1}$ ),  $\varepsilon$  is the medium dielectric constant (dimensionless),  $\kappa^{-1}$  is the Debye length (measured thickness of the double electric layer around the molecule) (nm),  $R_H$  is the particle radius (nm) and  $f(\kappa R_H)$  is Henry's function. Since the analysis was conducted in aqueous media, a value of 1.5 was adopted for  $f(\kappa R_H)$ , which is referred to as the Smoluchowski approximation.

#### 2.1.2.5 Heat coagulation time (HCT)

HCT is considered as the time required for the appearance of visible coagulation [122]. Using the method of Davies and White [133], 1.5 mL of sample were placed in 5 mL stoppered tubes and put in an oil bath. Samples were held with pliers and were manually and gently stirred continually to easily detect visible coagulation, without remove from the oil bath. These analyses were realized with heat-resistant gloves, laboratory pliers and safety glass in transparent oil. HCT was determined at 140 °C as a function of pH (pH values between 7.0 and 2.0). Experiments were performed in triplicate on 4 individual preparations.

#### 2.1.2.6 Ethanol stability

Following the method of [134], ethanol stability was determined by mixing 2 mL of sample (pH values between 7.0 and 2.0) with an equal volume of aqueous ethanol (0 – 100 % v/v at 2.5 % intervals) in a petri dish. Ethanol stability was determined by

visual coagulation of the sample at the lowest concentration of aqueous ethanol solution. All experiments were repeated in duplicate on 4 individual preparations.

### **2.1.2.7 Interactions among variables**

To understand the relationship between the stability of native CMs and CMs-GP against pH, temperature and ethanol, Pearson's correlation coefficients were determined using Microsoft Excel.

## **2.1.3 Results and discussion**

### **2.1.3.1 Z-average diameter**

DLS was used to investigate the size of the native and cross-linked CMs as a function of pH (Figure 7). The  $D_h$  of CMs showed stability in pH range from 7.0 to 5.5, with an average diameter of  $177 \pm 6$  nm. CMs-GP showed stability in the pH range from 7.0 to 5.0, with an average diameter of  $170 \pm 4$  nm. According to Nogueira-Silva et al.[129], this decrease can be explained by a collapse of the hairy layer of  $\kappa$ -casein at the surface of the micelle. Those authors confirmed this hypothesis with scanning electron microscopy analysis, through which a smoothing on CMs surface as a function of GP concentration was observed. At the same time, we observed that gelation of native CMs occurs at  $t = 10$  min, whereas no gelation was observed for CMs-GP after  $t = 25$  min of chymosin action (data not shown). These results confirm that GP affected the properties of the polyelectrolyte brush of  $\kappa$ -casein. In the pH range studied, native CMs and CMs-GP are negatively charged and are separated from each other due to electrostatic repulsion. When the pH value decreases to near the isoelectric point ( $pI$ ), the repulsion between casein micelles decreases and hydrophobic interactions increase. Native CMs precipitated below pH 5.5 and it was impossible to determine their physico-chemical characteristics below this pH value; CMs-GP were unstable only between 4.5 and 3.5 and no precipitation was observed from pH 2.0 to 3.0. When aggregates are formed, signals exceed the upper limit of the instrument (2000 nm). At pH between 2.0 and 3.0, CMs-GP presented an average  $D_h$  of  $181 \pm 5$  nm. Even if the colloidal calcium phosphate is mainly dissolved at these pH values, CMs-GP did not dissociate.

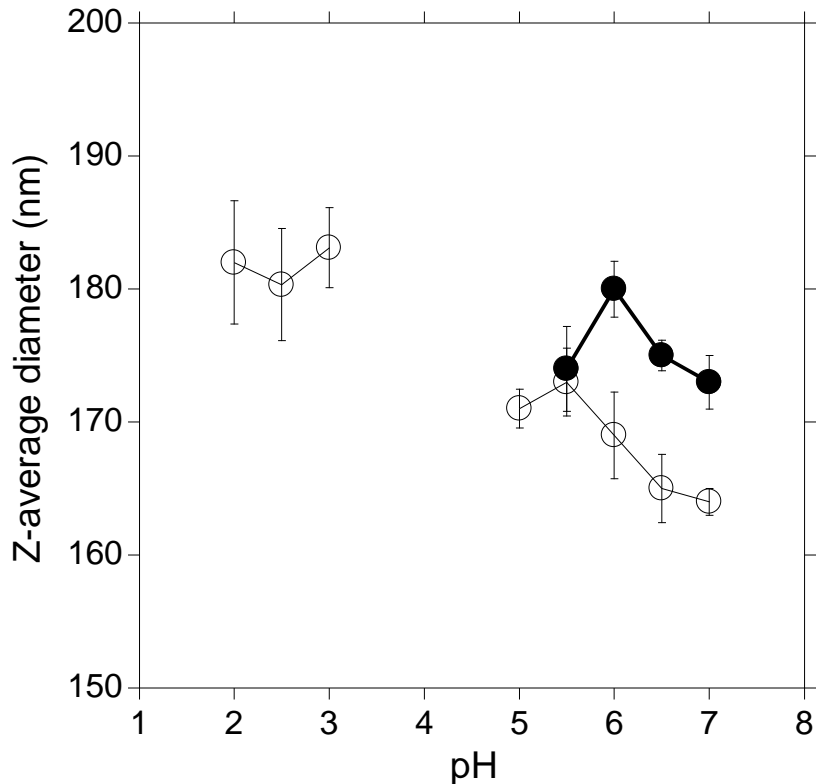


Figure 7 : Z-average diameter (nm) as a function of pH of native CMs (●) and CMs-GP (○). Data corresponded to average values (n=3) and the vertical error bars indicate the standard error. For native CMs and CMs-GP, the determinations between pH 5.0 and 3.0 were not possible due to the presence of precipitate. At pH below 3.0, native CMs were not monodisperse.

### 2.1.3.2 $\zeta$ -potential

The  $\zeta$ -potential of CMs is typically -20 mV in milk conditions [1]. During acidification of native CMs, their  $\zeta$ -potential increased, to a value close to  $-6.0 \pm 0.5$  mV at pH 5 (Figure 8). Under the same conditions,  $\zeta$ -potential of CMs-GP remained stable at  $-19.0 \pm 0.6$  mV. The value of  $\zeta$ -potential of cross-linked CMs was in accordance with the value at  $-23.4 \pm 2.8$  mV reported by [129]. This value was more negative than those of native CMs, because the amount of positive charges was decreased due to the reaction between lysyl and arginyl residues and GP.

As observed with native CMs, the  $\zeta$ -potential of cross-linked CMs also decreased as a function of acidification. At pH 2-3,  $\zeta$ -potential for native CMs and CMs-GP were  $9.7 \pm 0.2$  mV and  $14.3 \pm 1.1$  mV, respectively. By intersection of Y-axis curve on Z-axis at 0 mV, a pI value were measured as 4.7 for CMs and 3.7 for CMs-GP [135]. For native CMs, the conditions were not those of milk, because they were suspended in media containing only  $2 \text{ mmol}^{-1}$  Ca. Similar results were obtained by Famelart et al. [136].

For CMs-GP, the shift of  $pI$  corresponded to the decrease in positive charge of native CMs after reaction with GP.

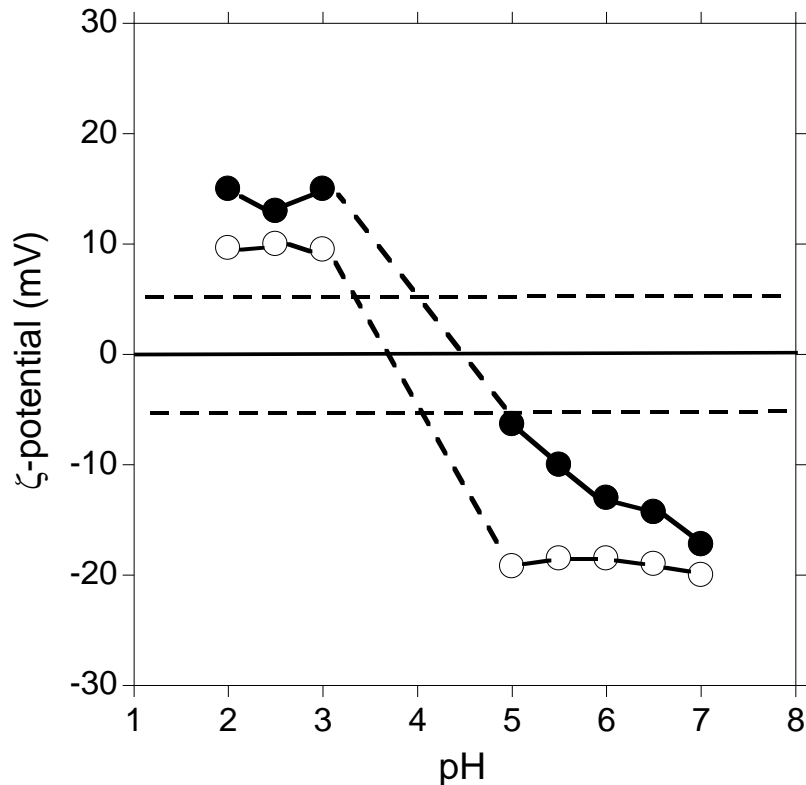


Figure 8 : $\zeta$ -potential (mV) as a function of pH of native CMs ( $\bullet$ ) and CMs-GP ( $\circ$ ). The determinations between -5 and +5 mV (horizontal dotted lines) were not possible due to the presence of visible aggregates. The standard deviation was < 5%.

### 2.1.3.3 Heat coagulation time (HCT)

Table 6 summarizes the average values of HCT for CMs and CMs-GP. Cross-linking by GP increased the heat stability of CMs. In the pH range 7.0 to 5.5, HCT of CMs decreased from 56 to 45 s, whereas the HCT of CMs-GP decreased from 115 to 89 s. Results suggest that, close to the  $pI$ , stability of native CMs and CMs-GP decreased. Highest stability was observed at pH 2, where CMs-GP presented a HCT of  $820 \pm 20$  s. According to the literature, cross-linking increase HCT of CMs. Smiddy et al. [137] studied the impact of enzymatic cross-linking of CMs with TGase on the stability of CMs against urea, sodium dodecyl sulfate, or heating in the presence of ethanol. TGase increased the stability of CMs against disruption or dissociation by stabilization of polyelectrolyte brush of  $\kappa$ -casein [138]. Removal or collapse of  $\kappa$ -casein induced instability of the CMs. Huppertz and de Kruif [139] observed that



cross-linking of CMs with TGase increased the stability of native CMs, but also affected the properties of the  $\kappa$ -casein brush, and thus micellar stability.

**Table 6 :HCT (s) at different pH values at 140 °C of native CMs and CMs-GP. Measurements were performed in triplicate for 3 different suspensions. For native CMs and CMs-GP, the determinations between pH 5.0 and 3.0 were not possible due to the presence of precipitate. At pH below 3.0, native CMs are not monodisperse.**

HCT (s)			
pH	CMs	CMs-GP	
7	36.5 ± 6.5	115.0 ± 21.2	
6.5	54.0 ± 4.2	302.4 ± 18.5	
6	56.3 ± 5.6	480.0 ± 24.5	
5.5	45.0 ± 1.7	303.3 ± 30.5	
5	-	89.0 ± 8.4	
3	-	397.0 ± 12.5	
2.5	-	496.0 ± 45.8	
2	-	817.5 ± 116.6	

#### 2.1.3.4 Ethanol stability

Ethanol stability of native CMs decreased as a function of pH, from 50 % at pH 7.0 to 7.5 % at pH 5.5 (Figure 9). Cross-linking of CMs with GP increased ethanol stability at all studied pH values. CMs-GP had an ethanol stability 25-40 % higher than that of native CMs in the same pH range (Fig. 3). In both cases, the presence of ethanol reduced the steric stabilisation of the CMs and CMs-GP [140]. Their resistance to ethanol were minimal approaching the zone of  $pI$ . Increasing concentrations of ethanol induce the collapse of  $\kappa$ -casein and the aggregation of casein micelles [141]. Below the  $pI$ , it was only possible to determine the ethanol stability of CMs-GP. At pH 3, the ethanol stability was 47.5 % whereas, at pH 2 and 2.5, it was 85 % and 87.5 %, respectively. Cross-linking of CMs by GP was mainly intra-micellar, with a decrease in micellar diameter (Fig. 1). Cross-linking increased their stability against ethanol-induced coagulation. Comparable results were observed for CMs cross-

linked with transglutaminase at 30 °C at different incubation times in pH range 7.0 – 5.0 [122]. In that study, the authors interpreted the results as a transformation of the original “absorbed” polyelectrolyte brush into a “grafted” polyelectrolyte brush on the surface of CMs. These “grafted” brushes induce a better stability against ethanol-induced coagulation. This interpretation can be also proposed for CMs cross-linked with GP.

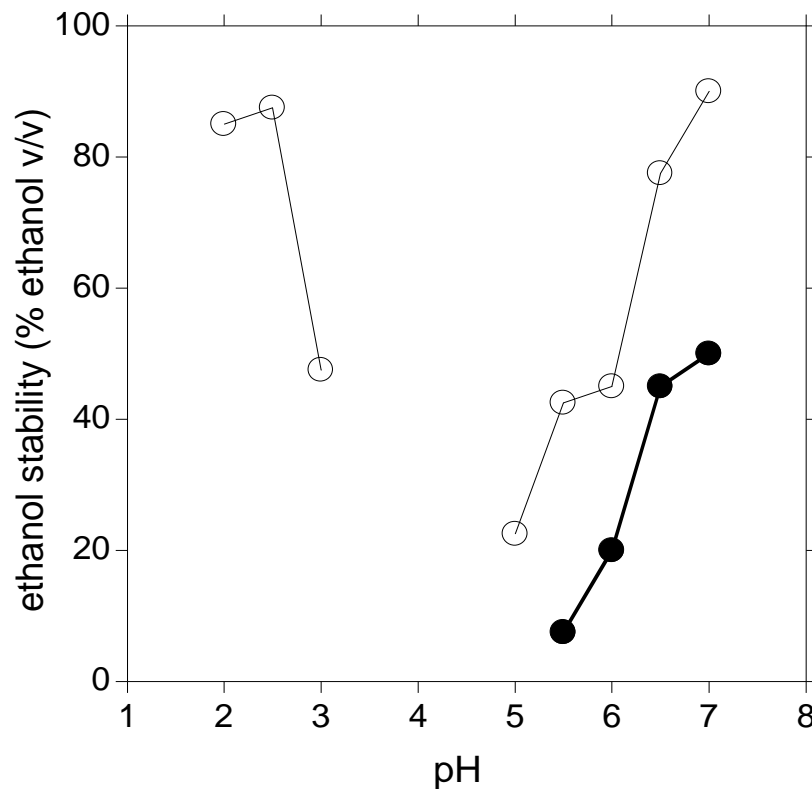


Figure 9 : Effect of pH on the ethanol stability for native CMs (●) and CMs-GP (○). Determinations were performed in triplicate for 3 different preparations of suspensions. The standard deviation was < 5%. For native CMs and CMs-GP, the determinations between pH 5.0 and 3.0 were not possible due to the presence of precipitate. At pH below 3.0, native CMs were not monodisperse.

### 2.1.3.5 Interactions among variables

Pearson’s correlation coefficients was used to analyze the experimental datas (Table 7); values close to -1 or 1 indicated a strong linear correlation between two variables. For native CMs, a high correlation between  $\zeta$ -potential and HCT (0.94) from pH 7.0 to 5.5, is observed. A mathematical empirical model of fourth degree was established for native CMs and is presented by equation 1, considering instantaneous coagulation as HCT equal to zero.

$$\text{HCT} = -5 \cdot 10^{-4} \cdot \zeta^5 - 6 \cdot 10^{-3} \zeta^4 + 2 \cdot 10^{-1} \cdot \zeta^3 - 2 \zeta^2 + 22 \zeta - 169 \quad (R^2 = 0.99) \quad (2)$$

However, a lower coefficient between  $\zeta$ -potential and HCT (0.70) was achieved for CMs-GP between pH 7.0 to 2.0. Consequently, a higher and negative correlation between pH and HTC was reached for native CMs (-0.97) but no significant correlation was achieved by CMs-GP (-0.71). CMs-GP were more stable to heat treatment and no correlation between the pH and HCT at 140°C was found. No significant correlation was established either between diameter and HCT for native CMs and CMs-GP (0.52 and 0.66, respectively). Regarding the ethanol test, the stability of native CMs was highly dependent on  $\zeta$ -potential, pH and diameter, with respective correlation coefficients of - 0.93, 0.97 and 0.80. However, no significant correlation was obtained with CMs-GP, with results of 0.35, -0.15 and 0.01, respectively. These low correlation coefficients confirmed that chemical cross-linking of CMs by GP conferred high stability against temperature and ethanol.

**Table 7: Pearson correlation coefficients among variables for native CMs and CMs-GP structures.  $\emptyset$  = diameter (nm); Eth = ethanol stability;  $\zeta$  =  $\zeta$  potential; HCT= Heat coagulation time. Correlation established from pH 7.0 to pH 2.0; \*correlations established from pH 7.0 to pH 5.5.**

<b>Coefficient Correlation</b>	<b>Native CMs</b>	<b>CMs-GP</b>
$\zeta$ x HCT	0.94*	0.70
pH x HTC	-0.97*	-0.71
$\emptyset$ x HCT	0.52*	0.66
$\zeta$ x Eth	-0.93*	0.35
pH x Eth	0.97*	-0.15
$\emptyset$ x Eth	-0.80*	0.01

#### 2.1.4 Conclusion

GP is a natural cross-linker, which is markedly less cytotoxic than glutaraldehyde. In this study, HTC and ethanol stability was explored in a pH range between 7.0 – 2.0. CMs cross-linked with GP showed higher stability than native CMs to all conditions studied. It is proposed that GP increased the stability of native CMs against disruption by stabilization of polyelectrolyte brush of  $\kappa$ -casein. Further investigations

are necessary in order to understand the mechanism of these factors on CMs structure. For example, it would be interesting to investigate the interfacial properties of CMs-GP as a function of pH. CMs-GP opens new perspectives for use as versatile vehicles that can tolerate a wide range of physico-chemical conditions, which have not yet been exploited due to sensitivity of protein particles. CMs-GP could replace native CMs for this purpose. This strategy was used by Anema and De Kruif (2012) for the study of binding of lactoferrin to transglutaminase cross-linked CMs.

## 2.2 Physico-chemical stability of casein micelles cross-linked with transglutaminase as a function of acidic pH

The content of this chapter is sent for a publication in:

*LWT – Food and Science Technology*

Márcio H. Nogueira, Guilherme M. Tavares, Naaman F. Nogueira Silva, Federico Casanova, Frédéric Gaucheron, Italo Tuler Perrone, Alvaro V. N. C. Teixeira, Antonio F. de Carvalho

The experimental part as well as the discussion of this paper was realized at the Inovaleite laboratory in collaboration with the department of physics at the Universidade Federal de Viçosa (Brazil). This project was realized by M. H. Nogueira during his Master's Thesis. I was associate as co-author in this work and I have participated in the discussions and corrections of the paper.

### 2.2.1 Introduction

Casein molecules are the major proteins in bovine milk (approximately 80% of the total milk proteins). They form structures called casein micelles (CMs) of 200 nm of hydrodynamic diameter. Their  $\zeta$ -potential were approximately -20 mV at neutral pH. CMs are colloidal particles consisting in phosphorylated  $\alpha$ S1- (40%)  $\alpha$ S2- (10%) and  $\beta$ -caseins (15%) interacting with colloidal calcium phosphate (CCP) at the interior of the micelles. K-casein (35%) is preferentially located at their surface, promoting their sterically stability [1]. The physiological function of CMs is associated to transport of calcium phosphate of the mammary gland to the mammal newborn [25]. In addition, CMs or their fractions (caseinate, purified casein molecules) are interesting materials to encapsulate different agents. In the last 10 years, different results reported their potential use as nanocarrier for protection of specific interest molecules, such as drugs, antioxidants and ingredients [142]. Although CMs are quite stable during heat treatments, physico-chemical conditions, especially acidic pH or modifications in the salt equilibrium, induce their destabilization by removal CCP. Several studies used cross-linking agents as an alternative to increase their stability under these stressing conditions. Nogueira Silva et al. [4][116] investigated the stability of CMs cross-linked by genipin (GP), a natural molecule extracted from *Gardenia jasminoides*[113]. Cross-linked CMs with GP were (1) formed *via* intra micellar cross-linkings with lysyl and arginyl residues, (2) smaller in size, and (3) more negatively charged with a smoother surface than native CMs. From pH 7 to pH 2, CMs cross-linked by GP have a higher stability compared to native CMs [117]. However, GP is not generally recognized as safe (GRAS) and further research on toxicity would be required to implement this material as a food-grade cross-linker. Casein can be enzymatically cross-linked by transglutaminase (Tgase), a natural agent of microbial origin recognized as safe. Tgase cross-links covalently proteins between the  $\gamma$ -carboxamide group of glutamine residues and the  $\epsilon$ -amino group of lysyl residues [118]. Analysis by X-ray scattering (SAXS) and small angle neutron scattering (SANS) showed that the internal structure of CMs was not affected [119]. Different authors investigated their stability. Thus, Huppertz et al. [120] demonstrated that CMs cross-linked with Tgase were stable to disruption by urea and/or citrate.

Subsequently, Huppertz and de Kruif [121] showed that reticulated CMs were more stable than native CMs against ethanol-induced coagulation. Huppertz [122] reported that incubation of milk with Tgase increased their heat stability by preventing dissociation of  $\kappa$ -casein. However, these studies were only conducted at neutral pH or around the isoelectrical point of casein.

The objective of this study was to evaluate the stability of CMs cross-linked with Tgase at acid pH (from 7.0 to 2.0), high temperature (140 °C), presence of ethanol, urea (8 M and from pH 7.0 to pH 2.0) or sodium citrate (100 mM and from pH 7.0 to pH 2.0). For each pH values,  $\zeta$ -potential and size of the particles were determined by Dynamic Light Scattering (DLS). Heat coagulation time (HCT) at 140 °C and ethanol stability (% ethanol, v/v) were also determined as a function of pH. The possibility of using this functional nanocarrier in acidic pH, for food or pharmaceuticals applications, was discussed.

## **2.2.2 Material and methods**

### **2.2.2.1 Sample preparation**

Purified native CMs was obtained by 2 successive microfiltration steps of raw skimmed milk and spray-drying. The first microfiltration step used a membrane with 1.4  $\mu\text{m}$  pore size (Membralox, Tetra Pak, Processing, Colombes, France), to remove bacteria. The operational conditions were a permeation flux of 145 L h<sup>-1</sup>, a total membrane area of 0.24 m<sup>2</sup> and a transmembrane pressure of 0.5 bar and a temperature of 38°C. The second was performed using a membrane with pore size 0.1  $\mu\text{m}$  (Membralox, Tetra Pak, Processing, Colombes, France), to remove constituents of the continuous phase (lactose, minerals, whey proteins). The operational conditions were a permeation flux of 35 L·h<sup>-1</sup>, a total membrane area of 0.24 m<sup>2</sup>, a transmembrane pressure of 0.5 bar and a temperature of about 45°C. A concentration factor equal to 3 was applied. This second microfiltration step was completed by diafiltration against Milli-Q water. The diafiltered retentate was spray-dried as described by [131][132]. The powder was composed of 96 % (w/w) of

proteins especially casein (97 %) (w/w). Residual whey proteins (3%) (w/w), lactose and diffusible calcium were also present in the powder but in small amounts.

A suspension containing 27.5 g L<sup>-1</sup> of CMs was obtained by powder solubilization in a buffer solution containing 25 mM 4-(2-hydroxyethyl)-1-piperazine ethanesulfonic acid (HEPES) and 2 mM CaCl<sub>2</sub> at pH 7.10. In order to prevent microbial growth, 0.30 g L<sup>-1</sup> sodium azide (Acros Organics, New Jersey, USA) was added. The suspension was incubated at 45°C with 3.0 units of Activa transglutaminase (Tgase) per gram of protein. Tgase, a gift from Ajinomoto Europe Sales (Hamburg, Germany), presented a declared activity of ~100 units/g. The CMs with TGase and the control native CMs (without TGase) were incubated in water bath at 45 °C for 24 h. Inactivation of the enzyme was performed by a heat treatment at 70 °C for 10 min. The samples were stored at 4 °C [137][144][145].

#### **2.2.2.2 Acidification**

Cold samples (4 °C) were acidified with HCl 1 M (Sigma Aldrich, São Paulo, Brazil) at different pH values from 7.0 to 2.0 with an interval of 0.5 unit. Then, the temperature was raised to 25 °C and the samples were stirred for 2 h before analysis.

#### **2.2.2.3 Dynamic light scattering (DLS)**

Hydrodynamic diameter ( $D_h$ ) was determined by DLS on a Zetasizer Nano-S (Malvern Instrument, Worcestershire, UK). Measurements were performed at a scattering angle of 173° and a wavelength of 633 nm. Suspensions were diluted 1/25 in their corresponding ultrafiltrate and left at room temperature for 20 min at 20 °C before analysis. Ultrafiltrate was obtained by centrifugation (25 min at 1800 g) with Vivaspin® centrifugal filters (10,000 Da molecular weight cut-off, Vivascience, Palaiseau, France) of suspensions at different pH values. The viscosity of solution was considered as the same than those of pure water (1.033 m Pa.s<sup>-1</sup>). The intensity correlation function was recorded after 4 min of accumulation and each experiment was repeated 6 times. Each correlogram was fitted by second order cumulant model, giving  $D_h$ , known as the so-called Z-average value. Experiment duration was 2 min and each experiment was repeated 5 times. Measurement of  $D_h$  was also used to study the resistance of particles against dissociating agents (same equipment and



conditions than those used for  $D_h$  determinations previously described). The suspensions were diluted 1/25 in 100 mM sodium citrate (Synth- P.A., SP, Brazil, purity > 99%) or in 8 M urea (Sigma-Aldrich, St. Louis, USA, purity > 98%) and studied from pH 7.0 to 2.0.

#### **2.2.2.4 $\zeta$ -Potential**

$\zeta$ -potential was determined with the Zetasizer Nano-ZS (Malvern Instruments, Worcestershire, UK) using capillary cells. Suspensions were previously diluted 1/25 in the corresponding ultrafiltrate and left at room temperature 20 min before analysis. The measurements were performed with an applied voltage of 50 V.  $\zeta$ -potential was calculated from the electrophoretic mobility ( $\mu$ ) using Henry equation, as follows:

$$\zeta = \frac{3\eta\mu}{2\varepsilon_f(\kappa R_h)} \quad (1)$$

where  $\eta$  is the viscosity of buffer ( $1.033 \times 10^{-3} \text{ Pa s}^{-1}$ ),  $\varepsilon$  is the medium dielectric constant (dimensionless),  $R_H$  is the complex radius (nm) and  $f(\kappa R_H)$  is the Henry's function. Since the analysis is conducted in aqueous media, a value of 1.5 was adopted for  $f(\kappa R_H)$ , which is referred to the Smoluchowski approximation.

#### **2.2.2.5 Heat coagulation time (HCT)**

HCT is considered as the time required for the appearance of visible coagulation [122]. Using the method of [133], 1.5 mL of suspensions (pH values between 7.0 and 2.0) were placed in 5 mL stoppered tubes and put in an oil bath at 140°C. Samples, held with pliers, were manually and gently stirred continually to easily detect visible coagulation, without remove them from the oil bath. Experiments were performed in triplicate on 3 individual preparations.

#### **2.2.2.6 Ethanol stability**

Following the method of [134], ethanol stability was determined by mixing 2 mL of suspensions (pH values between 7.0 and 2.0) with an equal volume of aqueous ethanol (Sigma-Aldrich, St. Louis, USA) at different % (between 0 and 100 % v/v with 2.5 % intervals) in a petri dish. Ethanol stability, determined by visual coagulation of

the sample, corresponded to the lowest concentration of aqueous ethanol solution. All experiments were repeated in duplicate on 3 individual preparations.

#### **2.2.2.7 Statistical interaction among variables**

Pearson's correlation coefficient were determined using Microsoft Excel to understand the stabilities of native CMs and CMs-Tgase against pH, temperature, ethanol and dissociating agents.

### **2.2.3 Results and discussion**

#### **2.2.3.1 Z-average diameter**

DLS was used to investigate the  $D_h$  of native and cross-linked CMs as a function of pH (Figure 10). Native CMs have a stable  $D_h$  ( $191 \pm 3$  nm) in pH range from 7.0 to 5.5. This value is in accordance with the literature [1]. In the same pH range, CM-Tgase presented a Z-average  $D_h$  of  $186 \pm 2$  nm. This difference of 5 nm between native and cross-linked CMs can be explained by a collapse of a  $\kappa$ -casein at the surface of CMs during the cross-linking process [146]. At pH value close to 5, *i.e* near their isoelectric point ( $pI$  of 4.6 for casein molecules), a reduction of  $D_h$ , due to a decrease of electrostatic repulsions associated to a solubilization of CCP from the CMs to the soluble phase, was observed [147,148]. Between pH 5.0 and 3.5, measurement was not possible due to the presence of precipitate generating inconstant intensity peaks. From pH 3.0 to 2.0, native CMs was not monodisperse and measurement was meaningless whereas CMs-Tgase presented a  $D_h$  between  $207 \pm 1$  nm and  $193 \pm 2$  nm. CMs-Tgase were not dissociated even when most of their CCP was dissolved. Similar results were founded by Casanova et al. [117] and [4] for cross-linked CMs with GP. In this last study, the authors showed that CMs-GP were unstable only between 4.5 and 3.5 and no precipitation was observed from pH 3.0 to 2.0. At acid pH, a variation of about 10 nm in size was observed. This variation can be explained by an anchorage of the hairy layer of  $\kappa$ -casein at the surface of the micelle.

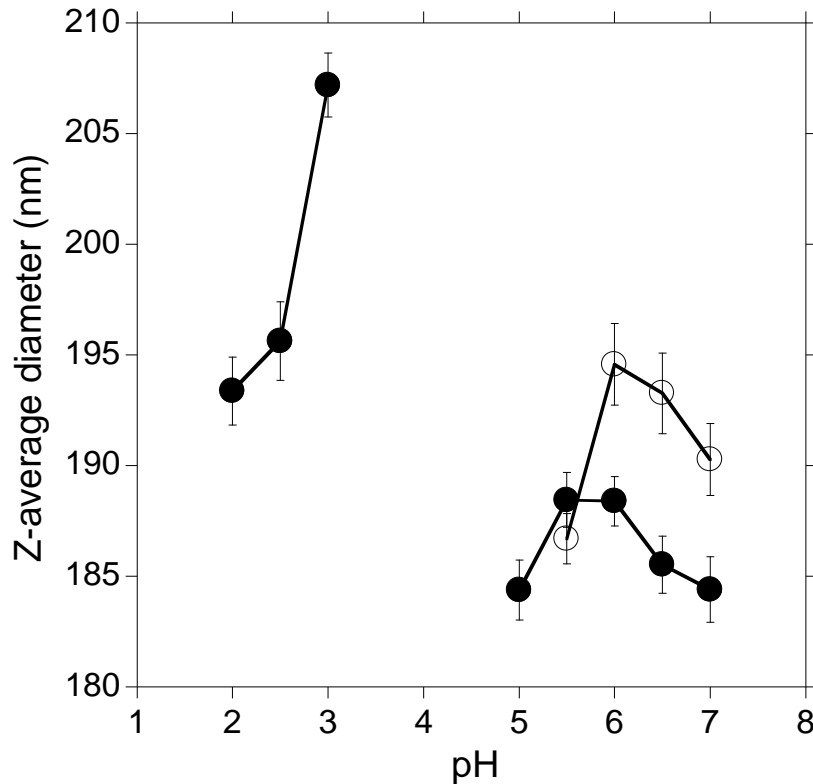


Figure 10: Z-average  $D_h$  (nm) as a function of pH of native CMs (○) and CM-Tgase (●). Data corresponded to an average of 3 determinations. The vertical error bars indicate the standard error. For native CMs and CMs-Tgase, the determinations between pH 5.0 and 3.0 were not possible due to the presence of precipitate. At pH below 3.0, native CMs were not monodisperse.

### 2.2.3.2 $\zeta$ -potential

The  $\zeta$ -potentials of native CMs and CM-Tgase were determined in the pH range from 7.0 to 2.0 (Figure 11). At pH 7.0, the  $\zeta$ -potential of native CMs was -22 mV. This value is in accordance with the literature [25]. During acidification their  $\zeta$ -potential increased to a value close to -7 mV. At the same pH values,  $\zeta$ -potential values of CMs-Tgase were -23 mV and -18 mV at pH 7.0 and 5.5 respectively. This decrease at pH 7.0 was probably due to the cross-linking where the lysyls and arginyls residues with positive charge were implicated. At pH between 2.0 and 3.0,  $\zeta$ -potentials for native CMs and CMs-Tgase were  $+28 \pm 1$  mV and  $+26 \pm 2$  mV, respectively. By intersection of Y-axis curve on Z-axis at 0 mV which corresponds to the isoelectric point, values of 4.6 for native CMs and 4.1 for CMs-Tgase were determined. For CMs-Tgase, the shift of isoelectric point compared to those of CMs corresponded to the decrease in positive charge of native CMs after cross-linking by

Tgase. For native CMs, the conditions were not those of milk, because they were suspended in media containing only 2 mM  $\text{Ca}^{2+}$ .

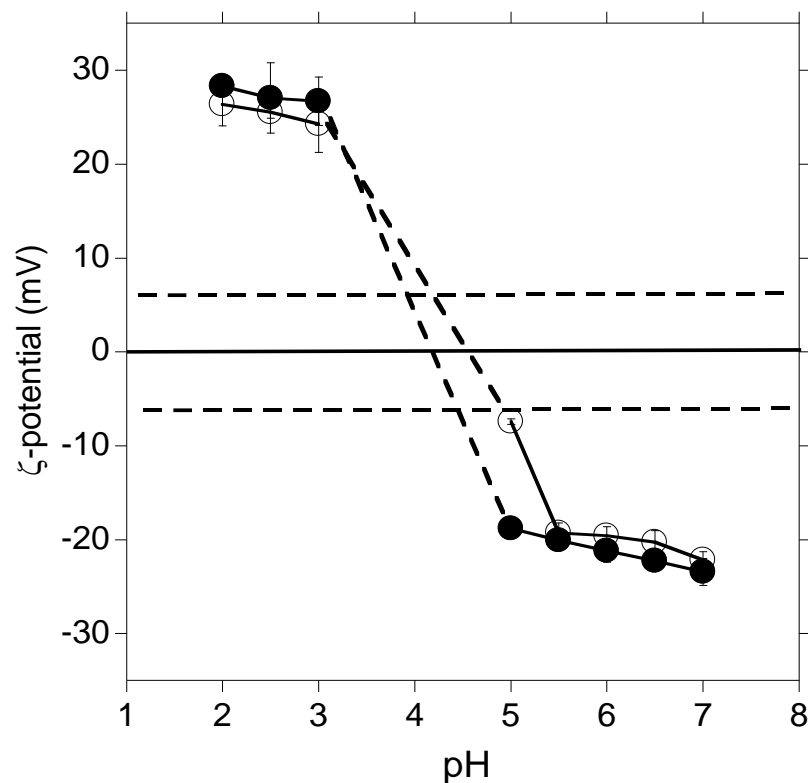


Figure 11:  $\zeta$ -potential as a function of pH of native CMs ( $\circ$ ) and CMs+Tgase ( $\bullet$ ). The determinations between -5 and +5 mV (horizontal dotted lines) were not possible due to the presence of visible aggregates. The standard deviation was < 5%. Data corresponded to an average of 4 determinations. The vertical error bars, comprised in points, indicate the standard error.

### 2.2.3.3 Addition of urea

It is well known that urea makes strong H-bonds with water and causes disruption of hydrophobic and hydrophilic interactions of proteins [25].  $D_h$  measurement evaluated the stability of native CMs and CM-Tgase in the presence of 8 M of urea (Figure 12). Native CMs in the presence of urea (8 M) were dissociated as a result of the rupture of hydrophobic interactions between the tails of caseins surrounding the nanoclusters of CCP and it was not possible to determine their  $D_h$  by DLS [25]. Cross-linked CMs were not dissociated and have a  $D_h$  of  $284 \pm 2$  nm. At acid pH, CMs-Tgase resisted to the dissociation and a significant decrease in  $D_h$  was observed between pH 2.5 and 2.0. Globally, CMs-Tgase swelled from pH 7.0 to 5.0 whereas their  $D_h$  decreased between pH 2.5 and 2.0. Comparable results were observed at neutral pH for CMs

cross-linked by TGase in the presence of 6 M urea [119][120]. Two explanations for this phenomenon were raised by the authors. In the first work, [119], the authors interpreted the swelling as a consequence of a “hydrophobic hydration” of the polymer chains within the CMs. In the second work, [120], the authors did not observe significant difference between the SANS spectra of control and cross-linked CMs, and attributed the increase in  $D_h$  to the presence of “dangling” ends formed after the disruption of weak interactions by urea. The colloidal properties of CMs were progressively changed by the Tgase cross-linking, whereas the micellar unit was preserved.

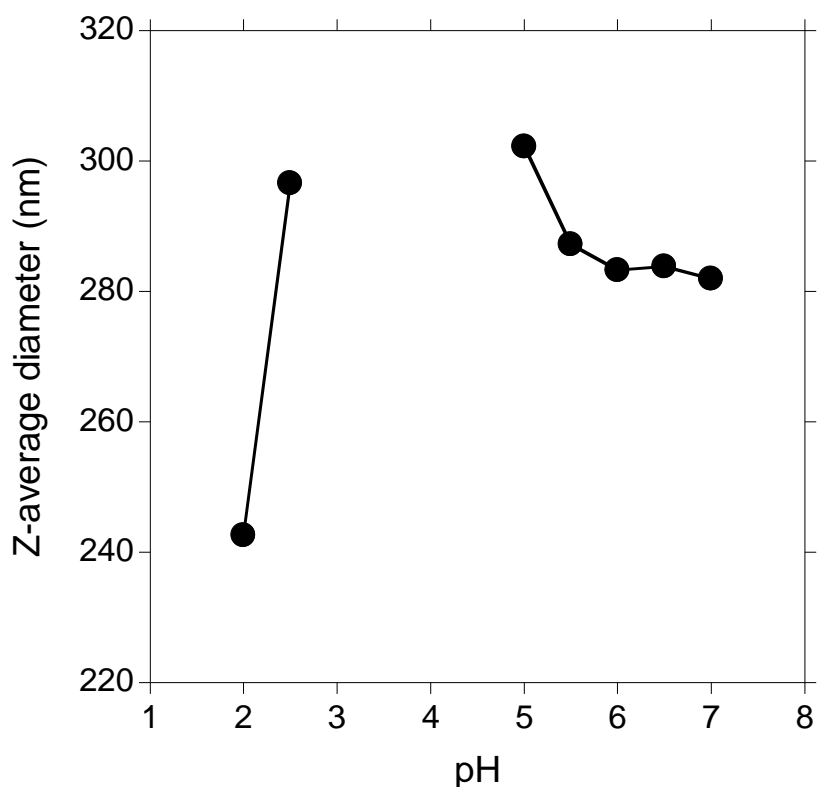


Figure 12: Z-average  $D_h$  (nm) as a function of pH of CMs-Tgase in presence of 8 M urea. Data corresponded to an average of 6 determinations. The standard deviation was < 5%. The vertical error bars, comprised in points, indicate the standard error. For native CMs the determinations were not possible due to their dissociation.

#### 2.2.3.4 Addition of sodium citrate

Addition of sodium citrate induces the solubilization of CCP and causes dissociation of CMs [149].  $D_h$  of cross-linked CMs in the presence of sodium citrate are presented in Figure 13. In the presence of 100 mM sodium citrate, native CMs were dissociated and their  $D_h$  were not measurable by DLS. On the contrary, cross-linked CMs were not dissociated and swelled inversely from pH 7.0 with an average  $D_h$  of 330 nm to pH 5.0 with an average  $D_h$  of 410 nm. In acid pH and close to their isoelectric point, CMs-Tgase have a significant decrease in  $D_h$ . Similar effects were observed in two studies. Huppertz et al. [120] observed that the presence of 50 mM of sodium citrate caused swelling of cross-linked CMs, rather than their disruption due to their internal cross-linking. The same behavior was also determined by Nogueira et al. [4] with cross-linked CMs with GP. The authors observed that CMs-GP did not dissociate and swelled inversely to GP concentration. According to the authors, when the CCP is solubilized at neutral pH in presence of citrate, the negative charges carried out by the phosphate centers of  $\alpha S_{1-}$ ,  $\alpha S_{2-}$ , and  $\beta$ -caseins were exposed. As a consequence, the cross-linked CMs were swollen due to the electrostatic repulsions generated in the core of the particles, and the increase in the hydration of the uncovered protein sequences containing the phosphate centers.

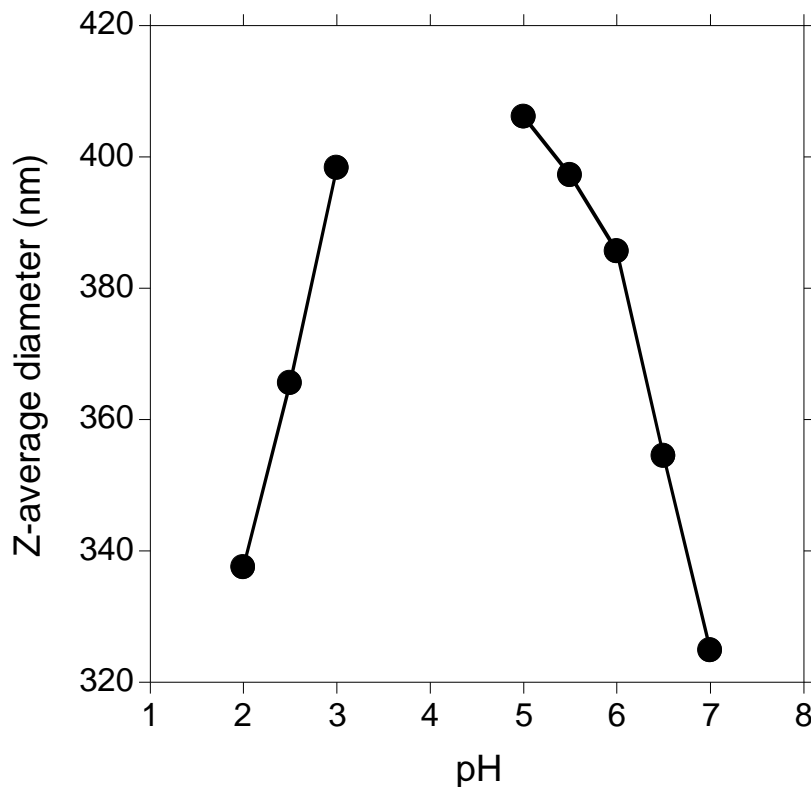


Figure 13: Z-average  $D_h$  (nm) as a function of pH of CMs+Tgase in the presence of 100 mM sodium citrate. Data correspond to an average of 6 determinations. The standard deviation was < 5%. The vertical error bars, comprised in points, indicate the standard error. For native CMs determination of  $D_h$  were not possible due to their dissociation.

### 2.2.3.5 Heat coagulation time (HCT)

The evolutions of the HCT of native CMs and CMs-Tgase, as a function of the pH, are showed in Table 8. In the pH range 7.0 to 5.0, HCT of native CMs decreased from 99 to 5 s whereas the HCT for CMs-Tgase decreased from 162 to 16 s.

The decrease of pH induces a decrease of  $\zeta$ -potential of the caseins (Fig. 2) therefore a decrease in their electrostatic repulsions which can lead to their aggregation caused by high temperature. This induce the increase of hydrophobic bonds, reducing the steric repulsions between the casein micelles and consequently promoting visible coagulation [150–153]. From pH 3.0 to pH 2.0 CMs-Tgase presented high stability against heat coagulation. HCT were 442 and 534 s at pH 3.0 and 2.0, respectively. These results may be explained by strong electrostatic repulsions between casein molecules. Indeed, as shown in Fig. 2, the  $\zeta$ -potentials of CMs and CMs-Tgase at pH 2.0 were approximately + 28 mV.

**Table 8 : Heat Coagulation Time (HCT) (s) at different pH values at 140 °C of native CMs and CMs-Tgase. Measurements were performed in triplicate for 3 different suspensions. For native CMs and CMs-Tgase, the determinations between pH 5.0 and 3.0 were not possible due to the presence of precipitate. At pH below 3.0, native CMs were not monodisperse and  $D_h$  was not determined.**

pH	HCT (s)	
	Native CMs	CMs-Tgase
7.0	99 ± 1	162 ± 3
6.5	71 ± 1	92 ± 3
6.0	47 ± 1	73 ± 4
5.5	21 ± 2	41 ± 2
5.0	5 ± 1	16 ± 1
3.0	-	442 ± 3
2.5	-	478 ± 4
2.0	-	534 ± 1

### 2.2.3.6 Ethanol stability

Table 9 reported the stability, expressed in % of ethanol, of native CMs and CMs-Tgase as a function of the pH. At all pH studied, CMs-Tgase presented higher stability compared to native CMs. Near the  $pI$ , increasing concentrations of ethanol induce the collapse of  $\kappa$ -casein and the aggregation of native and cross-linked CMs [141]. Below the  $pI$ , and at acidic pH, only the ethanol stability of CMs-Tgase was determined. In a pH range from 3.0 to 2.0, CMs-Tgase stability was observed at 99.5%. It is an indicative that in this condition the electrostatic repulsions were not sufficiently affected by the addition of ethanol [134]. Similar results were observed by Huppertz [134] for CMs cross-linked with transglutaminase at 30 °C at different incubation times in pH range 7.0 – 5.0. In this study, the authors interpreted the results as a transformation of the original “absorbed” polyelectrolyte brush into a



“grafted” polyelectrolyte brush on the surface of CMs. These “grafted” brushes induce a better stability against ethanol-induced coagulation.

**Table 9 : Ethanol stability (v/v) at different pH values of native CMs and CMs-Tgase. Measurements were performed in triplicate for 3 different suspensions. For native CMs and CMs-Tgase, the determinations between pH 5.0 and 3.0 were not possible due to the presence of precipitate. At pH below 3.0, native CMs were not monodisperse.**

Ethanol stability (% ethanol v/v)		
pH	Native CMs	CMs-Tgase
7.0	61 ± 2	88 ± 2
6.5	56 ± 2	81 ± 2
6.0	51 ± 2	76 ± 2
5.5	26 ± 2	71 ± 2
5.0	13 ± 2	56 ± 2
3.0	-	99 ± 0
2.5	-	99 ± 0
2.0	-	99 ± 0

### 2.2.3.7 Statistical interactions among variables

Pearson’s correlation coefficients were used to analyze the experimental datas. Values close to -1 or 1 indicated a strong linear correlation between 2 variables. Results are presented in Table 10. For native CMs and CMs-Tgase, a strong and negative correlation was established between  $\zeta$ -potential and pH. Equations 2 (native CMs) and 3 (CMs-Tgase) are empirical models of these relations.

$$\zeta = 1.8pH^3 - 25 pH^2 + 94.6 pH - 78.9 (R^2 = 0.970) \quad (2)$$

$$\zeta = 1.7pH^3 - 21 pH^2 + 68.9 pH - 38 (R^2 = 0.960) \quad (3)$$

Significant correlation was observed between stability at 140 °C (HCT) or stability in presence of ethanol (Eth) and pH. Compared to native CMs, CMs-Tgase were less sensitive to acidic pH in terms of precipitation by ethanol or during heat treatment. Similar behaviors were found for cross-linked CMs with GP, where correlation coefficient were -0.97 and -0.71 for native CMs and CMs-GP, respectively [117]. Regarding to their  $D_h$  in the presence of urea 5 M (results not shown), for native CMs, a high correlation was observed (-0.97), whereas for CMs-Tgase,  $D_h$  was not affected by the presence of this dissociating agents. Native CMs and cross-linked CMs were strongly modified in the presence of 100 mM citrate. Equations 4 and 5 were empirical models of these relations.

$$\varnothing = -3.0 pH^2 + 16.5 pH + 295 \quad (R^2 = 0.985) \quad (4)$$

$$\varnothing = -15.7pH^2 + 148 pH + 57 \quad (R^2 = 0.998) \quad (5)$$

High correlations was observed between  $\zeta$ -potential and ethanol stability for CMs-Tgase (-0.99). At the same time, a high but not significant coefficient (-0.84) was achieved for native CMs.

**Table 10 : Pearson correlation coefficients among variables for native CMs and CMs-Tgase structures.  $D_h$  = hydrodynamic diameter (nm); Eth = ethanol stability;  $\zeta$  = zeta potential; HCT= Heat coagulation time. <sup>1</sup>correlations established from pH 7.0 to 5.5 for native CMs; <sup>2</sup>correlation established from pH 7.0 to 2.0 for CMs-Tgase;**

<b>Coefficient Correlation</b>	<b>Native CMs<sup>1</sup></b>	<b>CMs-Tgase<sup>2</sup></b>
$\zeta$ x pH	-0.97*	-0.96
HCT x pH	0.99*	0.92
Eth x pH	0.95*	-0.77
$\varnothing$ x pH urea (8 M)	-0.97*	-0.86
$\varnothing$ x pH citrate (100 mM)	-	-0.97
$\zeta$ x Eth	-0.84*	-0.99

#### **2.2.4 Conclusion**

In this work, the stabilities of native CMs and CMs cross-linked by Tgase were studied. Their respective stabilities against dissociating agents, ethanol and HCT were explored in pH range between 7.0 to 2.0. Cross-linked CMs by Tgase showed a higher stability than native CMs in all studied conditions. Compared to native CMs, CMs-Tgase have higher stabilities at pH 2.0, in the presence of 100 mM of sodium citrate, 8 M urea, 99.5% (v/v) of ethanol and HCT superior to 500 s. According to literature, Tgase increased stability of CMs by their reticulation with a stabilization of polyelectrolyte brush of  $\kappa$ -casein. These results show the potential application of CMs-Tgase as functional nanocarrier for bioactive compounds, especially in acidic conditions at acid pH for example.

## PART B

Based on the results obtained in PART A, in this section we investigate first on the possible interactions between casein molecules and C3G under acidic (pH 2.0) and neutral (pH 7.0) conditions. Afterwards, we explored if CMs cross-linked with Tgase can be used as nanocarrier for C3G at pH 2.0 and at pH 7.0. The objective of this part is to determine binding constant and thermodynamic parameters.

### Questions

- What is the mechanism of interaction between C3G and casein?
- Cross-linking can be influenced the mechanism of interaction?
- Cross-linked CMs can be used as potential nanocarrier for C3G?

### **Main results**

- Casein and native or cross-linked CMs, binding spontaneously with C3G at pH 7.0 and pH 2.0.
- Based on the results, cross-linking don't affect the interaction between CMs and C3G. At pH 2, hydrophobic driven these interactions whereas at pH 7 electrostatic interactions, hydrogen bonding and Van der Waals forces are the dominant binding forces.
- Cross-linked CMs can be used as potential nanocarrier for C3G

## **2.3 Interaction of cyanidin-3-O-glucoside with sodium caseinate**

The content of this chapter is under submission to

*Food Chemistry*

Federico Casanova, Thomas Croguennec, Anne Laure Chapeau, Pascaline Hamon,  
Antonio F. de Carvalho, Saïd Bouhallab

The experimental part, the discussion and the redaction of the paper was realized at INRA-STLO (Rennes, France) in the ISF-PL team during my visiting as Ph.D. student.

### 2.3.1 Introduction

Anthocyanins are natural pigments widely distributed in flowers, vegetables and fruits, to which they give bright colours from red to blue [154]. Anthocyanins are sugar conjugates of flavonoids, which belong to the class of phenolic compounds [155]. Their basic structure is constituted with a flavylum cation (2-phenylbenzopyrylium) [156]. They are classified into various groups according to the different numbers and positions of hydroxyl and methoxyl groups, as well as to the various types of sugars attached to the benzene-ring [157]. Cyanidin-3-O-glucoside (C3G) is the most widespread anthocyanins in plants (Scheme 1).

In recent decades, interest for anthocyanins has been growing due to their putative health promoting properties. Numerous publications suggest that anthocyanins have vasoprotective [8], anti-inflammatory [9], anticancer [10], antimicrobial [11] and antidiabetic effects [12], all of which are more or less associated to anthocyanin antioxidant properties. Based on these reported properties it is of interest for food manufacturers to add anthocyanins in their products in order to improve consumer

health and well-being. However the chemical and structural stability of anthocyanins is affected by pH, temperature increase, UV light radiation and oxygen exposure [15][158]. In acidic pH conditions, anthocyanins can be found under different chemical forms in equilibrium (quinoidal blue species, colourless carbinol pseudobase and chalcone) but at pH values higher than 7, they are degraded in different species depending on their substituent groups [159]. The formation of anthocyanins/protein complexes was suggested to be a promising approach to overcome chemical instability drawbacks. In this way, several papers have studied the interactions between cyanidine and model proteins such as bovine serum albumin, hemoglobin, myoglobin [160],  $\alpha$ -casein,  $\beta$ -casein [61] and human serum albumins [161] at neutral pH.

In the present study the interaction between caseins (Cas) and C3G was investigated at pH 7 and pH 2, pHs for which the global charge of the caseins is negative and positive, respectively. Cas were selected because they were considered as intrinsically unfolded proteins due to their high poly-proline structural content [162], which were shown to have strong interactions with polyphenols [163]. Away from their pI (4.6), Cas exist as small assemblies of a tenth of caseins in loose electrostatic and hydrophobic interactions [164][149]. The Cas - C3G interaction was followed by fluorescence spectroscopy, which is an appropriate technique to characterize the binding properties (binding constant and number of binding sites) and the thermodynamic parameters of the interaction due to its high sensitivity and ease to implementation. Sodium caseinate, a well-known dairy protein ingredient was used as casein source.

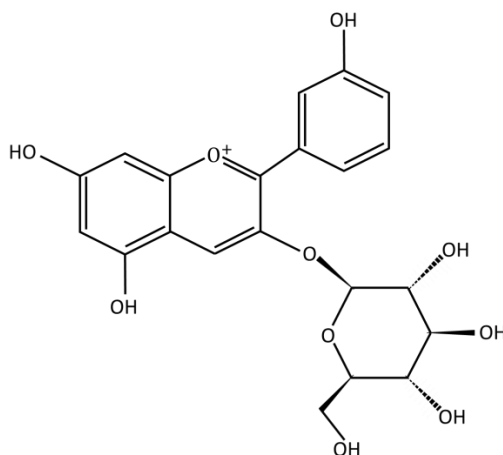


Figure 14 : Chemical structure of cyanidin-3-O-glucoside

## 2.3.2 Materials and methods

### 2.3.2.1 Sample preparation

Sodium caseinate powder was prepared in-house from raw skim milk according to [165]. Two stock solutions of Cas were prepared by dispersing sodium caseinate powder at  $27.5 \text{ g.L}^{-1}$  ( $1.2 \text{ mM}$ ) either in  $25 \text{ mmol.L}^{-1}$  of 4-(2-hydroxyethyl)-1-piperazine ethanesulfonic acid (HEPES) and  $2 \text{ mmol.L}^{-1}$   $\text{CaCl}_2$  at pH 7 or in  $25 \text{ mmol.L}^{-1}$  of KCl / HCl and  $2 \text{ mmol.L}^{-1}$   $\text{CaCl}_2$  at pH 2. Sodium azide (Acros Organics, New Jersey, USA) was added in the Cas stock solutions for having a final sodium azide concentration of  $0.30 \text{ g.L}^{-1}$  in order to prevent microbial growth. The solutions were slowly stirred during 48 h. Before analysis, the Cas stock solutions were further diluted at  $4 \text{ }\mu\text{M}$  with the appropriate buffer at pH 7 or at pH 2. In some Cas solutions NaCl was added. Cyanidin-3-O-glucoside (C3G) stock solution was prepared by diluting Cyanidin-3-O-glucoside (purity > 96 %) (Extrasynthese, Genay, France) at  $1 \text{ mM}$  in  $25 \text{ mmol.L}^{-1}$  KCl / HCl and  $2 \text{ mmol.L}^{-1}$   $\text{CaCl}_2$  at pH 2. The Cyanidin-3-O-glucoside stock solution was further diluted at  $40 \text{ }\mu\text{M}$  and  $100 \text{ }\mu\text{M}$  with the  $25 \text{ mmol.L}^{-1}$  KCl / HCl and  $2 \text{ mmol.L}^{-1}$   $\text{CaCl}_2$  buffer at pH 2 for titration at low and medium C3G/ Cas molar ratio.

### 2.3.2.2 Intrinsic fluorescence spectroscopy

Protein intrinsic fluorescence was determined using a Safas FLX-Xenius fluorimeter (Monaco, France) equipped with a temperature-controlled 96-wells microplate. Excitation wavelength was set at 280 nm and emission spectra were recorded between 300 and 450 nm. A volume of  $200 \text{ }\mu\text{l}$  of Cas solutions at  $4 \text{ }\mu\text{M}$  was placed in the wells and in each well one injection of C3G solution at  $40 \text{ }\mu\text{M}$ ,  $100 \text{ }\mu\text{M}$  or  $1 \text{ mM}$  was done in order to cover the C3G/ Cas molar ratio range from 0 to 10. The larger injection of C3G solution in the wells was  $20 \text{ }\mu\text{L}$  in order to avoid excessive Cas dilution. The mixtures were agitated and fluorescence measurements were taken after 5 min of equilibration. The titrations were conducted at 295, 299, 305, 309 and 315 °K. Each titration was performed twice using independent Cas and C3G solutions and in triplicate using the same Cas and C3G solutions. The fluorescence data were



analyzed on Kaleidagraph (Synergy Software) in order to determine the binding constant and the number of binding site of the interaction.

### 2.3.2.3 Hydrodynamic diameter and $\zeta$ -potential measurements

The hydrodynamic diameter ( $D_h$ ) and the zeta-potential ( $\zeta$ ) of C3G/Cas complexes were determined using a Zetasizer Nano-S (Malvern Instrument, Worcestershire, UK). Cas solutions was at 4 $\mu$ M and the C3G/ Cas molar ratio ranged from 0 to 10.

The hydrodynamic diameter ( $D_h$ ) of the C3G/Cas complexes at 22°C was obtained from dynamic light scattering measurements over 2 min using a backscattering angle of 173° and a wavelength of 633 nm. Experimental data were analyzed using the general purpose model. The  $D_h$  of C3G/Cas complexes was calculated by the Stokes-Einstein equation using the diffusion coefficient ( $D_t$ ) extracted from the fit of the correlation curve and solution viscosity,  $\eta$ , of 1.033 Pa.s<sup>-1</sup> as follow:

$$D_h = \frac{K_B T}{3\pi\eta D_t} \quad (1)$$

where  $K_B$  is the Boltzmann's constant and  $T$ , the temperature.  $D_h$  was expressed as Z-average value. Each experiment was repeated 5 times.

$\zeta$ -potential ( $\zeta$ ) measurements were performed at a voltage of 50 V.  $\zeta$ -potential was calculated from the electrophoretic mobility ( $\mu$ , V Pa<sup>-1</sup> s<sup>-1</sup>) of the C3G/Cas complexes using the Henry equation, as follow:

$$\zeta = \frac{3\eta\mu}{2\varepsilon f(\kappa R_H)} \quad (2)$$

where  $\eta$  is the viscosity of buffer (1.033 x 10<sup>-3</sup> Pa s<sup>-1</sup>),  $\varepsilon$  is the medium dielectric constant (dimensionless),  $R_H$  is the complex radius (nm) and  $f(\kappa R_H)$  is the Henry's function. Since the analysis is conducted in aqueous media a value of 1.5 was adopted for  $f(\kappa R_H)$ , which is referred to as the Smoluchowski approximation.

## 2.3.3 Results and discussion

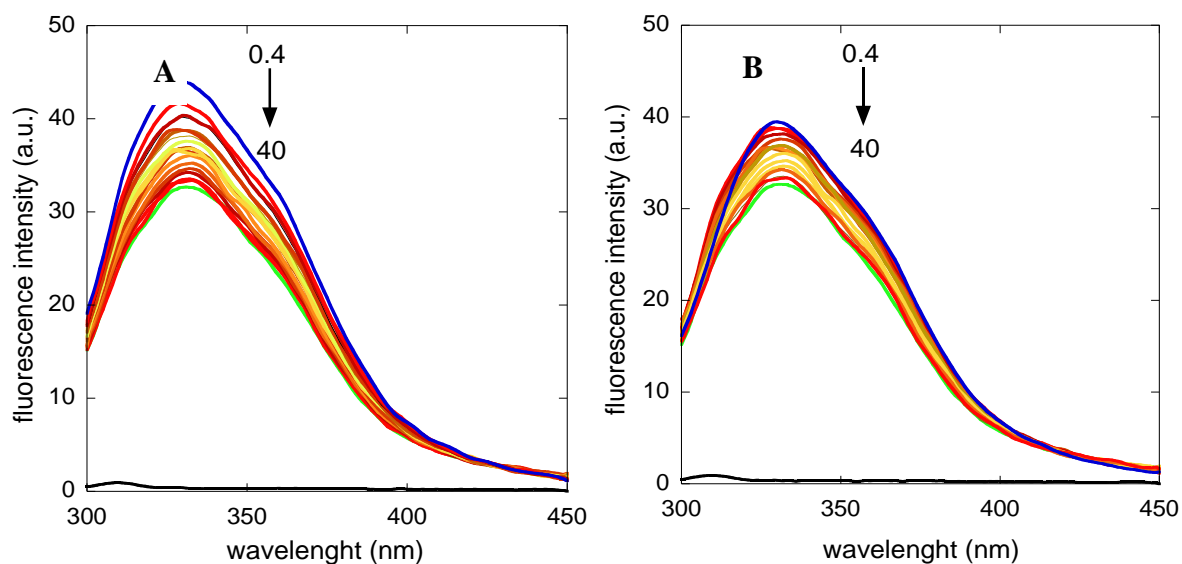
### 2.3.3.1 Cas intrinsic fluorescence quenching by C3G

Figure 15 shows the fluorescence emission spectra of the Cas solutions at pH 7 and pH 2 in the absence and presence of increasing concentrations of C3G (C3G / Cas molar ratio from 0 to 10). The maximum emission wavelength of Cas after excitation at 280 nm was around 330 nm for all samples. The fluorescence intensity of Cas decreased with increasing amount of C3G in the solution (quenching mechanism), suggesting an interaction between Cas and C3G. The intrinsic fluorescence of Cas was decreased of 27 % and 18 % after addition of 40  $\mu\text{M}$  of C3G at pH 7 and pH 2, respectively. Fluorescence quenching has two main mechanisms, generally divided into dynamic quenching and static quenching. According to Lakowicz [166], dynamic quenching results from collisional encounters between the fluorophore and the quencher, whereas static quenching results from the formation of a ground-state complex between the fluorophore and the quencher. To differentiate which one of the two quenching mechanisms was implicated in Cas - C3G interaction, the data were plotted using the Stern-Volmer equation (Figure 2):

$$F_0/F = 1 + K_{sv}[C3G] = K_q\tau_0[C3G] \quad (3)$$

Where  $F_0$  and  $F$  represent the fluorescence intensities of the protein in the absence and in the presence of increasing concentration of the C3G  $[C3G]$ , respectively.  $K_{sv}$  is the Stern-Volmer constant which can be written as  $K_{sv} = K_q\tau_0$  where  $K_q$  is the bimolecular quenching constant and  $\tau_0$  is the lifetime of the fluorophore in the absence of quencher. The value of  $\tau_0$  for Trp is equal to  $10^{-8}$  s [167].  $K_{sv}$  was obtained from the slope of the linear part of the titration curves (Figure 16). The non-monotonic evolution of the fluorescence ratio ( $F_0/F$ ) during titration suggested the existence of more than one quenching modes (in fact two quenching modes corresponding to the binding of C3G to two independent sets of binding sites on Cas as indicated by Scatchard plot, see below). At pH 7 and pH 2,  $K_{sv}$  had a magnitude order of  $10^4 \text{ M}^{-1}$  for the two quenching modes corresponding to  $K_q$  values of  $10^{12} \text{ M}^{-1} \cdot \text{s}^{-1}$ . These values were much higher than the diffusion limited quenching ( $2 \times 10^{10} \text{ M}^{-1} \cdot \text{s}^{-1}$ ) indicating that the quenching of Cas fluorescence by C3G followed a static mechanism [166]. In addition, Cas fluorescence quenching by C3G was studied at four other temperatures (299, 305, 309 and 315 °K). Increasing the temperature

induced a decrease of  $K_{SV}$  at pH 7 and 2 (data not show) confirming the Cas fluorescence quenching by C3G followed a static mechanism [61].



**Figure 15: Fluorescence emission spectra of Cas (4  $\mu\text{M}$ ) at pH 7 (A) and pH 2 (B) and at 295  $^{\circ}\text{K}$  in the absence and presence of increasing concentrations of C3G (from 0.4 to 40  $\mu\text{M}$ ). Black line corresponds to the fluorescence spectra of C3G at 40  $\mu\text{M}$  in the absence of caseins.**

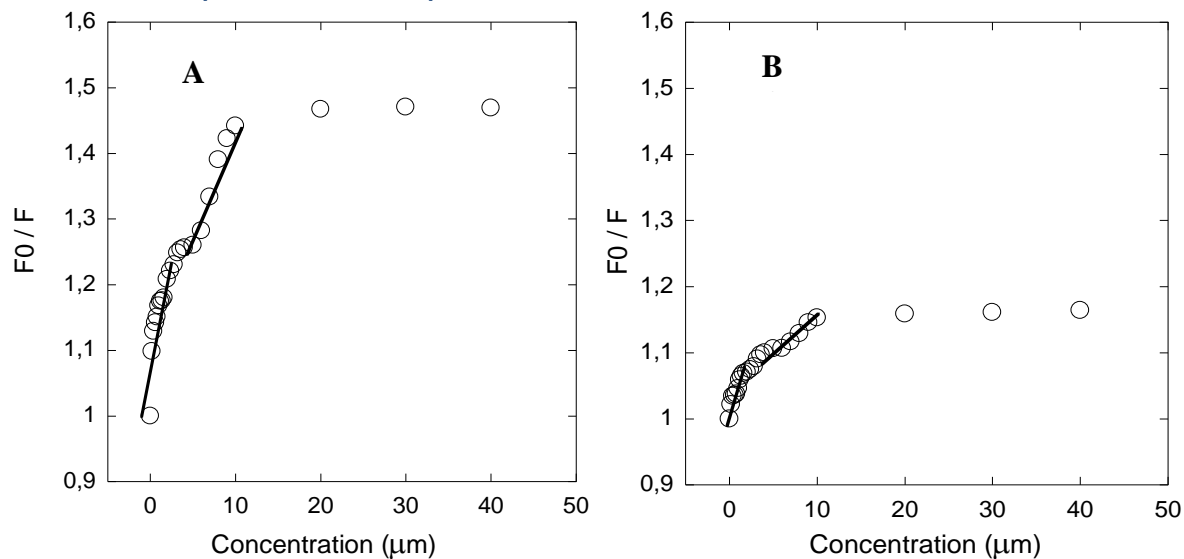


**Figure 16: Stern-Volmer plots of the quenching of Cas fluorescence by C3G at pH 7 (A) and Cas pH 2 (B) and at 295  $^{\circ}\text{K}$ .**

### 2.3.3.2 Binding constants

When ligands interact with a macromolecule according to a static mechanism, each ligand binding can be characterized by a binding constant,  $K_a$ . Firstly, for determining the binding constant of the interaction,  $K_a$ , experimental data were analyzed using the Scatchard representation, which consider the binding of C3G to independent sets of binding sites of Cas. In this representation  $\frac{fi P_{total}}{L_{total}}$  is plotted versus  $fi P_{total}$ , and the slope of the fit is used to determine  $K_a$ [168].  $fi$  is calculated using the Cas fluorescence intensity value in the absence of C3G ( $F_0$ ), the fluorescence intensity value during titration of Cas solutions with C3G ( $F$ ) and the fluorescence intensity value at saturation ( $F_{min}$ ) using the following equation:

$$fi = \frac{F_0 - F}{F_0 - F_{min}} \quad (4)$$

Figure 17 A and B shows the Scatchard plots for the Cas-C3G interaction at pH 7 and pH 2 at 295 °K. The plots show two well-separated domains suggesting the existence of two sets of binding sites for C3G on Cas at the two pHs. The data in these two domains were fitted independently by linear regression. The binding constants  $K_{a1}$  and  $K_{a2}$  (for the two sets of binding sites) were in the same range at pH 7 and pH 2 with  $K_{a1}$  larger than  $K_{a2}$  by a factor of around 10 (Table 1). These values indicated that the interaction between Cas and C3G was of strong affinity. They were in the same order of magnitude than the binding constants determined for the interaction between Cas and another flavonoid, pelargonidin [169]. These authors suggested that the high flexibility of Cas structure is responsible of the strength of the interactions.

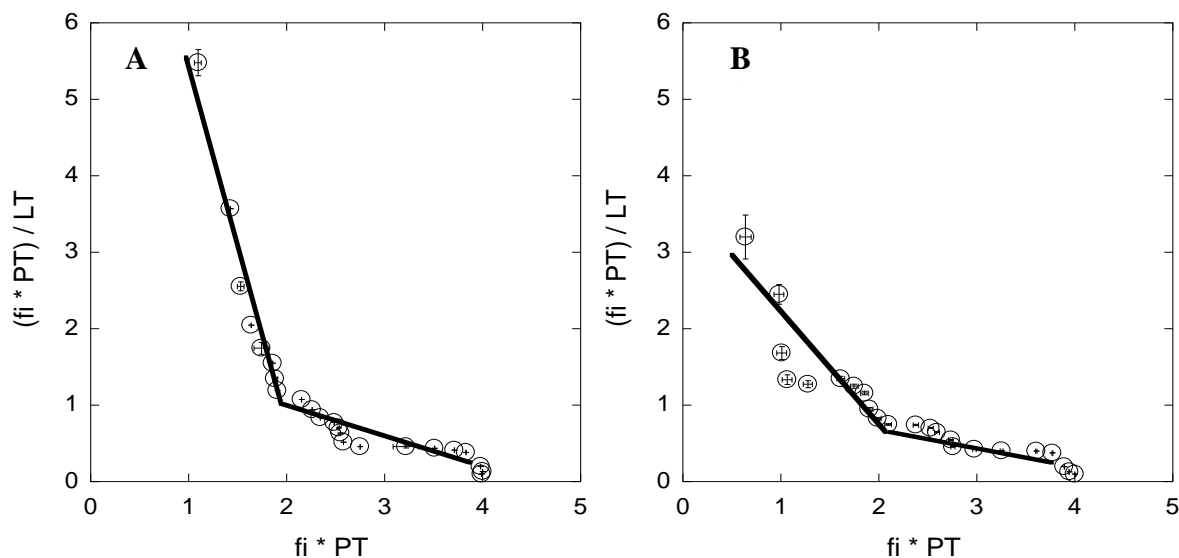


Figure 17: Scatchard plot of Cas (4  $\mu\text{M}$ ) at pH 7 (A) and pH 2 (B) titrated with an increasing concentration of C3G (from 0.4 to 40  $\mu\text{M}$ ) at 295  $^{\circ}\text{K}$ .

The binding constants were further determined at temperatures 299, 305, 309, 315  $^{\circ}\text{K}$  (Table 11).  $Ka_1$  and  $Ka_2$  decreased with increasing temperature at pH 7 whereas an increasing trend is observed at pH 2. In addition, the ratio between  $Ka_1$  and  $Ka_2$  decreased from 15 to 10 at pH 7 and increased from 5 to 10 at pH 2 in the investigated temperature range.

Table 11 : Binding affinity of C3G to Cas at different temperatures.

Compound	T ( $^{\circ}\text{K}$ )	$Ka_1$ ( $\times 10^6 \text{M}^{-1}$ )	$Ka_2$ ( $\times 10^6 \text{M}^{-1}$ )
----------	-----------------------------	---	---

Cas pH 7	295	5.11	0.33
	299	4.93	0.31
	305	3.26	0.21
	309	2.73	0.20
	315	2.12	0.21
Cas pH 2	295	1.31	0.26
	299	1.96	0.29
	305	2.98	0.37
	309	3.18	0.42
	315	6.51	0.65

### 2.3.3.3 Thermodynamic analysis and nature of the binding forces

The different temperature-dependent evolution of  $Ka$  at pH 7 and pH 2 suggested that the interaction mechanism between C3G and Cas was pH-specific. Indeed,  $Ka_1$  and  $Ka_2$  decreased at pH 7 when the temperature increased indicating that the binding reaction was exothermic. In the opposite, the temperature-dependent increase of  $Ka_1$  and  $Ka_2$  at pH 2 suggested an endothermic reaction [170]. Binding constants were used to analyze the thermodynamic parameters (enthalpy change,  $\Delta H$ ; entropy change,  $\Delta S$ ) of the interaction and to address the main binding forces involved [171]. Isothermal titration calorimetry experiments, titration of Cas solution by successive injection of C3G, confirmed the exothermic and endothermic signals at pH 7 and 2, respectively. Unfortunately, the very high energy associated to proper injection of C3G (dissociation energy) limited further use of this powerful technique. Basically, four types of non-covalent bonds (hydrogen, van der Waals, electrostatic and hydrophobic) participate in protein - ligand complex formation. They have specific thermodynamic signature [171], but the dissection of their contribution in a binding process is difficult because the formation and breaking of many bonds occurred simultaneous [172]. Only the dominant binding forces could be extracted from the analysis of the thermodynamic parameters of the binding reaction. These parameters were calculated by using Van't Hoff equation as follow:

$$\ln Ka = -\frac{\Delta H}{RT} + \frac{\Delta S}{R} \quad (8)$$

$$\Delta G = \Delta H - T \Delta S \quad (9)$$

Where  $R$  is the gas constant ( $8.314 \text{ J mol}^{-1} \text{ K}^{-1}$ ) and  $T$  is the temperature ( $^{\circ}\text{K}$ ). Thermodynamic parameters  $\Delta H$  and  $\Delta S$  were determined from the slope and abscissa of the plot  $\ln K_a$  versus  $1/T$  (Figure 18 A and B). The free energy change  $\Delta G$  of the interactions was calculated from (9). The values of  $\Delta G$  at different temperatures are listed in Table 12. The values of  $\Delta G$  for  $K_{a1}$  and  $K_{a2}$  at pH 7 and pH 2 are negative, indicating that the binding process is thermodynamically favorable (spontaneous). Cas-C3G interaction at pH 7 presented negative  $\Delta H$  ( $-36$  and  $-21 \text{ KJ mol}^{-1}$  for  $\Delta H_1$  and  $\Delta H_2$  respectively) and positive  $\Delta S$  ( $5$  and  $35 \text{ J mol}^{-1} \text{ K}^{-1}$  for  $\Delta S_1$  and  $\Delta S_2$  respectively) indicating that the binding reaction is enthalpy- and entropy-driven. Favorable enthalpy indicated that the interaction between Cas and C3G at pH 7 was governed by electrostatic and/or van der Waals bonds [171][173]. The entropic term probably came from the release water molecules bound to C3G and Cas upon complex formation [172]. It is interesting to note that enthalpy and entropy contributions differed for the 2 sets of binding sites. The first set of binding site was characterized by a large enthalpy of interaction and a minor favorable entropy of interaction ( $|\Delta H| > |T\Delta S|$ ) which could indicate a larger contribution of van der Waals bonds [173] while the second set of binding sites mainly involved electrostatic bonds [171]. In contrast, Cas – C3G interaction at pH 2 had positive  $\Delta H$  ( $57$  and  $34 \text{ KJ.mol}^{-1}$  for  $\Delta H_1$  and  $\Delta H_2$  respectively) and positive  $\Delta S$  ( $311$  and  $219 \text{ J mol}^{-1} \text{ K}^{-1}$  for  $\Delta S_1$  and  $\Delta S_2$  respectively) indicating an entropy-driven process typical of an interaction involving hydrophobic bonds [171]. This was confirmed by the more negative values of  $\Delta G$  with increasing temperature for the two sets of binding sites at pH 2. Regarding Cas and C3G structural features, “stacking” interactions between aromatic rings [174] and the displacement of bound water molecules upon C3G binding to Cas [172] could be the reason of this entropy-driven interactions at pH 2.

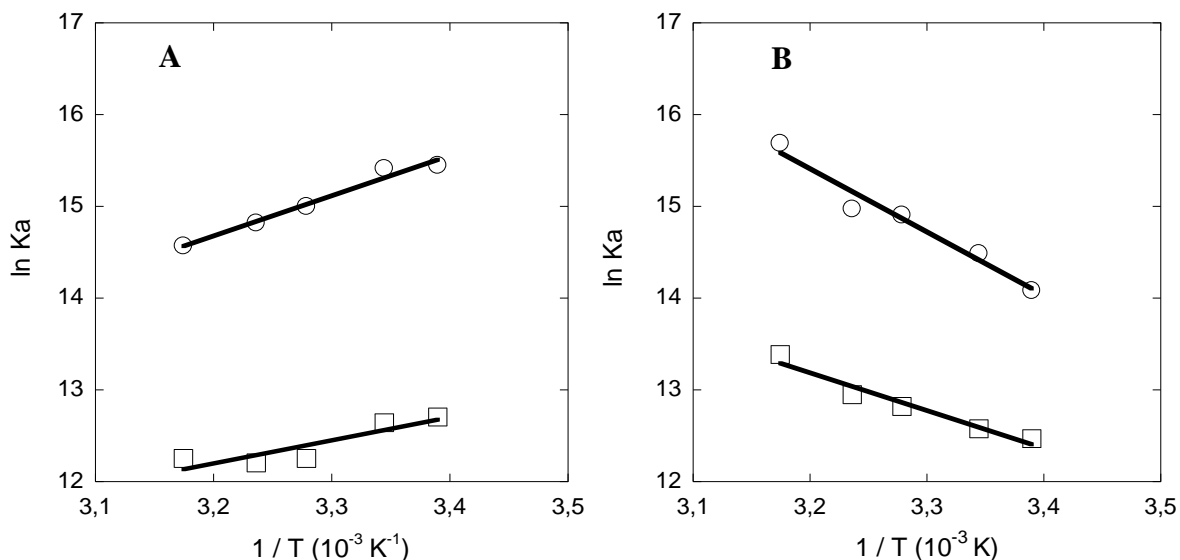


**Figure 18:** Variation of  $\ln K_a$  as a function of  $1/T$  for the two C3G classes of binding site on Cas at pH 7 (A) and at pH 2(B). ( $\circ$ ) correspond to the first class of binding site and ( $\square$ ) correspond to the second class of binding site.

**Table 12.** Thermodynamic parameters of Cas / C3G interaction at pH 7 and pH 2 at different temperatures.

Compound	T (°K)	$\Delta H_1$ (KJ / mol)	$\Delta S_1$ (J / mol K)	$\Delta G_1$ (KJ / mol)	$\Delta H_2$ (KJ / mol)	$\Delta S_2$ (J / mol K)	$\Delta G_2$ (KJ / mol)
Cas pH 7	295	- 36	5	- 38.0	- 21	35	- 31.1
	299			- 38.0			- 31.2
	305			- 38.1			- 31.4
	309			- 38.1			- 31.6
	315			- 38.1			- 31.8
Cas pH 2	295	57	311	- 37.1	34	219	- 31.9
	299			- 38.3			- 32.7
	305			- 40.1			- 34.0
	309			- 41.2			- 34.8
	315			- 43.0			- 36.1

#### 2.3.3.4 Effect of NaCl on Cas – C3G interaction

To confirm the main binding forces involved in Cas – C3G interaction, the same titrations were done at 295°K in the presence of various amounts of NaCl. Typical fluorescence emission spectra of Cas in the absence (blue line) or saturated with C3G (C3G/Cas molar ratio of 10) without NaCl added (green line) or with 100, 150, 200 mM NaCl (red, black and orange line respectively) at pH 7 and pH 2 were shown



on Figure 19 A and B, respectively. At pH 7, increasing NaCl concentration led to a progressive increase of Cas fluorescence up to values similar to the ones obtained in Cas solution in the absence of C3G (figure 6A). At 200 mM NaCl, the Cas fluorescence quenching by C3G vanished, indicating that the interaction between Cas and C3G was hindered. This result confirmed that electrostatic interactions strongly contributed to the formation of the Cas-C3G complexes at pH 7. It is interesting to note that at intermediate NaCl concentration (100 mM), Cas titration with C3G exhibited single exponential binding isotherm typical of the binding of C3G to one set of binding site on Cas. This was confirmed by the Scatchard plot of Cas titration with C3G at 100 mM NaCl (Figure 20). At 100 mM NaCl, the binding constant of C3G to Cas was still of strong affinity ( $K_a = 1.76 \times 10^6 \text{ M}^{-1}$ ). This Again, this confirmed Cas had two independent sets of binding sites for the binding of C3G, which had different response to NaCl concentration. The first set of binding sites was more resistant to NaCl addition probably because van der Waals bonds contributed to the binding forces in addition to electrostatic bonds. In contrast, electrostatics bonds are the main binding forces involved in the C3G interaction to Cas on the second set of binding site, which in consequence were more sensitive to NaCl addition.

On the other hand, increasing NaCl concentrations up to 200 mM in Cas solutions at pH 2 had no incidence on Cas fluorescence spectra (Figure 19 B). This result confirmed that the formation of Cas-C3G complexes at acidic pH was governed by another mechanism than at pH 7. Cas-C3G interaction at pH 2 was not governed by electrostatic but rather dominated by hydrophobic bonds.

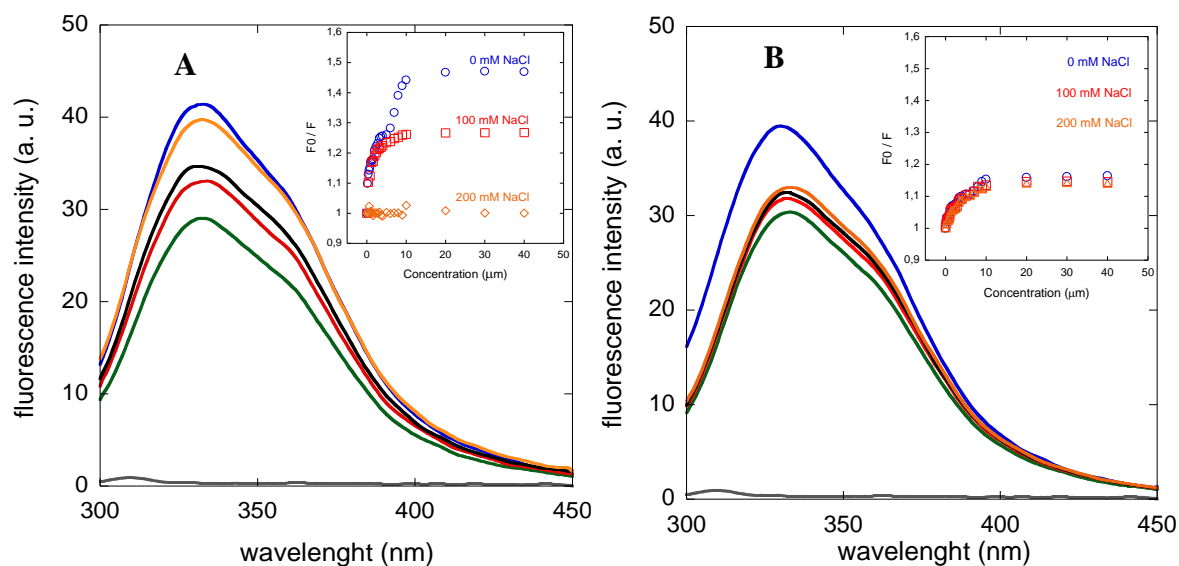


Figure 19: Fluorescence spectra (a. u.) of Cas (4  $\mu\text{M}$ ) in the absence (blue line) or saturated with C3G (C3G/Cas molar ratio of 10) without NaCl added (green line) or with 100, 150, 200 mM NaCl (red, black and orange line) at pH 7 (A) and pH 2 (B). Grey line represent C3G alone. Insert in (A) and (B) show the Stern-Volmer plot of the titration in the absence and the presence of 0 (O), 100 ( $\square$ ) and 200 ( $\diamond$ ) mM of NaCl.

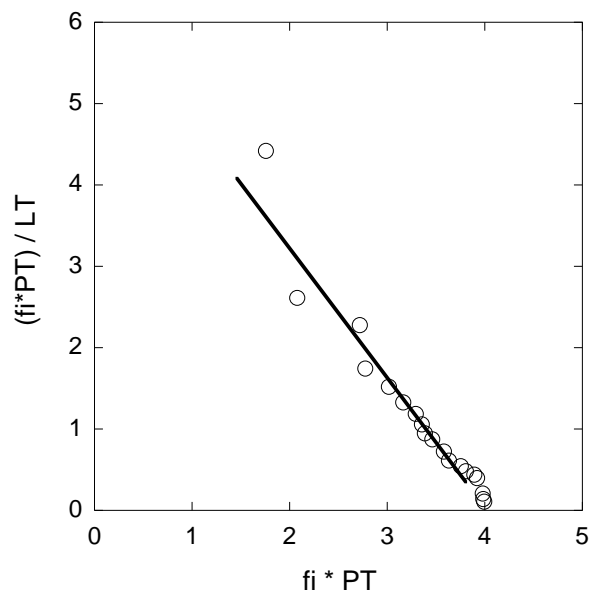


Figure 20: Scatchard plot of Cas (4  $\mu\text{M}$ ) at pH 7 and 100 mM NaCl titrated with an increasing concentration of C3G (from 0.4 to 40  $\mu\text{M}$ ) at 295 °K.

### 2.3.3.5 Z-average hydrodynamic diameter and $\zeta$ -potential of Cas in the presence of C3G

In the absence of  $\text{Ca}^{2+}$ , Cas solution consist of small assemblies of few Cas held together by hydrophobic and electrostatic interactions [164][175]. The assemblies expose to the solvent the most hydrophilic part of the caseins. In the present study these assemblies had a hydrodynamic diameter (Z-average) of  $20 \pm 2$  nm and  $25 \pm 2$  nm at pH 7 and pH 2 respectively (Figure 21). The  $\zeta$ -potential of the assemblies was -

$20 \pm 1$  mV and  $+16 \pm 1$  mV at pH 7 and pH 2, respectively. By increasing C3G concentration, the hydrodynamic diameter slightly increased and at saturation (C3G/Cas molar ratio of 10) this increase is only of 5 nm at pH 7 and pH 2 (Figure 7) but no change in the  $\zeta$ -potential of the assemblies was noticed (data not shown). The fact that the hydrodynamic diameter of the assemblies increased in the presence of C3G is in agreement with the above results showing an interaction between Cas and C3G. The absence of modification of the  $\zeta$ -potential of the assemblies suggested that the interactions between Cas and C3G was predominantly in the interior of the assemblies. Indeed, because of its positive charge, the binding of C3G on the surface of the assemblies would increase the positive charge of the Cas assemblies at pH 2 and would decrease its negative charge at pH 7. This result also explained that the Cas assemblies did not self-assemble into larger aggregates at pH 7 due to charge screening.

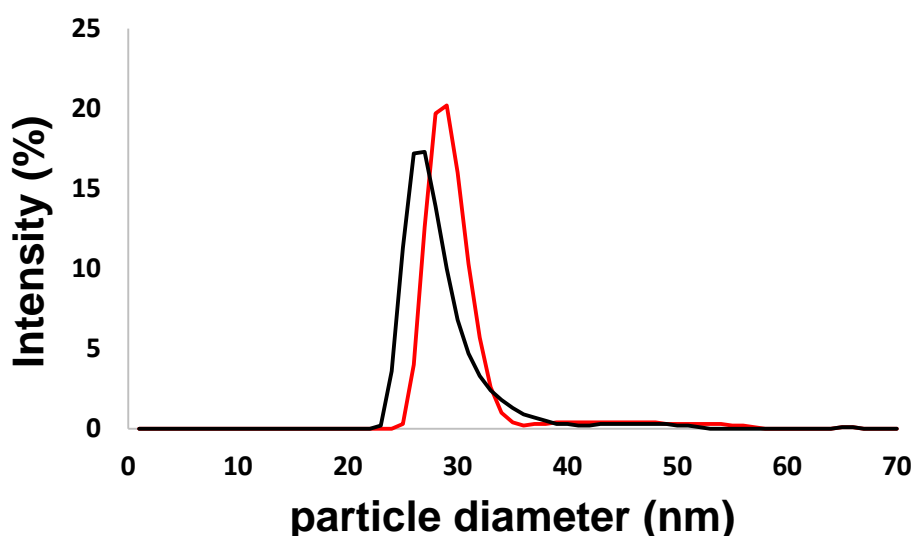


Figure 21: Intensity(%) as a function of particle diameter of Cas ( $0.4 \mu\text{M}$ ) in the absence (black line) and presence of  $40 \mu\text{M}$  of C3G (red line) at pH 2 monitored by dynamic light scattering (DLS).

### 2.3.4 Conclusion

C3G binds spontaneously to two independent sets of binding sites on Cas with a pH-specific mechanism. Hydrophobic-driven interactions were evidenced as the main binding forces in the C3G-Cas complex at pH 2, whereas NaCl-sensitive electrostatic interactions are the dominant binding forces at pH 7. C3G preferentially binds to the Cas part oriented in the interior of Cas assemblies resulting in a slight expansion of

its hydrodynamic diameter but the global charge and the stability in solution of the C3G loaded assemblies are unchanged. The results obtained in this study suggest that Cas assemblies constitute putative nanocarriers for bioactive anthocyanins at acidic and neutral pH. Studies on entrapped C3G stability to external stresses at pH 7 and pH 2 and on *in vitro* release of entrapped C3G are in progress.

## **2.4 Interaction between transglutaminase cross-linked casein micelles and cyanidin-3-O-glucoside**

The content of this chapter is under revision for a submission

Federico Casanova, Thomas Croguennec, Pascaline Hamon, Antonio F. de  
Carvalho, Saïd Bouhallab

The experimental part, the discussion and the redaction of the paper was realized at INRA-STLO (Rennes, France) in the ISF-PL team during my visiting as Ph.D. student.

### 2.4.1 Introduction

Caseins belong to the major protein fraction of bovine milk (approximately 80 %). In milk, caseins are organized as a complex assembly of highly phosphorylated  $\alpha$ S1- (40%),  $\alpha$ S- (10%),  $\beta$ - (35%) and K-casein (15%) with colloidal calcium phosphate (CCP), called casein micelle (CMs) [1]. CMs are highly hydrated (~ 4 g of water per g of protein [1]) with a hydrodynamic diameter of about 200 nm (De Kruif, 1998) and the  $\zeta$ -potential of -20 mV under physiological conditions [126]. CMs are used as functional ingredient in food [176], pharmaceutical [177] and chemical industries [178]. Integrity of CMs depends on the physicochemical conditions of the medium. The destabilization of the CMs and the subsequent coagulation of the caseins occurred when the external layer of K-casein collapse by urea addition, when CCP was solubilized by using calcium chelating salts or by acidification [3]. Their aggregation or coagulation can have a negative impact on the properties of the products they are used in. Hence, the production of stable CMs under various conditions such as at acidic pH could expand their spectra of utilization.

An interesting method to modify CMs structure consists on its cross-linking, by joining two or more molecules by covalent bonds. Glutaraldehyde for example, is a well know cross-linking agent. Silva et al. [112] showed that this compound was able to link lysyl residues of different molecules to form aggregates with high molecular weight. However, due to their toxicity the use of glutaraldehyde cross-linked CMs is limited. Another cross-linking agent is genipin (GP), a natural molecule extracted from *Gardenia jasminoides* [113]. In vitro studies showed that GP is  $10^4$  less cytotoxic than glutaraldehyde [114] and its role as cross-linking agents was investigated in some biological applications [115]. Silva et al. [4][116] have characterized the casein micelles cross-linked by GP. GP cross-linked CMs were (1) formed via cross-linking lysyl and arginyl residues, (2) smaller in size, and (3) more negatively charged with a smoother surface than native casein micelles. Compared to native CMs, GP cross-linked CMs had improved stability in pH range from 7 to 2 (Casanova et al., *paper under review*). Unfortunately, GP is not recognized as safe and further researches on toxicity would be required to implement this material as a food-grade cross-linker. Caseins can be enzymatically cross-linked by

transglutaminase (Tgase), a natural agent of microbial origin recognized as safe. Tgase cross-links proteins by forming covalent bonds between the  $\gamma$ -carboxamide group of glutamine residues and the  $\epsilon$ -amino group of lysyl residues [118]. Analysis by X-ray scattering (SAXS) and small angle neutron scattering (SANS) showed that the internal structure of Tgase cross-linked CMs was not affected [119]. Several authors investigated on the stability of Tgase cross-linked CMs. Huppertz et al. [120] demonstrated that CMs cross-linked with Tgase are entirely stable to disruption by urea and/or citrate. Subsequently, Huppertz and de Kruif [121] showed that reticulated CMs are more stable than native CMs against ethanol-induced coagulation. Huppertz [122] demonstrated that incubation of milk with Tgase improved milk heat stability by preventing the dissociation of  $\kappa$ -casein from CMs. Recently Nogueira et al. (paper under preparation) studied the stability of CMs-Tgase at acidic pH. Thus, Tgase cross-linked CMs can be used as putative nanocarrier in a wide range of pH under various physico-chemical conditions.

Cyanidin-3-O-glucoside (C3G) is an abundant, well-distributed anthocyanins, a group of water-soluble flavonoids subgroup, which belongs to the class of phenolic compounds. Numerous publications suggest that anthocyanins have health and wellness benefits for consumers: vasoprotective [8], anti-inflammatory [9], anticancer [10], antimicrobial [11] and antidiabetic [12]. All of which are more or less associated to anthocyanin antioxidant properties. However the stability of anthocyanins is strongly affected by pH, temperature increase, UV-light radiation, oxygen exposure and co-pigmentation [15]. Anthocyanins are stable at acidic pH (pH comprised between 2 and 3), conditions for which they can be found under different chemical forms in equilibrium (quinoidal blue species, colorless carbinol pseudobase and chalcone). At pH values higher than 7, they are degraded in different species depending on their substituent groups [159]. A possible way to stabilize anthocyanins is their interactions with proteins. Various papers have studied the interactions between cyanidine and model proteins such as bovine serum albumin, hemoglobin, myoglobin [160],  $\alpha$ -casein,  $\beta$ -casein [61] and human serum albumins [161] at neutral pH. In a previous study (Casanova et al., *paper under preparation*) investigated the interactions between the caseins and C3G at pH 7 and pH 2, pHs for which the global charge of the caseins is negative and positive, respectively.

In the present study we used Tgase cross-linked CMs (CMs-Tgase) to obtain a stable monodisperse nanocarrier of about 200 nm in acidic conditions. The aims of our work is to employ cross-linked CMs with Tgase as nanocarrier and explore their possible interactions with C3G at pH 7 and pH 2, where the global charge of CMs-Tgase is negative and positive respectively. Fluorescence spectroscopy and dynamic light scattering measurements were performed to determine the binding properties and thermodynamic parameters between Tgase cross-linked CMs and C3G.

## **2.4.2 Materials and methods**

### **2.4.2.1 Sample preparation**

Purified native CMs was obtained by two successive microfiltrations of raw skimmed milk. The first microfiltration used a 1.4  $\mu\text{m}$  pore size membrane with a total membrane area of 0.24  $\text{m}^2$  to remove bacteria. The microfiltration was conducted at an average permeation flux of 145  $\text{l}\cdot\text{h}^{-1}$ , and a transmembrane pressure of 0.5 bar at temperature of 38°C. The second microfiltration was performed using a 0.1  $\mu\text{m}$  pore size membrane with a total membrane area of 0.24  $\text{m}^2$  to remove constituents of the soluble phase (whey proteins, lactose, soluble minerals) and simultaneously concentrate CMs at; an average temperature for the process of 45°C. . A concentration factor equal to 3 was achieved using a permeation flux of 35  $\text{l}\cdot\text{h}^{-1}$  and a transmembrane pressure of 0.5 bar. The second microfiltration was completed by a diafiltration against Milli-Q water before the CMs concentrate was spray dried [131][132]. The powder had a protein content of 96 % (w/w on dry basis) mainly caseins (97 % (w/w on protein basis). Residual whey proteins (3%) (w/w on protein basis), lactose and diffusible calcium were also present in the powder. Suspension containing 27.5  $\text{g}\cdot\text{L}^{-1}$  of CMs was obtained by powder solubilization in a buffer solution containing 25  $\text{mmol}\cdot\text{L}^{-1}$  of 4-(2-hydroxyethyl)-1-piperazine ethanesulfonic acid (HEPES) and 2  $\text{mmol}\cdot\text{L}^{-1}$   $\text{CaCl}_2$  at pH 7. In order to prevent microbial growth, 0.30  $\text{g}\cdot\text{L}^{-1}$  of sodium azide (Acros Organics, New Jersey, USA) was added. Activa transglutaminase (Tgase), a gift from Ajinomoto Europe Sales (Hamburg, Germany) with a declared activity of  $\sim 1,000$  units/g, was employed to cross-link CMs. According



to [121][137] with slight modifications, cross-linking was obtained by addition of 3U of Tgase corresponding to 0.03 g Tgase. G<sup>-1</sup> of CMs. The reaction occurred at 45 °C for 24 h at pH 7. To obtain a final solution at pH 2 after enzymatic reaction, the sample was acidified with HCl (1 M) at 4 °C to prevent precipitation. Then, temperature was raised to 25 °C and the samples were kept under stirring for 2 h before analysis. Before analysis, solution of CMs-Tgase at pH 7 was further diluted at 4 μM with HEPES buffer, whereas solution of CMs-Tgase was diluted at 4 μM with KCl / HCl 2 mmol.L<sup>-1</sup> CaCl<sub>2</sub> at pH 2. A control sample consisting only of native CMs at pH 7 was treated in the same conditions. The preparation of native CMs solution at pH 2 was not possible due to the formation of visible aggregates. Cyanidin-3-O-glucoside (Extrasynthese, Genay, France, purity > 96 %, ) was prepared at 1 mM in 25 mmol.L<sup>-1</sup> KCl / HCl and 2 mmol.L<sup>-1</sup> CaCl<sub>2</sub> at pH 2. The stock solution was further diluted at 40 μM and 100 μM with the 25 mmol.L<sup>-1</sup> KCl / HCl and 2 mmol.L<sup>-1</sup> CaCl<sub>2</sub> buffer at pH 2 for titration at low and medium C3G/ CMs-Tgase molar ratio.

#### 2.4.2.2 Intrinsic fluorescence spectroscopy

Intrinsic fluorescence was determined using a Safas FLX-Xenius fluorimeter (Monaco, France) equipped with a temperature-controlled 96-wells microplate. Excitation wavelength was set at 280 nm and emission spectra were recorded between 300 and 450 nm. A volume of 200 μl of CMs-Tgase solutions at 4 μM was placed in the wells and in each well one injection of C3G solution at 40 μM, 100 μM or 1 mM was done in order to cover the C3G/ casein molar ratio range from 0 to 10. The larger injection of C3G solution in the wells was 20 μL in order to avoid excessive protein dilution. The mixtures were agitated and fluorescence measurements were taken after 5 min of equilibration. The titrations were conducted at 295, 299, 305, 309 and 315 °K. Each titration was performed twice using independent CMs-Tgase and C3G solutions and in triplicate using the same CMs-Tgase and C3G solutions. The fluorescence data were analyzed on Kaleidagraph (Synergy Software) in order to determine the binding constant of the reaction.

### 2.4.2.3 Hydrodynamic diameter and $\zeta$ -potential measurements

The hydrodynamic diameter ( $D_h$ ) and the zeta-potential ( $\zeta$ ) of the complexes were determined using a Zetasizer Nano-S (Malvern Instrument, Worcestershire, UK). Solutions was at 4 $\mu$ M and the C3G / casein molar ratio ranged from 0 to 10.

The hydrodynamic diameter ( $D_h$ ) of the complexes at 22°C was obtained from dynamic light scattering measurements over 2 min using a backscattering angle of 173° and a wavelength of 633 nm. Experimental data were analyzed using the general purpose model. The  $D_h$  of the complexes was calculated by the Stokes-Einstein equation using the diffusion coefficient ( $D_t$ ) extracted from the fit of the correlation curve and solution viscosity,  $\eta$ , of 1.033 Pa.s<sup>-1</sup> as follow:

$$D_h = \frac{K_B T}{3\pi\eta D_t} \quad (1)$$

where  $K_B$  is the Boltzmann's constant and  $T$ , the temperature.  $D_h$  was expressed as Z-average value. Each experiment was repeated 5 times.

$\zeta$ -potential ( $\zeta$ ) measurements were performed at a voltage of 50 V.  $\zeta$ -potential was calculated from the electrophoretic mobility ( $\mu$ , V Pa<sup>-1</sup> s<sup>-1</sup>) of the C3G/CMs-Tgase complexes using the Henry equation, as follow:

$$\zeta = \frac{3\eta\mu}{2\epsilon f(\kappa R_H)} \quad (2)$$

where  $\eta$  is the buffer viscosity (1.033 x 10<sup>-3</sup> Pa s<sup>-1</sup>),  $\epsilon$  is the medium dielectric constant (dimensionless),  $R_H$  is the radius of the complexes (nm) and  $f(\kappa R_H)$  is the Henry's function. Since the analysis is conducted in aqueous media a value of 1.5 was adopted for  $f(\kappa R_H)$ , which is referred to as the Smoluchowski approximation.

## 2.4.3 Results

### 2.4.3.1 Z-average hydrodynamic diameter and $\zeta$ -potential of CMs-Tgase in the presence of C3G

Native or cross-linked CMs presented an average diameter of 165 nm at pH 7 and pH 2 (data not shown) and a  $\zeta$ -potential of  $-20 \pm 2$  mV for native CMs,  $-23 \pm 1$  mV for CMs-Tgase at pH 7 and  $+21 \pm 1$  mV at pH 2 (data not shown). In the presence of C3G (C3G/CMs molar ratio of 10), the average hydrodynamic diameter of  $165 \pm 2$

nm (Figure 22) and the  $\zeta$ -potential of native CMs at pH 7, CMs-Tgase at pH 7 and at pH 2 were unchanged (data not shown).

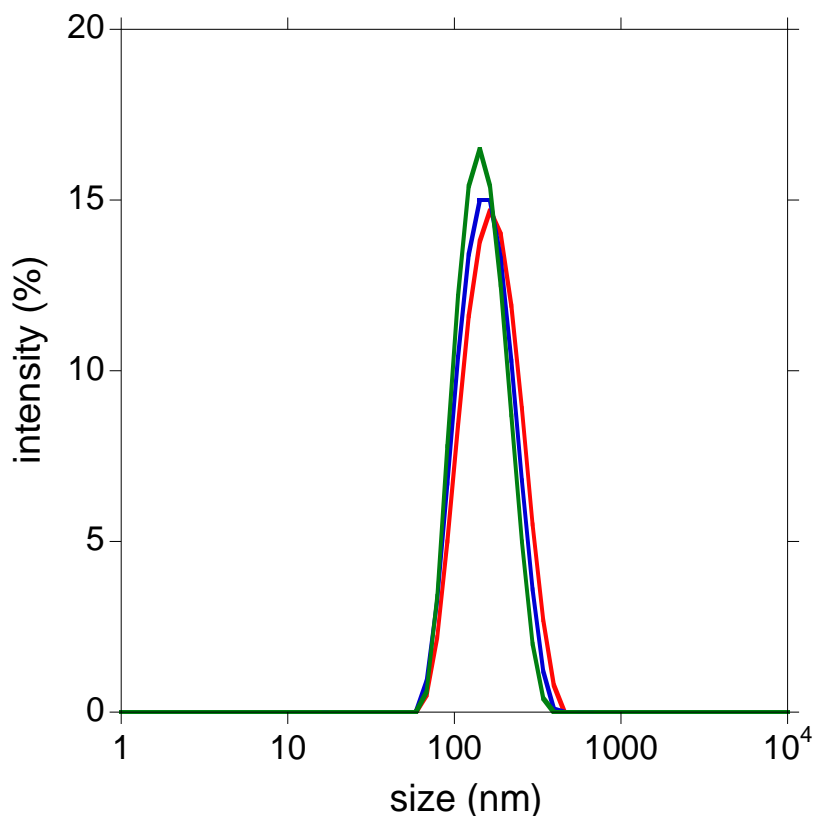


Figure 22 : Intensity (%) as a function of particle diameter of native CMs (red line), CMs-Tgase (blue line) at pH 7 and CMs-Tgase at pH 2 (green line) with 40  $\mu$ l of C3G monitored by dynamic light scattering (DLS).

#### 2.4.3.2 Intrinsic fluorescence quenching C3G / CMs-Tgase

Intrinsic fluorescence quenching for native CMs (data not show) and CMs-Tgase (Figure 23 A and B at pH 7 and pH 2 respectively) were measured in the absence and presence of increasing concentrations of C3G (C3G / casein molar ratio from 0 to 10). The maximum emission wavelength of native CMs and CMs-Tgase after excitation at 280 nm was around 330 nm. The fluorescence intensity decreased with increasing amount of C3G in the solution (quenching mechanism), suggesting an interaction between native CMs and CMs-Tgase with C3G. Fluorescence quenching can occur by two main mechanisms, generally divided into dynamic quenching and static quenching. According to Lakowicz [166], dynamic quenching results from random collisional encounters between the fluorophore and the quencher, whereas

static quenching results from the formation of a ground-state complex between the fluorophore and the quencher. To differentiate which one of the two quenching mechanisms was implicated in the interaction between CMs-Tgase and C3G, the data were plotted using the Stern-Volmer equation (Figure 1C and 1D):

$$F_0/F = 1 + K_{sv}[C3G] = K_q\tau_0[C3G] \quad (3)$$

Where  $F_0$  and  $F$  represent the fluorescence intensities of the protein in the absence and in the presence of increasing concentration of the C3G [C3G], respectively.  $K_{sv}$  is the Stern-Volmer constant which can be written as  $K_{sv} = K_q\tau_0$  where  $K_q$  is the bimolecular quenching constant and  $\tau_0$  is the lifetime of the fluorophore in the absence of quencher. The value of  $\tau_0$  for Trp is equal to  $10^{-8}$  s [167]. The non-monotonic evolution of the fluorescence ratio ( $F_0/F$ ) during titration suggested the existence of more than one quenching modes. For the data analysis, we consider two quenching modes corresponding to the binding of C3G to two independent sets of binding sites on native CMs and CMs-Tgase. At pH 7 and pH 2,  $K_{sv}$  was of  $10^4$  M<sup>-1</sup> for the two quenching modes corresponding to  $K_q$  values of  $10^{12}$  M<sup>-1</sup>.s<sup>-1</sup>. These values were much higher than the diffusion limited quenching ( $2 \times 10^{10}$  M<sup>-1</sup>.s<sup>-1</sup>) indicating that the quenching of native CMs and CMs-Tgase fluorescence by C3G followed a static mechanism [166]. In addition, native CMs and CMs-Tgase fluorescence quenching by C3G was studied at four other temperatures (299, 305, 309 and 315 °K). Increasing the temperature induced a decrease of  $K_{sv}$  at pH 7 and pH 2 (data not show) confirming the CMs-Tgase fluorescence quenching by C3G followed a static mechanism [61].

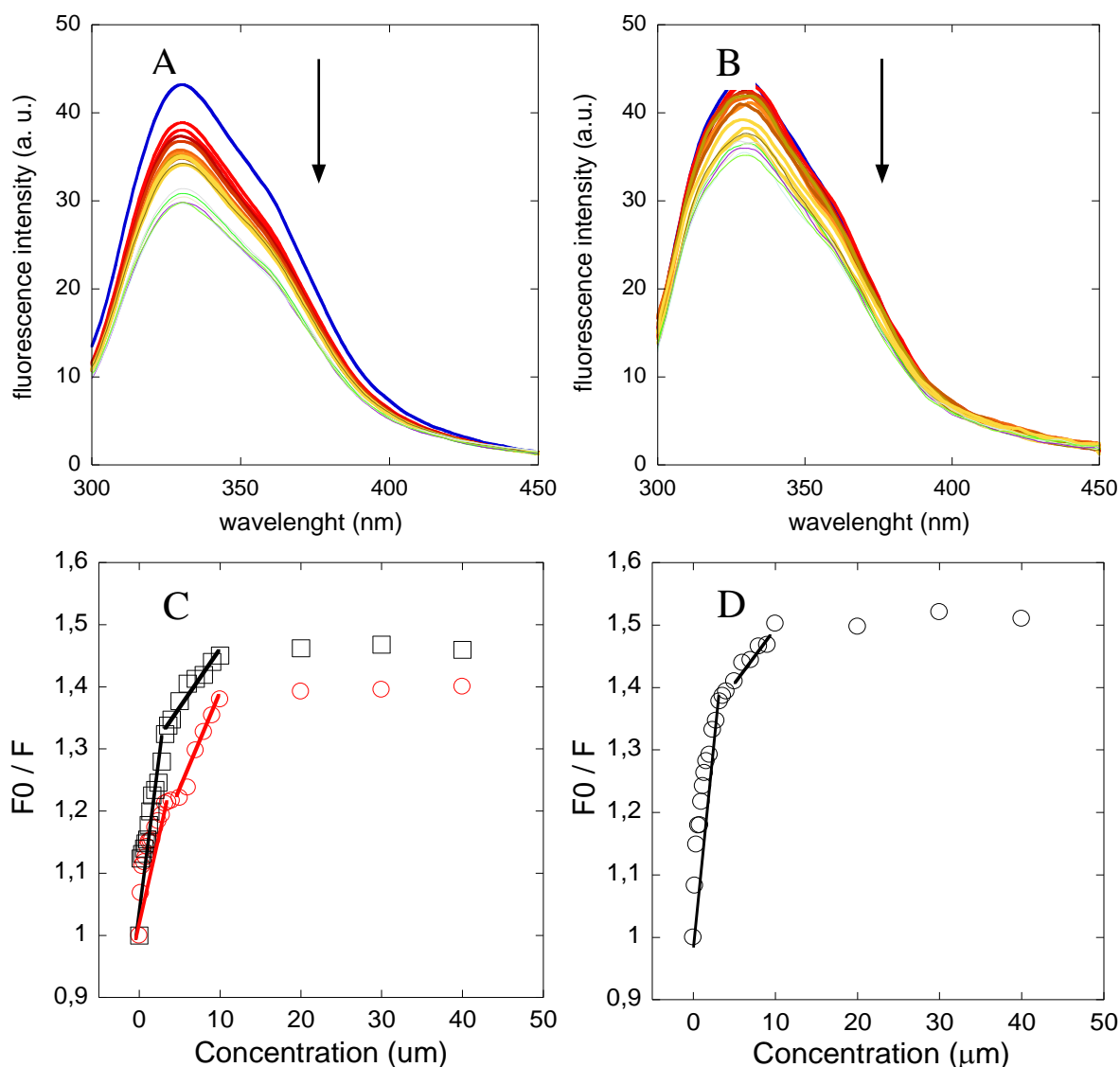


**Figure 23 :** Fluorescence emission spectra of native CMs-Tgase at pH 7 (A) and pH 2 (B) at 295 °C in the absence and presence of increasing concentrations of C3G (from 0.4 to 40 μM). Stern-Volmer plots of native CMs (O) and CMs-Tgase (□) at pH 7 (C) and CMs-Tgase at pH 2 (D).

### 2.4.3.3 Binding constant

To determine the binding constant of the interaction,  $K_a$ , experimental data were analyzed using the Scatchard representation, which consider the binding of C3G to independent sets of binding sites of CMs. In this representation  $\frac{fi P_{total}}{L_{total}}$  is plotted versus  $fi P_{total}$ , and the slope of the fit is used to determine  $K_a$ [168].  $fi$  is calculated using the native CMs fluorescence intensity value in the absence of C3G ( $F_0$ ), the

fluorescence intensity value during titration of native CMs solutions with C3G ( $F$ ) and the fluorescence intensity value at saturation ( $F_{min}$ ) using the following equation:

$$fi = \frac{F0 - F}{F0 - F_{min}} \quad (4)$$

Figure 24 A and B shows the Scatchard plots for the interaction of native CMs and CMs-Tgase with C3G at pH 7 and pH 2 at 295 °K. The plots show two well-separated domains suggesting the existence of two sets of binding sites for C3G on native CMs and CMs-Tgase at the two pH values. The data in these two domains were fitted independently by linear regression. The binding constants  $Ka_1$  and  $Ka_2$  (for the two sets of binding sites) were in the same range at pH 7 and pH 2 with  $Ka_1$  larger than  $Ka_2$  (Table 1). These values indicated that the interaction between native CMs and CMs-Tgase with C3G was of strong affinity.

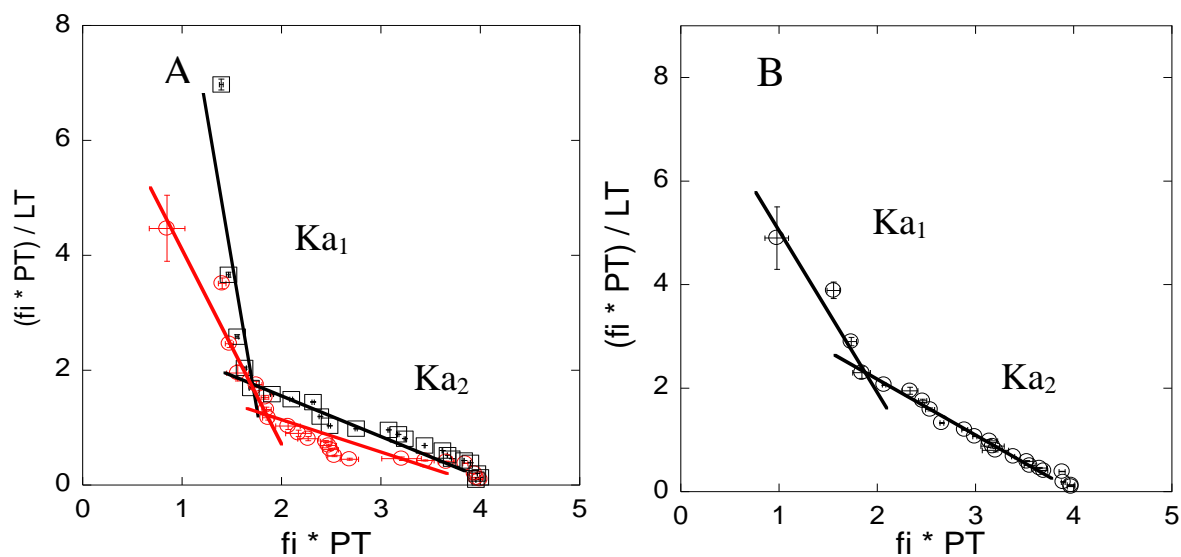


**Figure 24 : Scatchard plot of the interaction of C3G with native CMs (O) and CMs-Tgase (□) at pH 7 (A) and CMs-Tgase at pH 2 (B) at 295 °K.**

The binding constants were further determined at temperatures 299, 305, 309, 315 °K (Table 1).  $Ka_1$  and  $Ka_2$  decreased with increasing temperature at pH 7 whereas, at pH 2 an increase was observed. The ratio between  $Ka_1$  and  $Ka_2$ , at pH 7 decreased from 28 to 14 whereas at pH 2 increased from 3 to 20 in the investigated temperature range.

**Table 13: Binding parameters of the interaction of C3G with native CMs at pH 7 and CMs-Tgase at pH 7 and pH 2 at different temperatures.**

Compound	T (°K)	Ka <sub>1</sub> (x 10 <sup>6</sup> M <sup>-1</sup> )	Ka <sub>2</sub> (x 10 <sup>6</sup> M <sup>-1</sup> )
Native CMs pH 7	295	3.26	0.91
	299	3.02	0.93
	305	2.97	0.81
	309	2.20	0.72
	315	1.57	0.69
CMs-Tgase pH 7	295	16.14	0.58
	299	11.88	0.88
	305	10.30	0.49
	309	6.46	0.34
	315	5.09	0.36
CMs-Tgase pH 2	295	2.83	1.06
	299	4.81	0.64
	305	8.30	0.74
	309	10.68	0.88
	315	11.71	0.56

#### **2.4.3.4 Thermodynamic analysis and nature of the binding forces**

The evolution of  $Ka$  as a function of temperature, suggested that the interaction mechanisms of C3G with native CMs and CMs-Tgase are specific to the pH condition (Figure 25). At pH 7,  $Ka_1$  and  $Ka_2$  decreased when temperature increased indicating that the binding reaction was exothermic. In opposition, at pH 2,  $Ka_1$  and  $Ka_2$  increased with increasing the temperature, indicating that the binding reaction was endothermic [170]. Binding constant at different temperatures were used to analyze the thermodynamic parameters of the interaction: enthalpy, entropy and free energy. Protein-ligand interaction can occur via the formation of four types of non-covalent bond: hydrogen, van der Waals, electrostatic and hydrophobic. According to Ross and Subramanian [171] these interactions have specific thermodynamic signatures.

The main binding force can be deduced from the calculation of Van't Hoff equation as follow:

$$\ln K_a = -\frac{\Delta H}{RT} + \frac{\Delta S}{R} \quad (5)$$

$$\Delta G = \Delta H - T \Delta S \quad (6)$$

Where R is the gas constant (8.314 J mol<sup>-1</sup> K<sup>-1</sup>) and T is the temperature (°K). Thermodynamic parameters  $\Delta H$  and  $\Delta S$  were determined from the slope and abscissa of the plot  $\ln K_a$  versus  $1/T$  (Figure 3 A and 3 B). Results are listed in Table 2. The negative values of  $\Delta G$  for  $K_{a1}$  and  $K_{a2}$  at pH 7 and pH 2 suggested that the binding process is thermodynamically favorable (spontaneous).

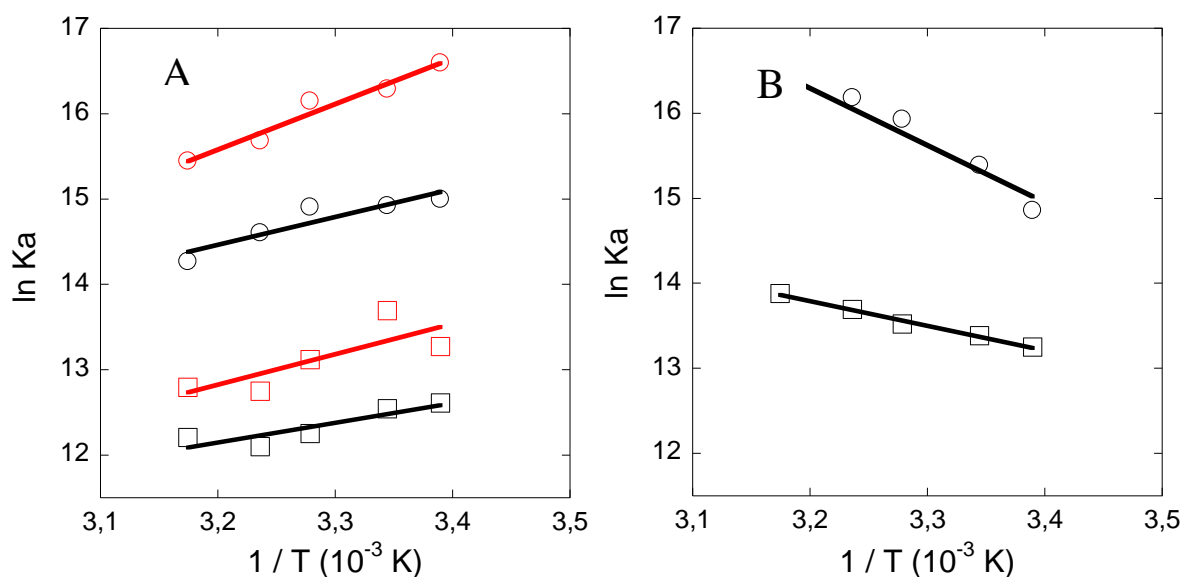


Figure 25 :  $\ln K_a$  as a function of  $1/T$  for the two classes of binding site. Figure 3 A represents the first (○ and ○) and the second (□ and □) class of C3G binding sites for native CMs and CMs-Tgase, respectively, at pH 7. Figure 3 B showed the first (○) and the second (□) class of C3G binding sites at pH 2.



**Table 14: Thermodynamic parameters of native CMs at pH 7 and CMs-Tgase at pH 7 and pH 2 at different temperatures.**

Compound	T (°K)	$\Delta H_1$ (KJ / mol)	$\Delta S_1$ (J / mol K)	$\Delta G_1$ (KJ / mol)	$\Delta H_2$ (KJ / mol)	$\Delta S_2$ (J / mol K)	$\Delta G_2$ (KJ / mol)
Native CMs pH 7	295	-27	33	-36.9	-12.4	72.3	-33.7
	299			-37.1			-34.0
	305			-37.3			-34.4
	309			-37.4			-34.7
	315			-37.6			-35.1
CMs-Tgase pH 7	295	-44	-13	-40.5	-29	12	-33.0
	299			-40.5			-33.1
	305			-40.4			-33.1
	309			-40.9			-33.2
	315			-40.3			-33.3
CMs-Tgase pH 2	295	56	314	-36.9	24	192	-32.5
	299			-38.1			-33.2
	305			-40.0			-34.4
	309			-41.2			-35.2
	315			-43.1			-36.3

## 2.4.4 Discussion

### 2.4.4.1 Quenching mechanism

At the excitation wavelength of 280 nm, native CMs and cross-linked CMs showed a strong fluorescence emission at 330 nm attributed to the presence of tryptophan in casein polypeptide chains. Stern-Volmer equation [Eq. (3)] is employed to describe the type of quenching between CMs and C3G. By using this approach, Stern-Volmer constant ( $K_{sv}$ ) and bimolecular rate constant ( $K_q$ ) were calculated.  $K_{sv}$  value was of an order of  $10^4 \text{ M}^{-1}$  with only a slight decrease when the temperature increases. Consequently, the corresponding  $K_q$  value had a magnitude order of  $10^{12} \text{ M}^{-1} \text{ s}^{-1}$  at all temperatures studied. The same behavior was observed at pH 7 and at pH 2 suggesting that the quenching originated from a static mechanism due to a specific interaction between protein and ligand [167]. Despite the fact that caseins has a

highly and flexible structure, no shift of spectral fluorescence was observed during the interactions with C3G, contrary to as observed by [169], [179]. This suggested that exposition of tryptophan to solvent do not change during the titration with C3G.

#### 2.4.4.2 Binding model

The absence of modification of the size and  $\zeta$ -potential of the assemblies suggested that the interaction is mainly intramicellar. Similar considerations were proposed by Sahu and collaborators [47] during the study of interactions between native CMs and curcumin. The same analysis conducted with a casein hydrolysate supported the hypothesis that the curcumin was bound to the hydrophobic regions of CM, which are located in the submicelles. For the static quenching constant, the binding constant  $K_a$  can be calculated by using the Scatchard plot [Eq. (4)]. Native CMs present binding association of  $3.3 \times 10^6 \text{ M}^{-1}$  whereas the maximum  $K_a$  was  $16.1 \times 10^6 \text{ M}^{-1}$ , observed at 295 °K. In a recent study, Lin et al. [160] observed that C3G interact with bovine serum albumin, hemoglobin and myoglobin in a static mode with a  $K_a$  of the order of  $10^4 \text{ M}^{-1}$  at 308 °K. Semo et al. [2] by using CMs as nanocarrier and curcumin as interest molecule, estimated a binding constant at  $1.5 \times 10^4 \text{ M}^{-1}$ . In our study, the larger value of  $K_a$  (magnitude order of  $10^6 \text{ M}^{-1}$ ) for the first and the second classes of binding sites suggested that the complexation of C3G with CMs is highly favorable. An analysis of the thermodynamics parameters of the binding at different temperatures gives information on the main kind of interactions involved. The thermodynamic parameters of the binding of native CMs and C3G, at pH 7 are negative enthalpy and positive entropy for both binding sites indicating that the reaction is enthalpy-entropy driven. According to Ross and Subramanian [171] this indicates that electrostatic and/or van der Waals interactions are the main contributors of the interaction. At the same pH value, during the interaction between CMs-Tgase and C3G,  $\Delta H$  was negative for both binding sites ( $-44$  and  $-29 \text{ KJ.mol}^{-1}$  for  $\Delta H_1$  and  $\Delta H_2$  respectively) whereas, for the second binding site,  $\Delta S$  is of low value either negative or positive ( $-13$  and  $+12 \text{ J.mol}^{-1} \text{ K}^{-1}$  for the first and second binding site respectively). In this case, we assume that, for the first binding site, the interaction was mainly electrostatically driven, due to the strong negative contribution of enthalpy. Whereas, for the second binding site, the interaction was mainly driven

by electrostatic and/or van der Waals forces. At pH 2, CMs-Tgase / C3G interaction, present positive  $\Delta H$  (56 and 314 KJ.mol<sup>-1</sup> for  $\Delta H_1$  and  $\Delta H_2$  respectively) and positive  $\Delta S$  (24 and 192 KJ.mol<sup>-1</sup> for  $\Delta S_1$  and  $\Delta S_2$  respectively). According to [169] high and positive value of entropy indicated water molecules that are arranged around the non-polar regions of ligand and protein molecules acquire a more random configuration as a results of hydrophobic protein-ligand interactions. The value observed for CMs-Tgase / C3G at pH 2 suggests that hydrophobic interactions play a major role in the binding interaction [171]. Hydrodynamic diameter of native CMs and CMs-Tgase at pH 7 and pH 2, remains stable during the titration with C3G at.  $\zeta$ -potential of the assemblies was negative at pH 7, with a slight difference between CMs-Tgase and CMs due to the cross-linking reaction by Tgase that reduce the number of positive charge, and positive at pH 2. However, no difference was observed after addition of C3G. These results strongly suggested that interactions between native CMs and CMs-Tgase with C3G are intramicellar.

CMs cross-linking by Tgase do not influence the binding with C3G at pH 7. The binding of CMs and C3G was affected by the pH. Affinity of native CMs and CMs-Tgase with C3G, at pH 7 and pH 2 was similar ( $\Delta G \sim 30$  KJ.mol<sup>-1</sup>) demonstrating that CMs or cross-linked CMs may be used a nanocarrier for C3G.

#### 2.4.5 Conclusion

Based on the results obtained by fluorescence spectroscopy, C3G binds spontaneously to native CMs and CMs-Tgase. At pH 2, hydrophobic forces drive the interactions between CMs-Tgase and C3G, whereas at pH 7, electrostatic interactions, hydrogen bonding and Van der Waals forces are the dominant binding forces. No difference in size and charge, after addition of C3G, was observed, indicating that interactions was mainly intramicellar. These results suggest that CMs-Tgase can be used as versatile nanocarriers for bioactive anthocyanins at acidic pH 2. It would be interesting to study *in vitro* release of entrapped C3G as well as stability of C3G at different pH. Protection of C3G against UV and light radiations by cross-linked CMs is also of interest.

## **5. GENERAL CONCLUSION AND PERSPECTIVES**

In the last three decades, world milk production has increased by more than 50 %, from 500 million tons in 1983 to 769 million tons in 2013. Milk and milk products are nutrient-dense foods and their consumption can add diversity to plant-based diets. Milk processing can produce a wide range of products such as liquid and fermented milks, cheeses, butter and ghee, condensed and evaporated milks, milk powder, cream, whey products and casein. Casein is the principal protein in bovine milk (approximately 80% of the total milk protein) and is used as an ingredient in several products, including cheese, bakery products, paints and glues. The singularity of caseins is their ability of self-assembling into natural micelles, called casein micelles (CMs). In the last 10 years, they are employed as versatile, cheap and raw materials for the development of nanocarrier with applications in food and pharmaceutical area. Although CMs are quite stable against heat, their structure is highly sensitive to ionic changes, especially at acid pH. An interesting method to stabilize casein structure consist on its cross-linking, by joining two or more molecules through covalent bonds. In this study we choice genipin (GP) and transglutaminase (Tgase) as natural cross-linker. The main results obtained in this thesis was divided in 2 parts, as following.

In a PART A of the manuscript, we investigated on the stability of CMs cross-linked with GP or Tgase against acid pH, dissociating agent, temperature and ethanol. Cross-linked CMs present high stability from pH 7.0 to pH 2.0, whereas native CMs precipitated at pH lower than 5.5. Isoelectric point for CMs-GP and CMs-Tgase was established at pH 3.6 and pH 4.1 respectively. Cross-linking protect CMs against disruption at pH 2.0, in the presence of 100 mM of sodium citrate, 8 M urea, 99.5% (v/v) of ethanol and HCT superior to 500 s. It is proposed that cross-linking increased the stability of native CMs against disruption by stabilization of polyelectrolyte brush of K-casein. These results confirm the potential application of cross-linked CMs as versatile nanocarrier for interest molecules in acid conditions.

In a PART B, with the perspectives of using cross-linked CMs for food applications, we choice Tgase as cross-linker. Cyanidine-3-O-glucoside (C3G) is an anthocyanin present in several Brazilian's fruits, especially Amazon açai and jaboticaba, which shows chemical stability and high antioxidant activity in acid conditions. Firstly we investigated on the possible interaction between casein molecules (sodium caseinate) and C3G under acidic (pH 2.0) and neutral (pH 7.0) conditions. Then, the use of Tgase cross-linked CMs as nanocarrier for C3G at pH 2.0 and at pH 7.0 is explored. Binding constant as well as driving forces at different pH values were determined by thermodynamic analysis at different temperatures. Casein molecules (sodium caseinate) and CMs exhibited two distinct binding sites for C3G with a respective affinities of  $10^6$  and  $10^5$  M<sup>-1</sup>. Comparing with the results present in Table 2, casein molecules and native or cross-linked CMs interact with C3G with high affinity. A thermodynamic analysis of the interactions indicated that the binding process was spontaneous. At pH 2.0, hydrophobic association drive the interactions between caseins and C3G, whereas at pH 7, electrostatic interactions are the dominant binding forces. CMs cross-linking by Tgase don't affect the interactions between C3G and caseins meaning it can be used as efficient nanocarriers for anthocyanins such as C3G under acid conditions.

Differents perspectives may be envisaged as a function of differents areas of interest. With a nutritional approach, it would be interesting to explore the antioxidant properties of C3G after interactions with CMs-Tgase as well as release properties during *in vitro* and *in vivo* studies (Figure 26). With a biophysical approach, SAXS analysis can be employed. This way can be used to confirm the results obtained by DLS analysis regarding the dispersity and the size of CMs before and after interaction with C3G. Furthermore, the structural change on CMs can be explored [180]. Another possible way is to encapsulated C3G in CMs by spray-dryer technique, to preserve antioxidant properties over the storage time. In this way, some experiments were conducted in the Inovaleite laboratory on the influence of the crosslinking of CMs on their dry ability, the powder quality and their potential use as encapsulation devices for polyphenols from jaboticaba fruit. According to the authors, cross-linked CMs presented better powder quality than native CMs [181]. Cross-linked CMs were able to protect the polyphenol extract from jaboticaba against

storage time and heat treatment, maintaining its antioxidant capacity mainly at pH 2.0. Based on these results, it would be interesting to employed the powder of encapsulated polyphenols from jaboticaba fruit in cross-linked CMs in food or pharmaceutical formulation for industrial applications.

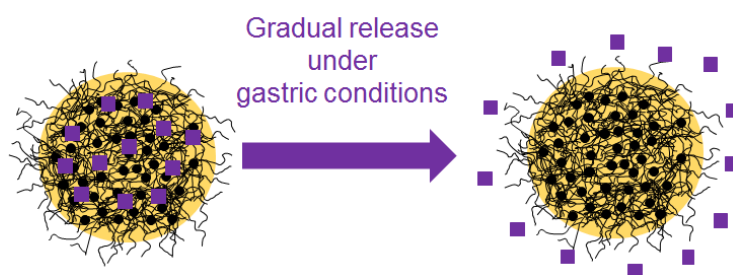


**Figure 26 : Gradual release of C3G molecules under gastric conditions (pH 2).**

## **6. REFERENCES**



- [1] D.G. Dalgleish, On the structural models of bovine casein micelles—review and possible improvements, *Soft Matter*. 7 (2010) 2265–2272.
- [2] E. Semo, E. Kesselman, D. Danino, Y.D. Livney, Casein micelle as a natural nano-capsular vehicle for nutraceuticals, *Food Hydrocoll.* 21 (2007) 936–942.
- [3] C. Broyard, F. Gaucheron, Modifications of structures and functions of caseins: a scientific and technological challenge, *Dairy Sci. Technol.* 95 (2015) 831–862.
- [4] N.F. Nogueira Silva, A. Saint-James, A. F. de Carvalho, F. Gaucheron, Development of casein microgels from cross-linking of casein micelles by genipin., *Langmuir*. 30 (2014) 10167–10175.
- [5] H. Jaros, D. Partschefeld, C. Henle, T. Rohm, Transglutaminase in dairy products: chemistry, physics, applications. *Journal, J. Texture Stud.* 37 (2006) 113–155.
- [6] V.F. De Lima Yamaguchi, K. K., Pereira, L. F. R., Lamarão, C. V., Lima, E. S., da Veiga-Junior, Amazon acai : Chemistry and biological activities : A review, *Food Chem.* 179 (2015) 137–151.
- [7] M.T.P.S. Clerici, L. B. Carvalho-Silva, Nutritional bioactive compounds and technological aspects of minor fruits grown in Brazil, *Food Res. Int.* 44 (2011) 1658–1670.
- [8] D.R. Bell, K. Gochenaur, Direct vasoactive and vasoprotective properties of anthocyanin-rich extracts., *J. Appl. Physiol.* 100 (2006) 1164–1170.
- [9] D.L. Wang, H. , Nair M. G. , Strasburg, M. G. , Chang, Y. C., Booren, A. M., Gray, J. I., DeWitt, Antyoxidant and Antiinflammatory Activities of Anthocyanins and Their Aglycon, Cyanidin, from Tart Cherries, *J. Nat. Prod.* 62 (1999) 294–296.
- [10] D. Hou, Potential mechanisms anthocyanins of cancer chemoprevention by anthocyanins, *Curr. Mol. Med.* 3 (2003) 149–159.
- [11] B.J. Mazza, G., Kay, C. D., Cottrell, T., Holub, Absorption of anthocyanins from blueberries and serum antioxidant status in human subjects, *J. Agric. Food Chem.* 50 (2002) 7731–7737.
- [12] M. Takikawa, S. Inoue, F. Horio, T. Tsuda, Dietary anthocyanin-rich bilberry extract ameliorates hyperglycemia and insulin sensitivity via activation of AMP-activated protein kinase in diabetic mice., *J. Nutr.* 140 (2010) 527–533.
- [13] N.H. Hurtado, A.L. Morales, M.L. González, M.L. Escudero-Gilete, F.J. Heredia, Colour, pH stability and antioxidant activity of anthocyanin rutinosides isolated from tamarillo fruit (*Solanum betaceum* Cav.), *Food Chem.* 117 (2009) 88–93.

- [14] C. Woodward, G., Cassidy, P. K. A., Kay, Anthocyanin stability and recovery: implications for the analysis of clinical and experimental samples, *J. Agric. Food Chem.* 57 (2009) 5271–5278.
- [15] R.N. Cavalcanti, D.T. Santos, M.A. Meireles, Non-thermal stabilization mechanisms of anthocyanins in model and food systems-An overview, *Food Res. Int.* 44 (2011) 499–509.
- [16] P.C. Lin, S. Lin, P.C. Wang, R. Sridhar, Techniques for physicochemical characterization of nanomaterials, *Biotechnol. Adv.* 32 (2014) 711–726.
- [17] P. Mondal, Author personal communication, (n.d.).
- [18] Y. Liu, L. Liu, M. Yuan, R. Guo, Preparation and characterization of casein-stabilized gold nanoparticles for catalytic applications, *Colloids Surfaces A Physicochem. Eng. Asp.* 417 (2013) 18–25.
- [19] J. Sangeetha, J. Philip, The interaction, stability and response to an external stimulus of iron oxide nanoparticle-casein nanocomplexes, *Colloids Surfaces A Physicochem. Eng. Asp.* 406 (2012) 52–60.
- [20] A. Bhogale, N. Patel, J. Mariam, P.M. Dongre, A. Miotello, D.C. Kothari, Comprehensive studies on the interaction of copper nanoparticles with bovine serum albumin using various spectroscopies, *Colloids Surfaces B Biointerfaces.* (2014).
- [21] K.E. Sapsford, K.M. Tyner, B.J. Dair, J.R. Deschamps, I.L. Medintz, Analyzing nanomaterial bioconjugates: a review of current and emerging purification and characterization techniques, *Anal. Chem.* 83 (2011) 4453–4488.
- [22] C. Sabliov, H. Chen, R. Ada, *Nanotechnology and functional foods: effective delivery of bioactive ingredients*, Wiley-Blackwell, 2015.
- [23] M.H. Abd El-Salam, S. El-Shibiny, Formation and potential uses of milk proteins as nano delivery vehicles for nutraceuticals: A review, *Int. J. Dairy Technol.* 65 (2012) 13–21.
- [24] S. Damodaran, K. Parkin, O. R. Fennema, *Fennema's Food Chemistry*, Fourth Edition, New York, 2007.
- [25] C. de Kruiff, C. G., Holt, Casein Micelle Structure Functions and Interactions 1, in: *Adv. Dairy Chem. - Proteins Part A*, 3rd Ed., Kluwer Aca, New York, 2003: pp. 233–276.
- [26] C. Holt, J.A. Carver, Darwinian transformation of a “scarcely nutritious fluid” into milk, *J. Evol. Biol.* (2012) 1–11.
- [27] L. Holt, C. Sawyer, Interpretation of primary and secondary structures of the  $\alpha$ -S1-Caseins,  $\beta$ -Caseins and K- Caseins, *J. Chem. Soc. Trans.* 89 (1993) 2683–2692.
- [28] J.W. Holland, Post-translational modifications of caseins, in: H. Thompson, A., Boland, M., Singh (Ed.), *Milk Proteins From Expr. to Food*, Elsevier Sc, San Diego, 2009: pp. 107–132.
- [29] E.W. Bingham, Influence of Temperature and pH on the Solubility of  $\alpha$ s1-,  $\beta$ - and  $\kappa$ -Casein., *J. Dairy Sci.* 54 (1971) 1077–1080.
- [30] P.L.H. McSweeney, P. F. Fox, *Advanced dairy chemistry Volume 1A: Proteins: Basic Aspects*, 4th Ed, Springer New York Heidelberg Dordrecht London, London, 2013.
- [31] D.T. Davies and A. J. R. Law, Content and composition of protein in creamery milks in southwest scotland, *J. Dairy Res.* 47 (1980) 83–90.

- [32] K.G. Jeurnik, T. J. M., and De Kruif, Changes in milk on heating: viscosity measurements, *J. Dairy Res.* 60 (1993) 139–150.
- [33] K. Makiko, A. Nemori, R. Ogiwara, Casein nanoparticles, US 2009/0280148 A1, 2009.
- [34] K. Kanazawa, Casein nanoparticles, US 2010/0143424 A1, 2010.
- [35] Y.D. Livney, D.G. Dalgleish, Casein micelles for nanoencapsulation of hydrophobic compounds, US 2009/0311329 A1, 2009.
- [36] A.M. Knoop, E. Knoop, A. Wiechen, Sub-structure of synthetic casein micelles, *J. Dairy Res.* 46 (1979) 347–350.
- [37] O. Menéndez-Aguirre, W. Stuetz, T. Grune, A. Kessler, J. Weiss, J. Hinrichs, High pressure-assisted encapsulation of vitamin D2 in reassembled casein micelles, *High Press. Res.* 31 (2011) 265–274.
- [38] O. Menéndez-Aguirre, A. Kessler, A. Stuetz, W. Grune, T. Weiss, J. Hinrichs, Increased loading of vitamin D2 in reassembled casein micelles, *Food Res. Int.* 64 (2014) 74–80.
- [39] M. Haham, S. Ish-Shalom, M. Nodelman, I. Duek, E. Segal, M. Kustanovich, Y. D. Livney, Stability and bioavailability of vitamin D nanoencapsulated in casein micelles, *Food Funct.* 3 (2012) 737–744.
- [40] Y. Levinson, S. Ish-Shalom, E. Segal, Y. D. Livney, Bioavailability, rheology and sensory evaluation of fat-free yogurt enriched with VD3 encapsulated in re-assembled casein micelles, *Food Funct.* 7 (2016) 1477–1482.
- [41] R. Penalva, I. Esparza, M. Agüeros, C.J. Gonzalez-Navarro, C. Gonzalez-Ferrero, J.M. Irache, Casein nanoparticles as carriers for the oral delivery of folic acid, *Food Hydrocoll.* 44 (2015) 399–406.
- [42] P. Bourassa, C.N. N'Soukpoé-Kossi, H.A. Tajmir-Riahi, Binding of vitamin A with milk  $\alpha$ - And  $\beta$ -caseins, *Food Chem.* 138 (2013) 444–453.
- [43] D. Chevalier-Lucia, C. Blayo, A. Gràcia-Julià, L. Picart-Palmade, E. Dumay, Processing of phosphocasein dispersions by dynamic high pressure: Effects on the dispersion physico-chemical characteristics and the binding of  $\alpha$ -tocopherol acetate to casein micelles, *Innov. Food Sci. Emerg. Technol.* 12 (2011) 416–425.
- [44] E. Frankel, Edwin N., Antioxidants in lipid foods and their impact on food quality, *Food Chem.* 57 (1996) 51–55.
- [45] M.J. Sáiz-Abajo, C. González-Ferrero, A. Moreno-Ruiz, A. Romo-Hualde, C.J. González-Navarro, Thermal protection of  $\beta$ -carotene in re-assembled casein micelles during different processing technologies applied in food industry, *Food Chem.* 138 (2013) 1581–1587.
- [46] T. Jarunglumlerta, K. Nakagawab, S. Adachi, Influence of aggregate structure of casein on the encapsulation efficiency of b-carotene entrapped via hydrophobic interaction, *Food Struct.* 5 (2015) 42–50.
- [47] A. Sahu, N. Kasoju, Bora U., Fluorescence study of the curcumin-casein micelle complexation and its application as a drug nanocarrier to cancer cells, *Biomacromolecules.* 9 (2008) 2905–2912.
- [48] S. Rahimi Yazdi, Corredig, M., Heating of milk alters the binding of curcumin to casein micelles. A fluorescence spectroscopy study, *Food Chem.* 132 (2012) 1143–1149.
- [49] A. Benzaria, M. Maresca, N. Taieb, E. Dumay, Interaction of curcumin with

- phosphocasein micelles processed or not by dynamic high-pressure, *Food Chem.* 138 (2013) 2327–2337.
- [50] A.N. Khanji, F. Michaux, J. Jasniewski, J. Petit, E. Lahimer, M. Cherif, D. Salameh, T. Rizk, S. Banon, Structure and gelation properties of casein micelles doped with curcumin under acidic conditions, *Food Funct.* 6 (2015) 3624–3633.
- [51] M. Esmaili, S.M. Ghaffari, Z. Moosavi-Movahedi, M.S. Atri, A. Sharifzadeh, M. Farhadi, R. Yousefi, J.M. Chobert, T. Haertlé, A.A. Moosavi-Movahedi, Beta casein-micelle as a nano vehicle for solubility enhancement of curcumin; food industry application, *LWT - Food Sci. Technol.* 44 (2011) 2166–2172.
- [52] K. Pan, Q. Zhong, S.J. Baek, Enhanced dispersibility and bioactivity of curcumin by encapsulation in casein nanocapsules, *J. Agric. Food Chem.* 61 (2013) 6036–43.
- [53] P. Bourassa, J. Bariyanga, H.A. Tajmir-Riahi, Binding sites of resveratrol, genistein, and curcumin with milk  $\alpha$ - And  $\beta$ -caseins, *J. Phys. Chem. B.* 117 (2013) 1287–1295.
- [54] K. Pan, Y. Luo, Y. Gan, S. J. Baekcand, Q. Zhong, pH-driven encapsulation of curcumin in self-assembled casein nanoparticles for enhanced dispersibility and bioactivity, *Soft Matter.* 10 (2014) 6820–6830.
- [55] F. Mehranfar, A.-K. Bordbar, N. Fani, M. Keyhanfar, Binding analysis for interaction of diacetylcurcumin with  $\beta$ -casein nanoparticles by using fluorescence spectroscopy and molecular docking calculations, *Spectrochim. Acta Part A Mol. Biomol. Spectrosc.* 115 (2013) 629–635.
- [56] R.K. Maheshwari, A.K. Singh, J. Gaddipati, R.C. Srimal, Multiple biological activities of curcumin: A short review, *Life Sci.* 78 (2006) 2081–2087.
- [57] K. Ono, K. Hasegawa, H. Naiki, M. Yamada, Curcumin Has Potent Anti-Amyloidogenic Effects for Alzheimer's beta-Amyloid Fibrils In Vitro, *J. Neurosci. Res.* 75 (2004) 742–750.
- [58] K.K. Li, S.W. Yin, X.Q. Yang, C.H. Tang, Z.H. Wei, Fabrication and characterization of novel antimicrobial films derived from thymol-loaded zein-sodium caseinate (SC) nanoparticles, *J. Agric. Food Chem.* 60 (2012) 11592–11600.
- [59] K. Pan, H. Chen, P.M. Davidson, Q. Zhong, Thymol nanoencapsulated by sodium caseinate: physical and antilisterial properties, *J. Agric. Food Chem.* 62 (2014) 1649–1657.
- [60] S. Zhou, S. Seo, I. Alli, Y.W. Chang, Interactions of caseins with phenolic acids found in chocolate, *Food Res. Int.* 74 (2015) 177–184.
- [61] Z. He, M. Xu, M. Zeng, F. Qin, J. Chen, Interactions of milk  $\alpha$ - and  $\beta$ -casein with malvidin-3-O-glucoside and their effects on the stability of grape skin anthocyanin extracts, *Food Chem.* 199 (2016) 314–322.
- [62] Y.L. Jianhui Ye, Fangyuan Fan, Xinqing Xu, Interactions of black and green tea polyphenols with whole milk, *Food Res. Int.* 53 (2013) 449–455.
- [63] I. Hasni, P. Bourassa, S. Hamdani, G. Samson, R. Carpentier, H.A. Tajmir-Riahi, Interaction of milk alfa and beta caseins with tea polyphenols, *Food Chem.* 126 (2011) 630–639.
- [64] M.C. Bohin, J.P. Vincken, A.H. Westphal, A.M. Tripp, P. Dekker, H.T.W.M. Van Der Hijden, H. Gruppen, Interaction of flavan-3-ol derivatives and different

- caseins is determined by more than proline content and number of proline repeats, *Food Chem.* 158 (2014) 408–416.
- [65] L. A. Kartsova and A. V. Alekseeva, Effect of Milk caseins on the concentration of polyphenolic compounds in tea, *J. Anal. Chem.* 63 (2008) 1211–1216.
- [66] E. Jöbstl, J.R. Howse, J.P.A. Fairclough, M.P. Williamson, Noncovalent cross-linking of casein by epigallocatechin gallate characterized by single molecule force microscopy, *J. Agric. Food Chem.* (2006).
- [67] J. Xue, C. Tan, X. Zhang, B. Feng, S. Xia, Fabrication of epigallocatechin-3-gallate nanocarrier based on glycosylated casein: Stability and interaction mechanism, *J. Agric. Food Chem.* (2014).
- [68] S. Haratifar, A. Meckling, M. Corredig, Antiproliferative activity of tea catechins associated with casein micelles, using HT29 colon cancer cells, *J. Dairy Sci.* 97 (2014) 672–678.
- [69] S. Haratifar, K. A. Mecklingband, M. Corredig, Bioefficacy of tea catechins encapsulated in casein micelles tested on a normal mouse cell line (4D/WT) and its cancerous counterpart (D/v-src) before and after in vitro digestion, *Food Funct.* 5 (2014) 1160–1166.
- [70] S. Haratifar, M. Corredig, Interactions between tea catechins and casein micelles and their impact on renneting functionality, *Food Chem.* 143 (2014) 27–32.
- [71] M. Sahlan, I. Pramadewi, Nanoencapsulation of the flavonoids isolated from *Phaleria macrocarpa* leaf by Casein micelle, *Int. J. Pharma Bio Sci.* 3 (2012) 472–478.
- [72] F. Mehranfar, A.K. Bordbar, H. Parastar, A combined spectroscopic, molecular docking and molecular dynamic simulation study on the interaction of quercetin with beta-casein nanoparticles, *J. Photochem. Photobiol. B Biol.* 127 (2013) 100–107.
- [73] A.-A. Moeniafshari, A. Zarrabi, A.-K. Bordbar, Exploring the interaction of naringenin with bovine beta-casein nanoparticles using spectroscopy, *Food Hydrocoll.* 51 (2015) 1–6.
- [74] V. Ferraro, A. R. Madureira, P. Fonte, B. Sarmiento, A. M. Gomes, M. E. Pintado, Evaluation of the interactions between rosmarinic acid and bovine milk casein, *RSC Adv.* 5 (2015) 88529–88538.
- [75] P. Zimet, D. Rosenberg, Y.D. Livney, Re-assembled casein micelles and casein nanoparticles as nano-vehicles for  $\omega$ -3 polyunsaturated fatty acids, *Food Hydrocoll.* 25 (2011) 1270–1276.
- [76] M. Sugiarto, A. Ye, H. Singh, Characterisation of binding of iron to sodium caseinate and whey protein isolate, *Food Chem.* 114 (2009) 1007–1013.
- [77] S. Raouche, M. Dobenesque, A. Bot, A. Lagaude, S. Marchesseau, Casein micelles as a vehicle for iron fortification of foods, *Eur. Food Res. Technol.* 229 (2009) 929–935.
- [78] V.A. Mittal, A. Ellis, A. Ye, P.J.B. Edwards, S. Das, H. Singh, Iron binding to caseins in the presence of orthophosphate, *Food Chem.* 190 (2016) 128–134.
- [79] M. Philippe, Y. Le Graët, F. Gaucheron, The effects of different cations on the physicochemical characteristics of casein micelles, *Food Chem.* (2005).
- [80] Ö. Demirbaş, M. Alkan, A. Demirbaş, Adsorption of casein onto some oxide minerals and electrokinetic properties of these particles, *Microporous*

- Mesoporous Mater. 204 (2015) 197–203.
- [81] P. Pomastowski, M. Sprynskyy, B. Buszewski, The study of zinc ions binding to casein, *Colloids Surfaces B Biointerfaces*. 120 (2014) 21–27.
- [82] P. Bourassa, L. Bekale, H.A. Tajmir-Riahi, Association of lipids with milk alpha- and beta-caseins, *Int. J. Biol. Macromol.* 70 (2014) 156–166.
- [83] M. Cheema, M.S. Mohan, S.R. Campagna, J.L. Jurat-Fuentes, F.M. Harte, The association of low-molecular-weight hydrophobic compounds with native casein micelles in bovine milk, *J Dairy Sci* . 8 (2015) 5155–5163.
- [84] M.G. Semenova, D. V. Zelikina, A.S. Antipova, E.I. Martirosova, N. V. Grigorovich, R.A. Obushaeva, E.A. Shumilina, N.S. Ozerova, N.P. Palmina, E.L. Maltseva, V. V. Kasparov, N.G. Bogdanova, A. V. Krivandin, Impact of the structure of polyunsaturated soy phospholipids on the structural parameters and functionality of their complexes with covalent conjugates combining sodium caseinate with maltodextrins, *Food Hydrocoll.* 52 (2016) 144–160.
- [85] G.A. Hussein, W.G. Pitt, Micelles and nanoparticles for ultrasonic drug and gene delivery, *Adv. Drug Deliv. Rev.* 60 (2008) 1137–1152.
- [86] A.O. Elzoghby, M. M. Elgohary, N. M. Kamel, Implications of protein- and Peptide-based nanoparticles as potential vehicles for anticancer drugs, *Adv. Protein Chem. Struct. Biol.* (2015).
- [87] M. Bachar, A. Mandelbaum, I. Portnaya, H. Perlstein, S. Even-Chen, Y. Barenholz, D. Danino, Development and characterization of a novel drug nanocarrier for oral delivery, based on self-assembled  $\beta$ -casein micelles, *J. Control. Release*. 160 (2012) 164–171.
- [88] T. Turovsky, R. Khalfin, S. Kababya, A. Schmidt, Y. Barenholz, D. Danino, Celecoxib Encapsulation in  $\beta$ -Casein Micelles: Structure, Interactions, and Conformation, *Langmuir* . 31 (2015) 7183–7192.
- [89] A. Shapira, Y.G. Assaraf, D. Epstein, Y.D. Livney, Beta-casein nanoparticles as an oral delivery system for chemotherapeutic drugs: Impact of drug structure and properties on co-assembly, *Pharm. Res.* 27 (2010) 2175–2186.
- [90] A. Shapira, Y.G. Assaraf, Y.D. Livney, Beta-casein nanovehicles for oral delivery of chemotherapeutic drugs, *Nanomedicine Nanotechnology, Biol. Med.* 6 (2010) 119–126.
- [91] A.O. Elzoghby, M. W. Helmy, W. M. Samy, N. A. Elgindy, Micellar Delivery of Flutamide Via Milk Protein Nanovehicles Enhances its Anti-Tumor Efficacy in Androgen-Dependent Prostate Cancer Rat Model, *Pharm Res.* 30 (2013) 2654–2633.
- [92] A.O. Elzoghby, M.W. Helmy, W.M. Samy, N.A. Elgindy, Spray-dried casein-based micelles as a vehicle for solubilization and controlled delivery of flutamide: Formulation, characterization, and in vivo pharmacokinetics, *Eur. J. Pharm. Biopharm.* 84 (2013) 487–496.
- [93] A.O. Elzoghby, N. I. Saad, M. W. Helmy, W. M. Samya, N. A. Elgindy, Ionically-crosslinked milk protein nanoparticles as flutamide carriers for effective anticancer activity in prostate cancer-bearing rats, *Eur. J. Pharm. Biopharm.* 85 (2013) 444–451.
- [94] A.O. Elzoghby, M.W. Helmy, W.M. Samy, N.A. Elgindy, Novel ionically crosslinked casein nanoparticles for flutamide delivery: Formulation, characterization, and in vivo pharmacokinetics, *Int. J. Nanomedicine.* 8 (2013)

- 1721–1732.
- [95] M. Razmi, A. Divsalar, A.A. Saboury, Z. Izadi, T. Haertlé, H. Mansuri-Torshizi, Beta-casein and its complexes with chitosan as nanovehicles for delivery of a platinum anticancer drug, *Colloids Surfaces B Biointerfaces*. 112 (2013) 362–367.
- [96] S. Narayanan, M. Pavithran, A. Viswanath, D. Narayanan, C.C. Mohan, K. Manzoor, D. Menon, Sequentially releasing dual-drug-loaded PLGA-casein core/shell nanomedicine: Design, synthesis, biocompatibility and pharmacokinetics, *Acta Biomater*. 10 (2014) 2112–2124.
- [97] D.P. Acharya, L. Sanguansri, M.A. Augustin, Binding of resveratrol with sodium caseinate in aqueous solutions, *Food Chem*. 141 (2013) 1050–1054.
- [98] X. Zhen, X. Wang, C. Xie, W. Wu, X. Jiang, Cellular uptake, antitumor response and tumor penetration of cisplatin-loaded milk protein nanoparticles, *Biomaterials*. 34 (2013) 1372–1382.
- [99] J. Raj, K. Babu Uppuluri, Metformin Loaded Casein Micelles for Sustained Delivery: Formulation, Characterization and In-vitro Evaluation, *Biomed. Pharmacol. J*. 8 (2015) 83–89.
- [100] M. Corzo-Martinez, M. Mohan, J. Dunlap, F. Harte, Effect of ultra-high pressure homogenization on the interaction between bovine casein micelles and ritonavir, *Pharm. Res*. 32 (2015) 1055–1071.
- [101] T. Turovsky, I. Portnaya, E. Kesselman, I. Ionita-Abutbul, N. Dan, D. Danino, Effect of temperature and loading on the structure of  $\beta$ -casein/ibuprofen assemblies, *J. Colloid Interface Sci*. 449 (2015) 514–521.
- [102] Z. Liefeng, J. Hui, Z. Wenjie, W. Lin, S. Lingling, W. Qiuyan, R. Yong, Improving the stability of insulin in solutions containing intestinal proteases in vitro, *Int. J. Mol. Sci*. 9 (2008) 2376–2387.
- [103] M.L. Kutt, J. Stagsted, Caseins from bovine colostrum and milk strongly bind piscidin-1, an antimicrobial peptide from fish, *Int. J. Biol. Macromol*. 70 (2014) 364–372.
- [104] Y. Liu, R. Guo, The interaction between casein micelles and gold nanoparticles, *J. Colloid Interface Sci*. 332 (2009) 265–269.
- [105] S.Z.H. Sumaira Ashrafa, Azhar Zahoor Abbasi, Christian Pfeiffer, I.H. Zafar Mahmood Khalid, Pilar Rivera Gil, Wolfgang J. Parak, Protein-mediated synthesis, pH-induced reversible agglomeration, toxicity and cellular interaction of silver nanoparticles, *Colloids Surfaces B Biointerfaces*. 102 (2013) 511–518.
- [106] J. Huang, L. Wang, R. Lin, A. Y. Wang, L. Yang, M. Kuang, W. Qian, H. Mao, Casein-Coated Iron Oxide Nanoparticles for High MRI Contrast Enhancement and Efficient Cell Targeting, *ACS Appl. Mater. Interfaces*. 5 (2013) 4632–4639.
- [107] J. Huang, Q. Shu, L. Wang, H.Wu, A.Y. Wang, H. Mao, Layer-by-layer assembled milk protein coated magnetic nanoparticle enabled oral Drug delivery with high stability in stomach and enzyme-responsive release in small intestine, *Biomaterials*. 39 (2015) 105–113.
- [108] T.A. Cowger, W. Tang, Z. Zhen, K. Hu, D.E. Rink, T.J. Todd, G.D. Wang, W. Zhang, H. Chen, J. Xie, Casein-Coated Fe<sub>3</sub>C<sub>2</sub> Nanoparticles with Superior r<sub>2</sub> Relaxivity for Liver-Specific Magnetic Resonance Imaging, *Theranostics*. 5 (2015) 1225–1232.
- [109] A. Singh, J. Bajpai, A.K. Bajpai, Investigation of magnetically controlled water

- intake behavior of iron oxide impregnated superparamagnetic casein nanoparticles (IOICNPs), *J. Nanobiotechnology*. 12:38 (2014) 1–13.
- [110] H. Chen, Q. Zhong, Processes improving the dispersibility of spray-dried zein nanoparticles using sodium caseinate, *Food Hydrocoll.* 35 (2014) 358–366.
- [111] Y.C. Yin, S.W. Yin, X.Q. Yang, C.H. Tang, S.H. Wen, Z. Chen, B. jie Xiao, L.Y. Wu, Surface modification of sodium caseinate films by zein coatings, *Food Hydrocoll.* 36 (2014) 1–8.
- [112] C.J.S.M. Silva, F. Sousa, F., G. Gübitz, A. Cavaco-Paulo, Chemical Modifications on Proteins Using Glutaraldehyde, *Food Technol. Biotechnol.* 42 (2004) 51–56.
- [113] T. Endo, H. Taguchi, The constituent of *Gardenia Jasminoides* Geniposide and genipin-gentiobioside, *Chem. Pharm. Bull.* 21 (1973) 2684–2688.
- [114] H.W. Sung, R. N. Huang, L. L. Huang, C. C. Tsai, In vitro evaluation of cytotoxicity of a naturally occurring cross-linking reagent for biological tissue fixation, *J. Biomater. Sci., Polym. Ed.* 10 (1999) 63–78.
- [115] Y. Chaubaroux, C., Vrana, E., Debry, C., Schaaf, P., Senger, B., Voegel, J. C., Haikel, F. Ringwald, C., Hemmerlé, J., Lavallo, P., Boulmedais, Collagen-based fibrillar multilayer films cross-linked by a natural agent, *Biomacromolecules*. 13 (2012) 2128–2135.
- [116] N. Nogueira Silva, A. Bahri, F. Guyomarc'h, E. Beaucher, F., Gaucheron, AFM study of casein micelles cross-linked by genipin: effects of acid pH and citrate, *Dairy Sci. Technol.* 95 (2015) 75–86.
- [117] F. Casanova, N.F.N., Silva, F. Gaucheron, M. H. Nogueira, A. V. N. C. Teixeira, I. T. Perrone, M. P. Alves, P. C. Fidelis, A. F. de Carvalho, Stability of casein micelles cross-linked with genipin: a physico-chemical study as a function of pH., *International Dairy J.* 68 (2017) 70–74.
- [118] H. Jaros, D., Partschefeld, C., Henle, T., Rohm, Transglutaminase in dairy product: chemistry, physics, applications, *J. Texture Stud.* 37 (2006) 113–155.
- [119] A. V. de Kruif, C. G., Huppertz, T., Urban, V. S., Petukhov, Casein micelles and their internal structure, *Adv. Colloid Interface Sci.* 172 (2012) 36–52.
- [120] C.G. Huppertz, T., Smiddy, M. M., de Kruif, Biocompatible micro-gel particles from cross-linked casein micelles, *Biomacromolecules*. 8 (2007) 1300–1305.
- [121] T. Huppertz, C. G. de Kruif, Ethanol stability of casein micelles cross-linked with transglutaminase, *Int. Dairy J.* 17 (2007) 436–441.
- [122] T. Huppertz, Heat stability of transglutaminase-treated milk, *Int. Dairy J.* 38 (2014) 183–186.
- [123] S.G. Anema, C. G. (Kees) de Kruif, Interaction of Lactoferrin and Lysozyme with Casein Micelles, *Biomacromolecules*. 12 (2011) 3970–3976.
- [124] S.G. Anema, C.G. (Kees) de Kruif, Lactoferrin binding to transglutaminase cross-linked casein micelles, *Int. Dairy J.* 26 (2012) 83–87.
- [125] C.G. de Kruif, Supra-aggregates of casein micelles as a prelude to coagulation, *J. Dairy Sci.* 81 (1998) 3019–3028.
- [126] G. Tuinier, R. & De Kruif, C., Stability of casein micelles in milk, *J. Chem. Phys.* 117 (2002) 1290–1295.
- [127] C. Kuraishi, K. Yamazaki, & Y. Susa Y., Transglutaminase: its utilization in the food industry, *Food Rev. Int.* 17 (2001) 221–246.
- [128] J.S. Mounsey, B.T. O 'kennedy, P.M. Kelly, Influence of transglutaminase



- treatment on properties of micellar casein and products made therefrom  
Influence of transglutaminase treatment on properties of micellar casein and products made therefrom, *Le Lait*, INRA Ed. 85 (2005) 405–418.
- [129] N. F. Nogueira Silva, A. Saint-Jalmes, A. F. de Carvalho, F. Gaucheron, Development of casein microgels from cross-linking of casein micelles by genipin., *Langmuir*. 30 (2014) 10167–10175.
- [130] M. Haham, S. Ish-Shalom, M. Nodelman, I. Duek, E. Segal, M. Kustanovich, Y. D. Livney, Stability and bioavailability of vitamin D nanoencapsulated in casein micelles, *Food Funct.* 3 (2012) 737–744.
- [131] A. Pierre, J. Fauquant, Y. Le Graet, M. Piot, J. L. Maubois, Préparation de phosphocaseinate natif par microfiltration sur membrane, *Lait*. 72 (1992) 461–474.
- [132] P. Schuck, M. Piot, S. Méjean, Y. Le Graet, J. Fauquant, G. Brulé, J. L. Maubois, Déshydratation par atomisation de phosphocaseinate natif obtenu par microfiltration sur membrane, *Lait*. 74 (1994) 375–388.
- [133] J.D.C. Davies, D. T. White, The stability of milk protein to heat. I. Subjective measurement of the heat stability of milk, *J. Dairy Res.* 33 (1966) 67–81.
- [134] T. Huppertz, C.G. de Kruif, Ethanol stability of casein micelles cross-linked with transglutaminase, *Int. Dairy J.* 17 (2007) 436–441.
- [135] L. Greenwood, R. & Bergstriim, Electroacoustic and Rheological Properties of Aqueous Ce-ZrO<sub>2</sub> (Ce-TZP) Suspensions, *JECs-Journal Eur. Ceram. Soc.* 17 (1997) 537–548.
- [136] M. Famelart, F. Lepesant, F. Gaucheron, L. Graet, P. Schuck, pH-Induced physicochemical modifications of native phosphocaseinate suspensions: Influence of aqueous phase, (n.d.).
- [137] M.A. Smiddy, J.-E. G. H. Martin, A. L. Kelly, C. G. de Kruif, T. Huppertz, Stability of casein micelles cross-linked by transglutaminase., *J. Dairy Sci.* 89 (2006) 1906–1914.
- [138] C.G. De Kruif, Casein micelle interactions, in: *Int. Dairy J.*, 1999: pp. 183–188.
- [139] T. Huppertz, C. G. de Kruif, Structure and stability of nanogel particles prepared by internal cross-linking of casein micelles, *Int. Dairy J.* 18 (2008) 556–565.
- [140] D.S. Horne, Steric effects in the coagulation of casein micelles by ethanol, *Biopolymers*. 23 (1984) 989–993.
- [141] D.S. Horne, Ethanol Stability, in: *Adv. Dairy Chem. (3rd Ed.). Proteins, Part A Vol. 1*, 2003: pp. 975–999.
- [142] C.S. Ranadheera, W.S. Liyanaarachchi, J. Chandrapala, M. Dissanayake, T. Vasiljevic, Utilizing unique properties of caseins and the casein micelle for delivery of sensitive food ingredients and bioactives, *Trends Food Sci. Technol.* 57 (2016) 178–187.
- [143] W.M. Elzoghby, A. O., Samy, N.A. Elgindy, Novel spray-dried genipin-crosslinked casein nanoparticles for prolonged release of alfuzosin hydrochloride, *Pharm. Res.* 30 (2013) 512–522.
- [144] B.M. Christensen, E.S. Sørensen, P. Højrup, T.E. Petersen, L.K. Rasmussen, Localization of Potential Transglutaminase Cross-Linking Sites in Bovine Caseins, *J. Agric. Food Chem.* 44 (1996) 1943–1947.
- [145] H. Ikuraa, K., Kometania, T., Yoshikawaa, M., Sasaki, R., & Chibaa,

- Crosslinking of Casein Components by Transglutaminase, *Agric. Biol. Chem.* 44 (1980) 1567–1573.
- [146] J.H. Moon, Y.H. Hong, T. Huppertz, P.F. Fox, A.L. Kelly, Properties of casein micelles cross-linked by transglutaminase, *Int. J. Dairy Technol.* 62 (2009) 27–32.
- [147] G. Koutina, J.C. Knudsen, U. Andersen, L.H. Skibsted, Temperature effect on calcium and phosphorus equilibria in relation to gel formation during acidification of skim milk, *Int. Dairy J.* 36 (2014) 65–73.
- [148] G. Koutina, J.C. Knudsen, U. Andersen, L.H. Skibsted, Influence of colloidal calcium phosphate level on the microstructure and rheological properties of rennet-induced skim milk gels, *LWT - Food Sci. Technol.* 63 (2015) 654–659.
- [149] A. Pitkowski, T. Nicolai, D. Durand, Scattering and turbidity study of the dissociation of Casein by calcium chelation, *Biomacromolecules.* 9 (2008) 369–375.
- [150] B.Y. Kim, N.A. Bringe, J.E. Kinsella, Effects of calcium anions on the rates of casein aggregation, *Food Hydrocoll.* 4 (1990) 239–244.
- [151] A. Tsioulpas, M.J. Lewis, A.S. Grandison, Effect of minerals on casein micelle stability of cows' milk., *J. Dairy Res.* 74 (2007) 167–173.
- [152] A. Sauer, C. I. Moraru, Heat stability of micellar casein concentrates as affected by temperature and pH, *J. Dairy Sci.* 95 (2012) 6339–50.
- [153] S. Sandra, M. Ho, M. Alexander, M. Corredig, Effect of soluble calcium on the renneting properties of casein micelles as measured by rheology and diffusing wave spectroscopy., *J. Dairy Sci.* 95 (2012) 75–82.
- [154] A.G. Bueno, J. M., Plaza, S., Ramos-Escudero, F., Jiménez, A. M., Fett, R., & Asuero, Analysis and Antioxidant Capacity of Anthocyanin Pigments. Part II: Chemical Structure, Color, and Intake of Anthocyanins, *Crit. Rev. Anal. Chem.* 42 (2012) 126–151.
- [155] K. Jaakola, L., Määttä, A.M. Pirttilä, R. Törrönen, S. Kärenlampi, A. Hohtola, Expression of genes involved in anthocyanin biosynthesis in relation to anthocyanin, proanthocyanidin, and flavonol levels during bilberry fruit development., *Plant Physiol.* 130 (2002) 729–739.
- [156] R. Brouillard, Chemical structure of anthocyanins, in: *Anthocyanins as Food Color.*, Pericles M, ACADEMIC PRESS INC., London, 1982: pp. 1–40.
- [157] L. Wu, X., Prior, R., Systematic identification and characterization of anthocyanins by HPLC-ESI-MS/MS in common foods in the United States: fruits and berries., *J Agric Food Chem.* 6 (2005) 2589–2599.
- [158] V. Kopjar, M., Orsolic, M., & Pilizota, Anthocyanins, phenols, and antioxidant activity of sour cherry puree extracts and their stability during storage., *Int. J. Food Prop.* 17 (2014) 1393–1405.
- [159] A. Castañeda-Ovando, M. de L. Pacheco-Hernández, M.E. Páez-Hernández, J.A. Rodríguez, C.A. Galán-Vidal, Chemical studies of anthocyanins: A review, *Food Chem.* 113 (2009) 859–871.
- [160] L. Tang, S. Li, H. Bi, X. Gao, Interaction of cyanidin-3-O-glucoside with three proteins, *Food Chem.* 196 (2016) 550–559.
- [161] S. Wiese, S. Gärtner, H.M. Rawel, P. Winterhalter, S.E. Kulling, Protein interactions with cyanidin-3-glucoside and its influence on  $\alpha$ -amylase activity, *J. Sci. Food Agric.* 89 (2009) 33–40.

- [162] H.M. Farrell, E.L. Malin, E.M. Brown, P.X. Qi, Casein micelle structure: What can be learned from milk synthesis and structural biology?, *Curr. Opin. Colloid Interface Sci.* 11 (2006) 135–147.
- [163] M.P. Baxter, N. J., Lilley, T. H., Haslam, E. & Williamson, Multiple interactions between polyphenols and a salivary proline-rich protein repeat result in complexation and precipitation, *Biochemistry.* 36 (1997) 5566–5577. doi:10.1021/bi9700328.
- [164] J.A. Lucey, M. Srinivasan, H. Singh, P.A. Munro, Characterization of commercial and experimental sodium caseinates by multiangle laser light scattering and size-exclusion chromatography, *J. Agric. Food Chem.* 48 (2000) 1610–1616.
- [165] F. Gaucheron, D. Mollé, R. Pannetier, Influence of pH on the heat-induced proteolysis of casein molecules, *J. Dairy Res.* 68 (2001) 71–80.
- [166] J.R. Lakowicz, Principles of fluorescence spectroscopy (2nd ed.), Publisher, Kluwer Academic/Plenum, New York, USA, 1999.
- [167] G. Lakowicz, J. R., Weber, Quenching of fluorescence by oxygen. A probe for structural fluctuations in macromolecules, *Biochemistry.* 21 (1973) 4161–4170.
- [168] G. Scatchard, The attractions of proteins for small molecules and ions, *Ann. New York Accademy Sci.* 51 (1949) 660–672.
- [169] I.J. Arroyo-Maya, J. Campos-Terán, A. Hernández-Arana, D.J. McClements, Characterization of flavonoid-protein interactions using fluorescence spectroscopy: Binding of pelargonidin to dairy proteins, *Food Chem.* 213 (2016) 431–439.
- [170] L. Tang, H. Zuo, L. Shu, Comparison of the interaction between three anthocyanins and human serum albumins by spectroscopy, *J. Lumin.* 153 (2014) 54–63.
- [171] S. Ross, P. D., Subramanian, Thermodynamics of protein association reactions: Forces contributing to stability., *Biochemistry.* 20 (1981) 3096–3102.
- [172] R. Perozzo, G. Folkers, L. Scapozza, Thermodynamics of Protein–Ligand Interactions: History, Presence, and Future Aspects, *J. Recept. Signal Transduct.* 24 (2004) 1–52.
- [173] K. Bouchemal, New challenges for pharmaceutical formulations and drug delivery systems characterization using isothermal titration calorimetry, *Drug Discov. Today.* 13 (2008) 960–972.
- [174] C. Bissantz, B. Kuhn, M. Stahl, A medicinal chemist’s guide to molecular interactions, *J. Med. Chem.* 5061 (2010) 5061–5084.
- [175] A. Pitkowski, T. Nicolai, D. Durand, Scattering and turbidity study of the dissociation of Casein by calcium chelation, *Biomacromolecules.* 9 (2008) 369–375. doi:10.1021/bm7006899.
- [176] D.G. Dalgleish, M. Corredig, The Structure of the Casein Micelle of Milk and Its Changes During Processing, *Annu. Rev. Food Sci. Technol.* 3 (2012) 449–467.
- [177] O. Elzoghby, A, W.M. Helmy, M. W., Samy, N.A. Elgindy, Spray-dried casein-based micelles as a vehicle for solubilization and controlled delivery of flutamide: Formulation, characterization, and in vivo pharmacokinetics, *Eur. J. Pharm. Biopharm.* 84 (2013) 487–496.
- [178] G. Audic, J. L., Chaufer, B., Daufin, Non-food applications of milk components and dairy co-products: A review, *Lait.* 83 (2003) 417–438.

- [179] P. Klajnert, B., Stanislawska, L., Bryszewska, M., Bartłomiej, Interactions between PAMAM dendrimers and bovine serum albumin, *Biochim. Biophys. Acta.* 1648 (2003) 115–126.
- [180] A. Shukla, T. Narayanan, D. Zanchi, Structure of casein micelles and their complexation with tannins, *Soft Matter.* 5 (2009) 2884.
- [181] M.H. Nogueira, Crosslinked casein micelles by transglutaminase: stability, drying and use as encapsulation device, Master Thesis, Universidade Federal de Viçosa, 2016.